UNDERSTANDING SPATIAL AND TEMPORAL VARIABILITY OF CORN YIELD TO IMPROVE NITROGEN USE EFFICIENCY

By

Olivia Davidson

A THESIS

Submitted to
Michigan State University
in partial fulfillment of the requirements
for the degree of

Environmental Geosciences – Master of Science

2020

ABSTRACT

UNDERSTANDING SPATIAL AND TEMPORAL VARIABILITY OF CORN YIELD TO IMPROVE NITROGEN USE EFFICIENCY

By

Olivia Davidson

Two field scale studies were performed in five corn fields across southwest Michigan over three years in order to examine i) the influence of delayed corn plant emergence on final yield, and ii) the effect of strategic, varied nitrogen management on final yield, profit, and nitrogen use efficiency. Individual corn plant emergence date was documented, and kernel weight, kernel number, and biomass weights were analyzed in order to examine the importance of uniform plant stands in achieving high yields, analyzed by the known historical yield stability (Basso et al., 2019). The results showed a 22-gram decrease from early to late emergence and a 15-gram decrease in total kernel weight from early to medium emergence date, equivalent to 1,825 and 1,244 kg/ha decrease in yield. Yield stability zones differentiation showed a 19.9-gram decrease in relative total kernel weight (1,651 kg/ha) from historically high and stable yield to low and stable yield. More variability in days after planting and decreased yields were seen in the low and medium yielding zones. For the second field study, a procedure was created to variably rate nitrogen fertilization using remotely sensed imagery and crop modelling using the SALUS crop model. Whole plant destructive samples and yield monitor data were analyzed to examine the spatial and temporal variability in differing yield stability zones among all study sites. The results showed no statistically significant difference in yield or profit between nitrogen fertilization zones in most fields, while increases in nitrogen use efficiency were seen in all tactically reduced fertilization rate zones.

ACKNOWLEDGEMENTS

First and foremost, I would like to thank my parents, Bill and Paula, whose support has been most important in achieving my career and life goals. I have been beyond lucky to have parents that have supported and inspired me to achieve higher education and have been there to help me through all of life's big and small moments. Further, thanks are owed to my friends Katelyn, Carlee, Lauren, Erin, Julia, and Alisha who have done nothing but lift me up and encourage me to continue to pursue my career goals.

I would also like to thank my advisor Bruno Basso for providing funding and guidance throughout my undergraduate and graduate career at Michigan State and for giving me opportunities that many do not receive because of his faith in my ability to perform research and create a positive graduate assistant experience. Additionally, I would like to thank my lab members for assisting me both in the field collecting samples, and in the lab processing and analyzing data, as well as my committee members, Dr. Jeff Andresen and Dr. Dave Hyndman for supporting my research goals.

I have been fortunate to attend higher education for eight years and am excited for the opportunities my time at Michigan State has created for me. This experience has brought me to a place where my career goals are achievable, and I thank the university for its focus on research endeavors that made my time here plausible.

TABLE OF CONTENTS

LIST OF TABLES	vi
LIST OF FIGURES	viii
KEY TO ABBREVIATIONS	xi
CHAPTER I: History of Precision Agriculture	1
CHAPTER II: Yield Response to Variable Corn Emergence and Plant Population	12
Introduction	12
Research Question and Objectives	15
Methods	15
Plot Selection and Creation	19
Yield Stability Zone Creation	20
Stealth Cam Imagery Analysis	21
Within-Row Plant Spacing Variability	22
Processing Field Samples	22
Statistical Analysis	22
Results	15
Plant Emergence	23
Tillage and Days After Planting	24
Uniformity of Stand Among Stability Zones	26
Yield Effects of Delayed Emergence	29
Plant Spacing Variability	33
Discussion	38
CHAPTER III: Spatial and Temporal Analysis of Nitrogen Use Efficiency Using Remotely Sensed	
Imagery and Crop Modeling	
Introduction	
Overview of Remotely Sensed Imagery and Nitrogen	
Spectral Reflectance and Plant Health	
Crop Modeling Integration Precision Nitrogen Management Adoption	
Research Question and Objectives	
Methods	
Field Experiment	
Tactical Management and In-Season Destructive Sampling	
UAV Imagery and Chlorophyll Meter Measurements	
DALOD CIUD MUUCIIIE	J∠

Procedure to Develop Nitrogen Fertilization Prescription Map (Rx)	53
Industry Methodology	53
UAV Imagery Prescription Aided by Systems Crop Modeling	
Statistical Analysis	
Nitrogen Use Efficiency	59
Spatial Analysis	
Results	
Chlorophyll Meter Analysis	63
Reflectance from Remotely Sensed Imagery and Nitrogen Status	65
Yield and Use Efficiency Response to Variable Rate Application	66
Field Summaries.	67
Discussion	75
CONCLUSIONS	77
APPENDIX	79
REFERENCES	87

LIST OF TABLES

Table 1. Description of field size by study year from 2016 to 2018 field sites in Portland and Springport, MI
Table 2. Delineation into early, medium and late emergence by field, year, and replicate of sampling point within each field
Table 3. Output of field 105 in 2018 in which different emergence plots received differing nitrogen applications relating total kernel number per plant in comparison to the total amount of nitrogen applied and the yield stability zone
Table 4. Analysis considering all fields in one mixed model $kernel\ weight = D0E + Zone + growing\ space + D0E:Zone:growing\ space$ with replicate as the random variable. Letter separation was performed using Tukey's test of mean separation calculated by zone32
Table 5. Anova table by each field in each year of study. Letter separation was performed using Tukey's test of mean separation calculated by zone in the mixed model $y = DOE + Zone + DOE:Zone:growingspace$ with replicate as the random variable
Table 6. The growing space is calculated by stability zone, and shown with standard error, and Tukey's mean separation performed to visualize any statistically significant differences of growing space between stability zones. This incorporated all study sites and all years of study35
Table 7. ANOVA Table of predicting total grain weight using growing space, yield stability zone and their interaction
Table 8(a-b). The fertilizer application dates (a) and amounts (b) for six research fields from 2016 through 2018
Table 9. Description of wavelengths pertaining to visible, multispectral, and thermal imagery and the pertaining vegetation indices produced
Table 10. The chosen application rates based on the segmentation of NDRE imagery of field 105 in 2018. After performing segmentation, each class of pixels is assigned a rate based on agreed upon rates with the farmer, as well as crop modeling results (Figure 17) showing the tradeoff of yield probability with application amount
Table 11. The chosen application rates based on the segmentation of ExG imagery of field NC12 in 2018. After performing segmentation, each class of pixels is assigned a rate based on agreed upon rates with the farmer, as well as crop modeling results showing the tradeoff of yield probability with application amount
Table 12. Values used for spaital NUE calculation in ArcGIS using the raster caculator tool. The HI is the same for both treatments because only camera zones had HI values but they were placed in conventional only. The asterisk next to the N values indicates this was an arbitrary value chosen from literature
Table 13. Single variate regression analysis with profit, yield, or ANUE as the dependent variable and treatment as the covariate by field. The letters represent the Tukey's mean

separation test showing if profit, yield, and ANUE are statistically significantly different from one another
Table 14(a-b). Regression using equation $y = \mu + stability + N$ applied $+$ replicate $+$ error with mean separation using Tukey adjustment. The letters represent the Tukey's mean separation test showing if yields were significantly different between stability zones and by amount of fertilization.
Table 15. ANOVA significance results (p values) relating relative chlorophyll from photosynQ measurements to date of measurements, yield stability zone, and nitrogen treatment type (tactical or conventional, trt=treatment) and their interactions, indicated by a colon

LIST OF FIGURES

Figure 1. Industry 4.0 in agriculture: Focus on IoT aspects. (2017). Diagram showing the steps of development in precision agriculture
Figure 2. Research design of Lauer and Rankin et al., 2004, deliberately altering plant spacing in order to examine yield effects
Figure 3. Climagraphs showing weather observed from 2016 to 2018 relative to historical observed weather in Portland and Springport, MI
Figure 4. Relationship between Days After Planting and cumulative rainfall from the day of planting by stability zone. Each figure contains all fields analyzed. Low and stable yielding zones were not represented in 2018.
Figure 5. Cumulative rainfall and cumulative plants emerged by stability zone and field from 2016 to 2018.
Figure 6. Stealth Cam image of emergence plot in field JS1 in 2017, the technique utilized in each emergence plot from 2016-2018, sizing four rows by two meters
Figure 7. Showing emergence difference between no-till (darker shade) and tilled fields using data from 2016-2018, separated by yield stability zone
Figure 8. Frequency diagram of the amount of corn plants emerged by yield stability zone and categorical emergence of early, medium, and late. Categorical emergence was determined each year for each field using quartiles
Figure 9. Frequency diagrams of emergence days by year and stability zone, where each plot shows the two study sites utilized for emergence studies in the given year
Figure 10. Coefficient of variation of days after planting (DAP) for each study year by stability zone
Figure 11. Illustrating the accumulation of emerged plants in all plots at each study site by stability zone. Some study plots were randomly excluded to have an equal number of plots in each stability zone, and hence comparison between the plots is not encouraged
Figure 12. (a) average number of kernels, (b) Average total kernel weight per plant, and (c) Average weight per kernel by plant, for each emergence category grouped by yield zone
Figure 13. Average number of kernels and average total kernel weight per plant shown by days after planting and separated by yield stability zone. Each plot represents a different study site and includes all of the emergence plots at the site
Figure 14. Coefficient of variation of growing space using equation 1 is shown versus the point yield (calculated using row spacing and plants per hectare calculations from number of plants within the sample plot) and grams of grain per plant, and converted to kilograms per hectare, and grouped by stability zone

Figure 15. Coefficient of variation of growing space using equation 1 is shown versus the point yield (calculated using row spacing and plants per hectare calculations from number of plants within the sample plot) and grams of grain per plant, and converted to kilograms per hectare, and grouped by stability zone and separated by field with regression equation and coefficient of determination
Figure 16. Utilizing by-plant grain weights to examine growing space (in square centimeters) vs the total kernel weight per plant in grams. Performed by field and separated by stability zone by color
Figure 17. The nitrogen cycle pertaining to agricultural sources of fertilizer, and its effects on the atmosphere, surface water and ground water from North Carolina State Extension
Figure 18. This image is a segmentation of NDRE imagery taken on July 24, 2018 and used to create the nitrogen prescription used. The yellow represents low reflectance, increasing to green, blue and at the highest reflectance, purple
Figure 19. ECDF of field 105 in 2018 several days before the planned fertilization date. This ECDF was made from SALUS output data utiling the current conditions from soil sampling, and 30 potential weather scenarios. This plot shows the probability of achieving a certain level of yield dependent upon the level of fertilization. It is visible here that in many circumstances, yields will be incredibly similar regardless of application type, and visualizes the trade-off of no nitrogen application.
Figure 20. Segmentation of the ExG index, with suggested N rates of 40 gpa (gallons per acre, as the farmer applies liquid fertilizer) for green areas, or lower values of excessive greenness, and increased rates of 50 gpa for blue or yellow areas. On top of the segmentation image is the fishnet tool the width of the planter, which can be directly loaded into the farmer's applicator as a shapefile
Figure 21. The plots show simulated vegetation index (NDVI, NDRE and GNDVI) using Photosynq measurement parameters versus the true vegetation index value from UAV imagery (a). The correlation of nitrogen in biomass to the relative chlorophyll estimated from SPAD reflectance values from the PhotosynQ devices. Each color indicated a different field from 2017 to 2018 (b)
Figure 22. Plots of the red band, green band, blue band, red edge band, NDVI, NDRE, GNDVI and ADVI reflectance values, plotted against the nitrogen content in the biomass. This content was calculated using biomass weight values, referenced to percent nitrogen analyzed from a subsample of the ground biomass
Figure 23. Yield, Nitrogen Use Efficiency, and profit by each application in six field studies from 2016-2018
Figure 24. Differences in yield between stability zones by application types for each study field between 2016- 2018. In 2016 field 222 received different color scheme because the difference in application was timing of fertilization, and not application amount
Figure 25. Nitrogen Supplied by Soil, Nitrogen Use Efficiency, ANUE, and Nitrogen Uptake were calculated using N data from plant samples and yield monitor data from all six study sites

from 2016-2018, using raster calculation in ArcMap and extracting point data74
Figure 26. Nitrogen fertilizer sidedress prescription developed from remotely sensed imagery for field NC12 in 2018
Figure 27. Nitrogen fertilizer sidedress prescription developed from remotely sensed imagery for field 105 in 2018, created in ESRI ArcGIS80
Figure 28. NUE, Profit, Yield, and Fertilizer Efficiency/ANUE maps created in ArcMap from yield monitor data and N data from hand samples
Figure 29. Yield monitor data of field ZC1 in 2016 showing sampling locations where N was overloaded by hand

KEY TO ABBREVIATIONS

ADVI Advanced Difference Vegetation Index

ANUE Agronomic Nitrogen Use Efficiency

CCCI Canopy Chlorophyll Content Index

CERES Crop Environment Resource Synthesis)

DAP Days After Planting

DOP Dilution of Precision

ECDF Empirical Cumulative Density Function

ExG Excessive Greenness

GIS Geographic Information System

GNDVI Green Normalized Difference Vegetation Index

GPS Global Position System

HI Harvest Index

LAI Leaf Area Index

N Nitrogen

NDRE Normalized Difference Red Edge

NDVI Normalized Difference Vegetation Index

NFE Nitrogen Fertilizer Efficiency

NIR Near Infrared

NSI Nitrogen Stress Index

NUE Nitrogen Use Efficiency

PA Precision Agriculture

RGB Red Green Blue

RTK Real Time Kinetics

SA Selective Availability

SALUS System Approach to Land Use Sustainability

SPAD Soil Plant Analysis Development

UAV Unmanned Aerial Vehicles

USDA United States Department of Agriculture

CHAPTER I: History of Precision Agriculture

The cultivation of corn (Zea Mais) has been instrumental in sustaining food production across the world for decades and remains critical today, with a different focus - eliminating detrimental environmental impact from its current agronomic management (Basso et al., 2019). While ongoing studies of sustainable management practices have existed for decades, there is still much to be learned, and the balance between producing high yields and profit and mitigating environmental impact has yet to be achieved. Understanding the degree of spatial and temporal variability across a region, a county, and at the field-scale is key to developing management practices adoptable by farmers and demonstrated by research to be a means of increasing sustainability of the agricultural industry.

Precision agriculture (PA), defined by Pierce and Novak (1999) as "the application of technologies and principles to manage spatial and temporal variability associated with all aspects of agricultural production for the purpose of improving crop performance and environmental quality" has led the way to increasing sustainable management practices, mostly due to advances in technology and a deeper understanding of the controlling systems for the adoption of sustainable practices. The core of precision agriculture lies in the ability to measure spatial and temporal variability. For this to be possible, positional data needs to be obtainable for the information to be useful for site-specific management. The establishment of technology capable of measuring positional data came from humble beginnings. Before the creation of GPS (global position systems), position was measured relatively, using radar or ultrasound, and direction using a gyroscope or an angle-sensor if permanent wheel tracks (tramlines) existed in the farming system. Spatial variability had been measured far before the technology to record exact

spatial location existed by (Nielsen et al., 1973) using time-consuming measures of distance by hand in a grid fashion with rows and columns (Vieira et al., 1981) and lacked precision.

Following this dead reckoning methodology came triangulation, where the known location of two or more radio transmitters sends radio waves to a handheld unit, giving positional accuracy up to 15 cm (Pierce and Novak, 1999). These systems were expensive, time consuming and ease of use was limited.

Grain flow monitoring systems to measure yield were created in 1985, which use a load cell, or a transducer that translates a force such as pressure or torque into an electric signal that can be measured with an impact plate to measure grain mass flow, which is then calibrated to an average grain impact force. This is attached to the grain elevator, a conveyor that lifts the grain within the combine to measure yield by field, and once GPS was utilized, by each meter in a single field. Yield monitor systems utilizing GPS did not become a commercial product in the US until 1992 (Pierce and Novak, 1999). Along with yield monitoring systems came autosteering tractors in the 1990's, alluring to farmers to cut down on labor costs and worker fatigue/human error, and reduce overlaps and skips, reduce drift and increase the land area planted in the optimal planting period (Shockley et al., 2011). Variate rate technology was also first introduced in 1985, patented by SoilTeq Inc (Pierce and Novak, 1999) when they created a computer-controlled fertilizer spreader (Mulla, 2013). The rates were based on digitized soil maps identified using dead reckoning or triangulation techniques. Extensive variable fertilization trials were performed by Mulla (1992) using 15 meter transects and manually applying variable rates (Mulla and Khosla, 2016) to assess profitability of variate rate technology due to savings in fertilizer quantity. From this technology came variable rate herbicide technology, and variable rate irrigation in the 1990's.

The rise of precision agriculture is attributed with the creation of GPS technology. This technology enabled a new level of spatial awareness and facilitated all other forms of precision agriculture technology used today. GPS utilizes the known location of satellites orbiting earth, and transmits the location to a GPS receiver, with which the receiver's location is calculated based on the time elapsed until the satellite signal reaches the receiver. It was first made available to the general public in 1983 and has had the largest influence on the technology used to examine temporal and spatial variability in soil and yield (Schimmelpfennig, 2016). The first GPS satellite was launched in 1978, while GPS was not made available for civilian use until 1983. The full 24 GPS NAVSTAR satellite group was launched intermittently until being completed in 1994. The first handheld GPS system was released by Magellan in 1989, with a cost of \$3000 and battery power lasting only few hours. For this reason, GPS was not used widespread until years later, when the full constellation of satellites was available. GPS still suffered from accuracy and addressing the dilution of precision (DOP) was the first step in creating the spatial accuracy we have today. DOP relates to the geometric error from the multiple satellites and GPS receiver in location prediction (PFost et al., 1998). Further, errors were introduced from selective availability (SA) implemented by the US Department of Defensive in 1990 to purposefully skew the positional accuracy by up to 100 meters, later turned off in 2000 (Mulla and Khosla, 2016).

Utilization of GPS technology for yield monitoring and auto-steering became more alluring with the invention of Real Time Kinetics (RTK) by O'Connor et al. (1996) (Mulla, 2013), which is a processor that increases accuracy of positional data by correcting GPS signal, and stores the information in real time, constantly updating the corrections as the RTK is moved. Because stationary receivers have a known fixed location, the difference between this value (true

range from satellite) and the value given after SA error and all other error is introduced (pseudorange from satellite) is known as the differential correction. Stationary receivers use differential corrections to eliminate SA, dilution of error, and other variable atmospheric conditions introducing further error. This can be especially important for the creation of terrain maps and can lead to one-centimeter accuracy (Schimmelpfennig and Ebel, 2011). Previously, differential corrections on GPS positional data suffered from the need for expensive antennae and receivers, and inconsistent connection depending on distance from a base station and topography and landscape of the area, as well as requiring a fee for commercial use (Pierce and Novak, 1999; Mulla and Khosla 2016). Despite the initial limitations, swift advancement of GPS technology has led to sub centimeter resolution for positional accuracy that makes precision agriculture as we know it today, possible.

Another technology that makes the use of spatial data attainable are Geographic Information Systems (GIS). A GIS is a suite of hardware and software used for the visualization and manipulation of spatial data, which first became possible on desktop computer with limited capacity in the 1990's. The most limiting factor of GIS came from the complexity of the programs, making it unreasonable to expect adoption until ease of use was established. By the late 1980's software existed to interpolate soil fertility data and created management zones based on extensive transect soil sampling (Mulla and Khosla, 2016). While this was a large feat in the 1980's, GIS software has gone from clunky desktop computer applications to geographically referenced yield data automatically uploaded to a storage disk using GIS software, most often, ESRI (Environmental Systems Research International) Arc software (Schimmelpfennig and Ebel, 2011) directly from the harvester for on-the-go data collection without extra labor.

Crop modeling has become an integral technology in assessing spatial and temporal crop growth variation (Basso et al., 2016). Many crop models use a process-based approach, integrating environmental and management information such as weather, soil information, crop genetic information, fertilization management, planting information and more to simulate possible yield outcomes. These outcomes can be validated with yield monitor data, hand samples of plant material and soil analyzed for nitrogen content. Error of yield simulation can likely be attributed to incorrect initial environmental conditions, often approximated, of which the crop model was ran. These can be altered using informed trial and error decisions and simulated again to have high accuracy of simulation, and hence validate the model for the specific region of interest. Error of yield estimation can also come from a variety of other sources, including genetic coefficients from new hybrids and weather extremes, as there is not as much validation under these conditions. It is important to note that a small amount of error in the initial conditions can be exacerbated by the end of the season yield estimation, but it is impossible to eliminate all sources of error. In a study assessing the CERES crop model in 43 different countries, Basso et al. (2016) found that the error associated with phenological maturity was less than 7 days across all study sites, and yield estimation was less than 10%, while nitrogen dynamics errors were as high as 80%. Continued validation at high frequency can only make a crop model more accurate, but multiple sources of error will always be present.

The integration of GPS, GIS, crop modelling and mechanized farm equipment are the key mechanisms needed for PA techniques to be fully realized. The future of precision agriculture lies in adapting to a systems approach rather than traditional management schemes, using today's advanced technology for site specific management based on plant and soil needs detected from a variety of sensor data and high resolution yield data, all of which can be stored within GIS

software, continually adapting for ease of use and utilized for crop modelling (Figure 1). While many of these technologies have become a reality in the research realm, adoption among farmers is still struggling when tradition is favored, and ease of use is not guaranteed.

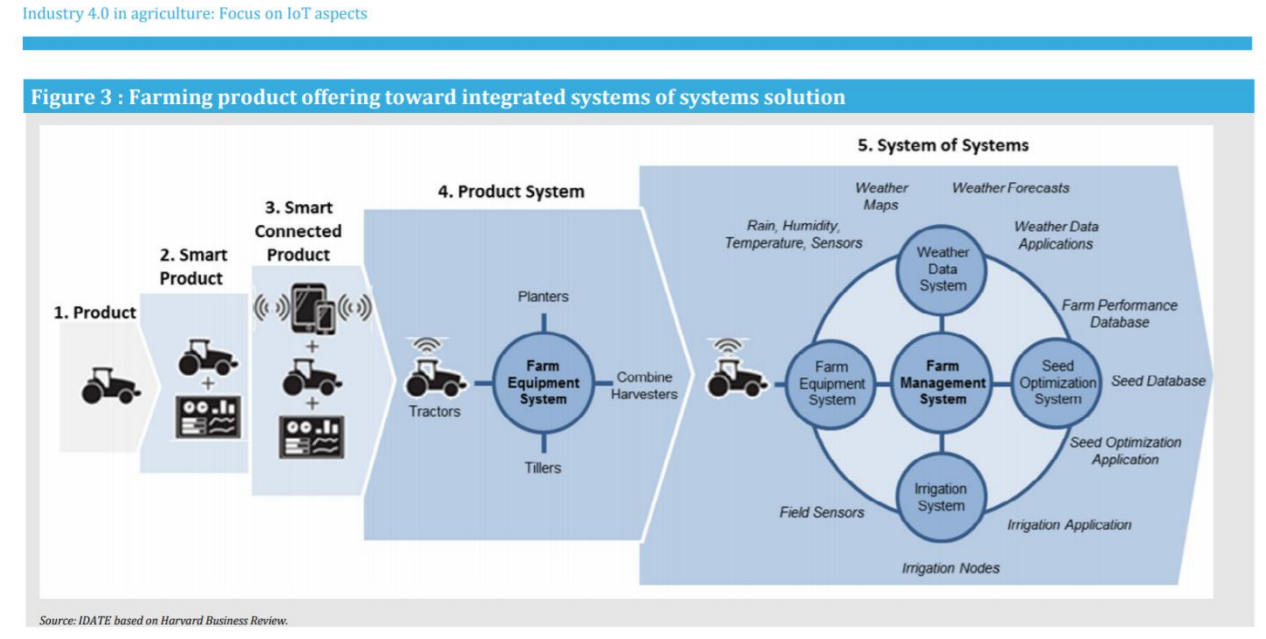


Figure 1. Industry 4.0 in agriculture: Focus on IoT aspects. (2017). Diagram showing the steps of development in precision agriculture.

Yield monitoring systems and GPS allowed farmers to visualize spatial and temporal variation in their fields at a higher resolution for a better understanding of plant-to-plant variation and needs and illuminated the potential of high-resolution field sensors to monitor variable crop development over a field. From the technological advancements of yield monitor technology and variable rate fertilization came the utilization of remotely sensed imagery for site specific management. Remote sensing in precision agriculture began with sensors to monitor soil properties such as organic matter and water content in the 1990's (Mulla, 2013) using light emitting diode (LED) sensor that emitted radiation mounted to a tractor. Satellite data imagery developed in the 60's has been used for agricultural research for decades, but it suffered from

low resolution and was only useful for large-scale research. Increases in spatial resolution in the 90's as low as 0.6 meters of the IKONOS satellite lead to the use of satellite imagery for agricultural research (Mulla, 2013). Many of these spatially evolved satellites were operated by privately funded companies, of which the costs limited the number of farmers willing to work with the data. Data provided by government-operated satellites is most often free but remains limited by spatial resolution for field scale precision agricultural techniques. Satellites are also limited by weather conditions, as cloudy skies limit some to all visibility many days of the year. Throughout the decades remotely sensed imagery has gone from grainy satellite imagery to Unmanned Aerial Vehicles (UAV) imagery, beginning in the early 2000's. Analysis of vegetation indices such as NDVI (Normalized Difference Vegetation Index) to assess crop health has become a popular technological advancement, most specifically in the research realm, while adoption by farmers is becoming more and more realized as research establishing the benefits continues to be published (Mulla, 2013; Shanahan et al., 2001; Basso, et al., 2016; Maestrini, and Basso, 2018; Moran, et al., 1997; etc.). While soil and handheld sensor capabilities have expanded precision agriculture methods, yield monitors continue to be one the most important tools in evaluating variation, surpassed only by the implementation of remotely sensed imagery with the capability of assessing variation more frequently without the need for time consuming field sampling.

Given the clearly appealable aspects of PA in relation to improved yield, reduced cost, and improved environmental impact, what is its current adoption? As of 2012, 50 percent of corn and soybean farmers had adopted yield monitor systems, while only a third of these farms had adopted auto-steer technology and a quarter had adopted variable rate technology and GPS yield mapping (Schimmelpfennig, 2016). This statistic is extremely different if looking at farms that

have over 2,900 acres, in which almost 80 percent have adopted mapping and guidance techniques, and almost 40 percent variable rate technology. Adoption of GPS mapping from 2012 data showed it is most often independently adopted rather than adopted with other precision agriculture techniques. Only 3.8 percent of farms adopted guidance systems, variable rate technology, and GPS mapping (Schimmelpfennig, 2016) while conversely, farmers that adopt conservation tilling are more likely to adopt yield monitoring technology (Schimmelpfennig and Ebel, 2011). Research has shown that money spent on labor is increased with adoption of precision agriculture most likely due to the increased need for skilled employees to operate and interpret the newest technology platforms, as well as increased spending on equipment and machinery. Despite this, average profit of farmers that don't adopt precision agriculture is \$66 per acre less than farmers who choose to invest in precision agriculture technologies (Schimmelpfennig and Ebel, 2011). This number is very dependent on farm size and location of the operation, and therefore it must be understood that some smaller farm sizes do see decreased profit, while larger farms see significant increases. Survey data from Erickson et al., 2013 showed that 70 percent of farming precision agriculture providers reported profitability of soil sampling with GPS, 50 percent showed planting guidance systems were profitable, and 80 percent of variable rate technology adopters saw profit increases. The profit of variable rate technology was found to be largely dependent on the variability within the field, where homogeneous fields do not show a response from variable fertilization. Overall, smaller operations suffer from initial operation and machinery costs and lessened variability on smaller land area which shows lessened profitability with adoption of variable rate technology, and adoption of these environmentally sound practices needs to be encouraged by private industry and government policy.

For adoption of precision agriculture techniques to increase, policy will need to advance with technological advancement, not only providing incentives but continually developing user-friendly services to accomplish sustainability goals (Rosegrant et al., 2014). This does not come without caveats, as policies meant to increase sustainable practices can have the opposite desired effect, for example, as subsidies for no-till management to increase carbon sequestration can increase the need for weed control, with additional environmental concerns of higher herbicide applications. Similarly, subsidies for nitrogen application can lead to increased inputs and diminish the industry of efficient fertilizer application technology (Schimmelpfennig and Ebel, 2011). The future of governmental advocation of precision agriculture techniques lies in the partnership of private industry and research and government, such as insurance companies and research institutions continuing to provide advanced technologies for new crop varieties and informed variable rate fertilization strategies/mechanization.

Collection of remotely sensed imagery through UAV's has created the capability of assessing plant health throughout the growing season using multispectral imagery, providing farmers information to make in-season management decisions (Raun, 2002; Basso, 2015, Solie, 2012). Gathering data on well and poor performing regions on the field scale and investigating the environmental factors that contribute to these yield variations using sensor data, historical yield data and field sampling provides the means to adjust fertilization management based on known yield performance, and create informed explanations on why certain regions perform better than others. Plant stresses from water or nutrients can be detected through remotely sensed imagery based on the relative reflectance values from multispectral imagery, as well as water retention soil characteristics and estimation of soil organic matter using thermal imagery (Mulla et al., 2013). Many underperforming regions do not utilize applied fertilizer due to water

limitation retention constraints, topography, and soil type, and can be analyzed to understand the environmental and cost benefit of choosing not to apply fertilization or applying a reduced quantity. This can be achieved on a scale as small as a fertilizer applicator allows. Further technological advances in fertilization applicators could further increase the resolution of prescription fertilization once adoption of precision agriculture techniques is fully realized.

Understanding plant-to-plant variation can aide in better informed fertilization management and create an agricultural industry that is economically viable, socially conscious, and environmentally sound (Ikerd et al., 1993). The future of precision agriculture comes down to acquiring more data than ever before at the field scale, to ensure the five R's of management are achieved; doing the right thing, at the right time, in the right place, in the right way, with the right inputs. Much of this data can be understood with crop modelling, using a systems approach to consider many management decisions and environmental conditions in order to simulate yield and make informed fertilization decisions based on the best scenario for the predicted weather, soil, and management ensuring profitability and sustainability (Basso et al., 2016). This becomes even more important as climatic conditions change across the globe, creating more extreme weather events including cases of extreme precipitation and drought (IPCC, 2014). Expected climatic changes are implemented into crop models to examine yield and environmental effects in upcoming years, encouraging preemptive ideas of management (Liu and Basso, 2020). Predicted extreme weather conditions can be extremely detrimental to uniform plant stands stemming from flooding or extreme lack of water (Martinez-Feria and Basso, 2019). Liu and Basso (2020) found that while practices such as no-till management can help decrease yield loss in corn and retain soil structure and soil organic carbon, it is not enough to mitigate predicted climatic change unless new corn drought-resistant hybrids are developed. Identifying

regions of the field more susceptible to excess or lack of water and creating management strategies for either circumstance using remotely sensed imagery and crop modelling can create an adaptable, weather-dependent management scheme ready to face climatic change that may arise in the years to come implementing using advanced drought-resistant hybrids and variable rate fertilization. Basso and Antle (2020) have recently discussed about the critical role that Digital Agriculture covers in designing future sustainable agricultural systems.

This objective of this study is to evaluate two specific aspects of precision agriculture: i) assessing and analyzing plant to plant variability (Chapter II), and ii) improve N fertilizer application to increase productivity where possible and reduce N loss in areas of lower response to fertilizer (Chapter III).

CHAPTER II: Yield Response to Variable Corn Emergence and Plant Population

Introduction

Understanding spatial and temporal variability of plant emergence is important because uneven emergence and lower plant stands decreases yield (Nafziger, 1991). Heterogeneous plant stands cause a larger yield gap and in turn can decrease nitrogen use efficiency as well as water use efficiency in irrigated fields. Researchers have deliberately planted at later dates to examine implications of late or early emergence. These studies found that delayed emergence decreased final yield in areas where some or all plants emerged late (Ford, 2013; Liu, 2004; Rutto, 2014). Rutto et al., (2014) found a mean grain decrease of 122 kg/ha per day of delayed emergence compared to adjacent plants. When one out of six plants experienced delayed emergence, Liu et al., (2004) found a 4 percent yield decrease in two leaf stage delay, and 8 percent yield loss in four leaf stage delay. Yield compensation in nearby plants did not occur as strongly for late emerged plants than for skipped or unmerged plants. Liu et al., (2004) also addressed that in fields where plant populations are high as is competition, late emerged plants act as weeds and reduce compensatory growth. Rows with skips of unemerged plants refer to mechanical error of the planter, in contrast to environmental factors of unemerged plants. The physiological source of the decreased grain yield pertains to the number of kernels rather than the weight per kernel (Pommel, 2002). Pommel et al., (2002) found that compensatory growth accounted for much of unmerged plant yield loss, as 7 to 15 percent grain yield per area was observed and validated with model values simulating 6 to 11 percent, but simulations without compensation with the CERES (Crop Environment Resource Synthesis) model showed 20 percent yield loss. The main causes for uneven emergence have been identified as soil characteristics, including moisture, texture, and temperature (Blacklow, 1974), and management such as tilling, planting density and depth, and genetics (Nielson, 2001). Nielsen (2001) showed that a growth stage difference of two leaves or greater between adjacent plants can result in the younger plant being barren at end of the season. Absence of tillage was shown to lower the number of emerged plants by up to 26 percent (Lithourgidis, 2005) attributed to dry soils, but some field study sites showed no statistical difference, although no yield differences were found between tillage and no tillage management. Conversely, Hughes et al., (1992) found plots with no tillage had 16% yield loss in comparison to tilled fields. Genetics or hybrid type is also a complicating factor in understanding how late emergence affects final grain yield. The difficulty in producing homogeneous plant stands, due to the many environmental factors causing delayed emergence, creates the need for additional research on the degree to which yield will be affected in a uniformly planted field. This natural heterogeneity cannot be corrected to create an even stand; however, a more informed perspective on the yield effects can create better management standards to correct for these yield losses through practices such as variable fertilization.

Plant spacing is another aspect of potential yield growth and variability and can be used alongside delayed emergence to assess possible yield loss due to natural variation and management decisions. The effect of plant spacing on yield has been debated in literature, as Liu et al., (2004) found no effect of increased plant spacing variability (PSV) on grain yield as well as no significant effect on yield when considering the interaction of delayed emergence and increased PSV. The study found that the variability in plant spacing was reflected in the individual dry plant matter, but the average dry matter across emergence types was not affected. Liu et al., (2004) found that increased variability had no effect on grain yield, leaf number, plant height, Leaf Area Index (LAI), or Harvest Index (HI) when evaluating across two locations and two years. Similarly, J. Lauer et al., (2004) concluded that PSV did not affect grain weight

besides in cases with more extreme topography. Hilled areas have shown to decrease grain yield in comparison to lower elevations of the field. The study found that PSV did not affect absolute grain weight, but when using relative grain yield calculated from the highest yielding PSV of each study site and density tested, each cm over 12 cm decreased grain weight by one percent. B. Pommel (2002) found that grain yield lost due to skips varied from seven to fifteen percent per unit area. Nielsen (2001) reported grain loss for each 2.54 cm increase in the standard deviation of plant spacing. Most studies evaluating the effect of PSV on grain yield have utilized a similar design of manually planting a control with a goal of 0 PSV, and then planting 2 or more plants more closely together in a pattern such as the image below (Figure 2). The argument for a limited effect of PSV arises from the standard that compensatory growth yield due to increased PSV or skips outweighs the competition established between early and late emerged plants. The more significant factor in decreased grain yield has shown to be the temporal variation of plant emergence, while in certain scenarios, a combination of management and environmental factors can cause increased plant spacing variation to decrease yield.

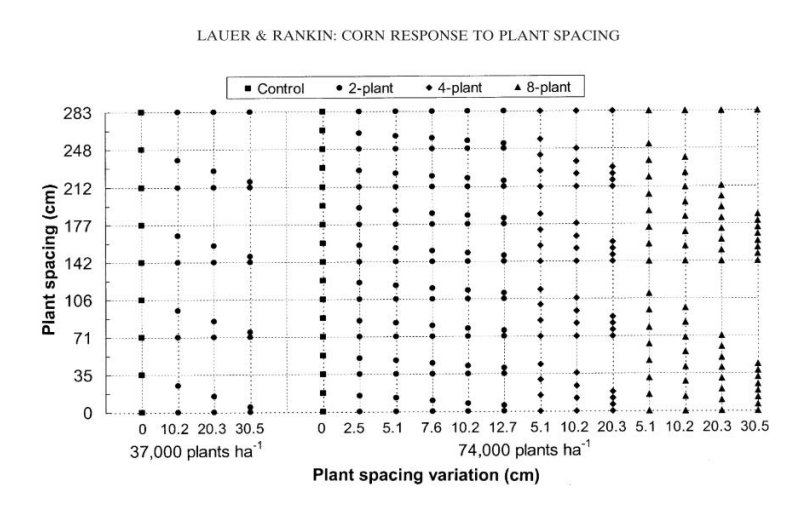


Figure 2. Research design of Lauer and Rankin et al., 2004, deliberately altering plant spacing to examine yield effects.

Research Questions and Objective

In the first study (Study 1), we aim to understand processes affecting plant-to-plant scale emergence of corn in response to spatial and temporal interaction between soil type, weather, topography and management (tillage and no tillage). This study examines the yield effects of delayed corn plant emergence, and question whether this suggested yield loss is primarily related to a decrease in the number of kernels produced, or the weight of the individual kernels. The study also investigated if significant differences exist in plant emergence between yield stability zones, established based on historical yield data compiled from yield monitor data from private farmers in Portland and Springport, Michigan. Our hypothesis is that delay in corn plant emergence decreases yields due to lower number of kernels rather than the weight per kernel and that these results vary over different stability zones.

Methods

Measurements were taken from three corn fields ZC1 (2016), JS1 (2017), and NC12 (2018) in Portland, Michigan, and corn fields 222 (2016 & 2017) and 105 (2018) in Springport, Michigan. The study areas are characterized as Warm Humid Continental Climate (Dfb) and have a growing season varying from May/June to September-November with rain totals averaging 750-900 mm of rain annually. The total in-season rainfall (May 1st to October 1st) varied from 485 to 530 mm in 2016, 255 in 2017 and 490 to 508 in 2018 (Figure 3). Rainfall after the day of planting demonstrated differences in the number of days after planting that plants emerged (Figure 4). In 2016, rainfall after the day of planting was present, but not large (5-12 mm) and yielded strong initial plant emergence, and when more rain fell after the initial emergence, more plants emerged in each stability zone. Interestingly, although 2017 showed a lack of rainfall throughout the growing season, there was an abundance of rainfall after the day

of planting (30-45 mm). Despite this, the low rainfall throughout the 2017 season appeared to create a larger range of days when plants emerged, perhaps due to more isolated, stronger instances of rain. The low and stable yielding zones had low initial emerged plants than other stability zones but increased as days after planting increased. In 2018, field 105 saw a large rain event of over 20 mm after planting as well, which showed strong initial emergence, but as in 2016, more rain after initial emergence increased delayed emergence. Similar results were seen in field NC12 despite over a month difference in planting date. Looking at all plants emerged in each field separated by stability zone (Figure 5), we see a positive correlation between days after planting and cumulative rainfall. This relationship appears to begin after 20 mm of rainfall. In the low and stable yielding zone, this relationship is less clear, as other environmental factors such as topography in the landscape and soil conditions show more variable days after planting despite cumulative rainfall values.

Fields 105 and 222 were planted with corn hybrid Dekalb seeds DKC46-18, field NC12, JS1 and ZC1 planted with Golden Harvest hybrids G95D32-3220-EZ1, G01P52-3122A EZ, and G01P52 respectively. Fields in Springport received no tillage, while fields in Portland were turbo tilled with a tandem disk 4 inches deep. Fields in Springport are planted at 76 cm row spacing while Portland fields maintain 50.8 cm.

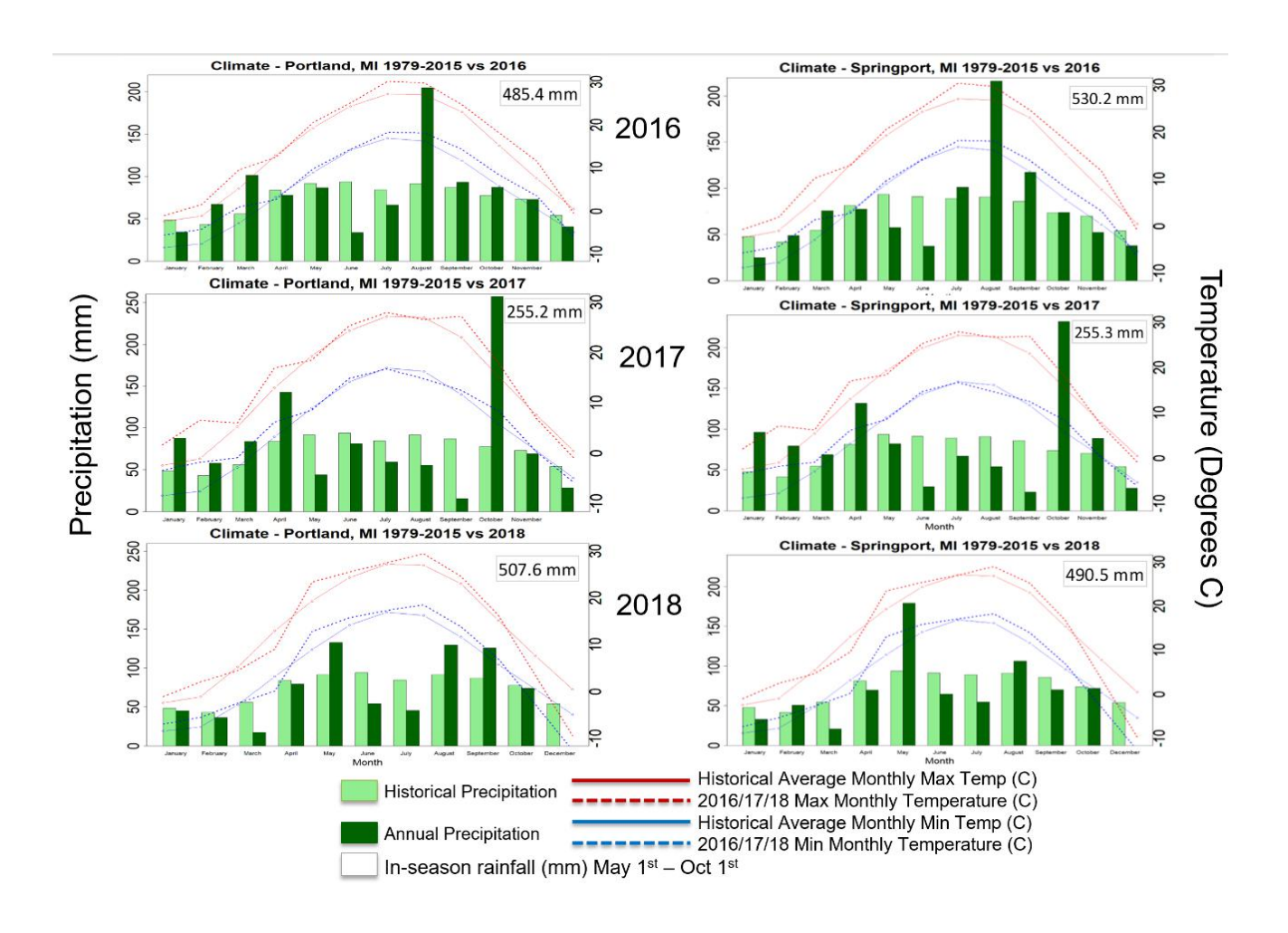
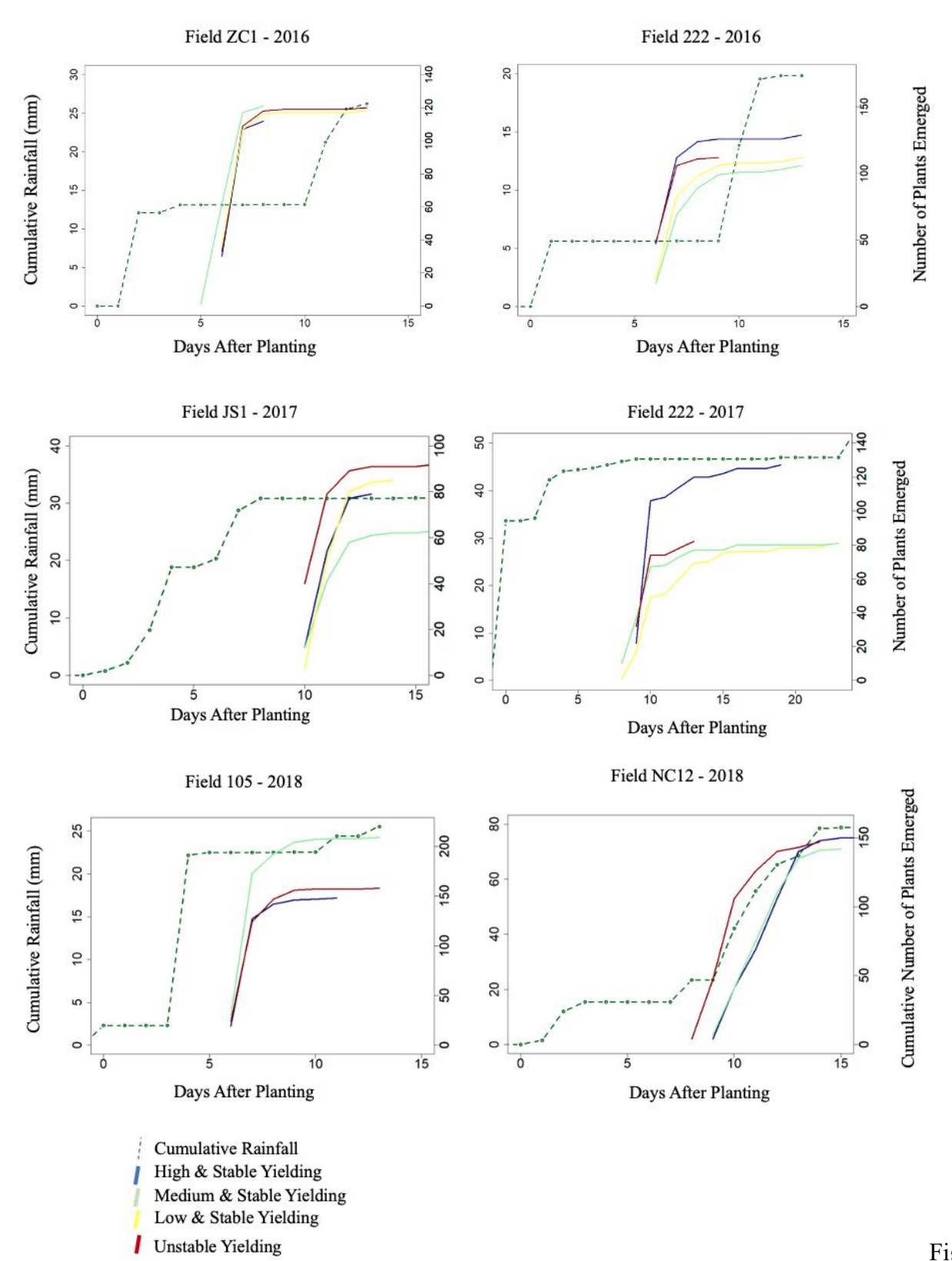


Figure 3. Climagraphs showing weather observed from 2016 to 2018 relative to historical observed weather in Portland and Springport, MI.



ure 4. Relationship between Days After Planting and cumulative rainfall from the day of planting by stability zone. Each figure contains all fields analyzed. Low and stable yielding zones were not represented in 2018.

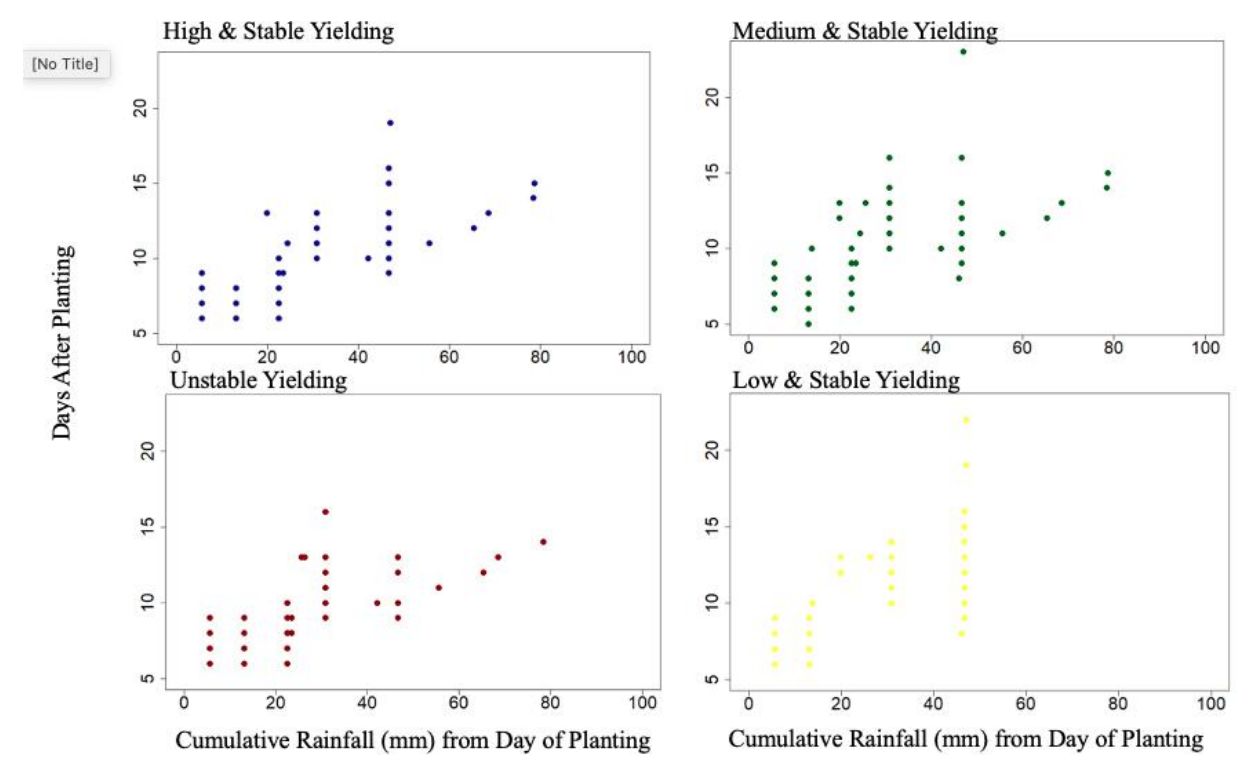


Figure 5. Cumulative rainfall and cumulative plants emerged by stability zone and field from 2016 to 2018



Figure 6. Stealth Cam image of emergence plot in field JS1 in 2017, the technique utilized in each emergence plot from 2016-2018, sizing four rows by two meters.

In 2016 and 2017, shortly after corn planting, high, medium, and low stable zones were first identified, and unstable yield zones based on historical yield considered, to establish two meters by four row plots (Figure 6) with three replicates in each of the yield stability zones totaling twelve plots per field (Basso et al., 2011) in two research fields per year. In 2018, twelve sampling plots were established based on the tactical N treatment they would receive (Basso et al., 2016) instead of yield stability zone. Plots were outlined by orange marking stakes and visited often during the May to October field season and together this totaled six field studies over three years (Table 1). The plot size allowed for up to 13 plants in each row, totaling a maximum of around 50 plants per plot. In 2016 and 2017, 'Stealth Cam' trail cameras were drilled to a post 5 rows in front of the plot. The stealth cams recorded one picture an hour from dawn to dusk and were used to gain emergence dates. Resolution of the 'Stealth Cam' was 16-22 MP and therefore it was not always possible to use the imagery to visually determine emergence. To aid in documenting emergence, white stakes labeled with the days after planting (DAP), or the number of days after planting until emergence, were set in the soil behind the plant on field visits and served as a ground truth aid.

Table 1. Description of field size and dominant soil type by study year from 2016 to 2018 field sites in Portland and Springport, MI.

Field	Study Year	Size (Hectares)	Dominant Soil Type
ZC1	2016	32	Parkhill loam
222	2016-2017	35	Riddles sandy loam
JS1	2017	34	Conover loam
105	2018	106	Riddles sandy loam
NC12	2018	28	Dryden sandy loam

Yield Stability Zone Creation

Yield will be further delineated for analysis by yield stability zones, created from yield monitor data collected from farmers (Maestrini and Basso, 2018). A map is created based on the spatial and temporal variability, first by normalizing the yield across all years of yield data in order for crop rotations to be considered in stability analysis, and establishing regions of variability, or high standard deviation of yield temporally (unstable zones or UN). Areas not considered unstable are classed as low, medium, or high and stable yield (LS, MS, and HS) (Basso et al., 2019).

Stealth Cam Imagery Analysis

The emergence dates were extracted by analyzing the Stealth Cam imagery using ESRI ArcGIS Image Analysis toolbox to emphasize green color and mark the locations of emerged plants, using a backwards time-lapse approach. This process was done manually, using circles marking the plant location from later dates when all plants had emerged and working backwards in time for each plant in each row, zone, and plot. In these years (2016-2017), all fields were planted within the same week, making it impossible to travel to every field every day to note emergence, hence the stealth cams assured emergence days were not missed. In 2018, the study fields were planted over a month apart, so stealth cams were excluded, and each field was visited once a day during the period of emergence to eliminate any possible error of image analysis.

Each plant within the plots was harvested at maturity and processed for dry biomass weight and nitrogen concentration of leaves and stalks, reproductive material (the tassel and husk), and ears. In 2016 and 2017, leaves and stalks biomass were grouped by row, while ears and reproductive material were grouped by early, medium and late emergence, retaining the yield zone and replicate. In 2018, while all ears were still harvested, only 15 to 16 whole plants from each plot

for leaves and stalks and reproductive material were harvested, selected randomly from emergence categories early, medium, and late.

Within-Row Plant Spacing Variability

Plant spacing between each plant within the plot was recorded by hand at several sample plots during 2016, and every sample plot in 2017 and 2018. Growing space (Martin, 2005) was calculated per plant (Equation 1) and used with grain yields and emergence dates to assess yield response. Plant populations between the Portland and Springport fields vary in row spacing and serve as another variable in growing space.

$$A_{i} = \left[\frac{d_{i} - d_{i-1}}{2} + \frac{d_{i+1} - d_{i}}{2}\right] x R \tag{1}$$

Where A_i is the growing space, R is the row spacing, and d_i , $d_{i+1} d_{i-1}$ represent the distances to the nearest plant on either side within-row, using cumulative distance measurements.

Processing Field Samples

In all years, each ear was counted once for width and five times for length, and then averaged for kernel number. In-season one meter squared destructive samples were taken four rows diagonal from each plot to examine biomass differences and N concentrations under different yield stabilities and N management, completed twice in 2016 and three times in 2017-2018. All biomass and grain were dried at 90 degrees C for 10 days. Biomass was weighed wet and ground using a woodchipper, and a subsample was weighed before and after drying in order to get whole plant dry weight and moisture. Grain was separated into early, medium and late

DAP by field, stability zone, treatment and replicate when grinding occurred totaling 60-70 groupings instead of grinding each plant individually, in order to have timely results for analysis.

Statistical Analysis

In all cases mixed model analysis was performed using replicate of field sample point as a random variable, considering categorial emergence and yield stability zone (YSZ), and where indicated, also considered growing space in R studio. Tukey's method is used to analyze mean separation between groups, performing pairwise comparisons to identify differences greater than the expected standard error. It is especially conservative when utilized with unequal sample sizes.

Results

Plant Emergence

DAP ranged from 5 to 23 days from 2016 to 2018. Each year, early, medium and late emergence was determined by field using quantile analysis (Table 2). Considering all study sites in the three years of study, emergence category showed a 22-gram decrease from early to late emergence and a 15-gram decrease in total kernel weight from early to medium emergence date, equivalent to 1,825and 1,149 kg/ha decrease in yield respectively when utilizing growing space calculated from equation 1. Emergence category showed a 77 total kernel decrease per plant from early to late emergence, and 49-kernel decrease from early to medium emergence. Significant differences were observed in the weight per kernel among early, medium and late emergence only up to the p<0.1 significance level (Figure 12) and hence was not further considered in analysis. Additionally, analysis of DAP and total nitrogen application for field 105 in 2018 that received differing amounts of N showed that total N application did not have a significant effect on the days after planting or the total grain weight or the weight per kernel,

while it did have a slightly significant effect on the amount of kernels per plant (p<.10). Further analysis showed no difference in total number of kernels per plant between the differing nitrogen applications when examining least squared means of total nitrogen applied separated by yield stability zone (Table 2). Because there was only one emergence plot with different total nitrogen application amount in field NC12, differences in yield between management zones were not

Year	Field	Categorical	Days after planting
		Emergence	
2016	ZC1	Early	[6,7)
		Medium	[7, 8)
		Late	[8, 13]
	222	Early	[6,7)
		Medium	[7, 8)
		Late	[8, 13]
2017	222	Early	[8,9]
		Medium	(9,10]
		Late	(10,25]
	SR2	Early	[6, 8]
		Medium	(8,10]
		Late	(10, 16]
	JS1	Early	[9,10]
		Medium	(10,11]
		Late	(11,22]
2018	NC12	Early	[8,10]
		Medium	(10,12]
		Late	(12,20]
	105	Early	[6,7]
		Medium	(7,13]
		Late	NA

considered. Differences among application types will be further discussed in Chapter 2.

Table 2. Delineation into early, medium and late emergence by field, year, and replicate of sampling point within each field.

Tillage and Days After Planting

Histograms for number of plants emerged for each day of emergence (Figure 7) showed a trend of increased number of plants emerging more quickly in a no-till management scheme than in a tilled field, even when tilling was conservative at four inches deep. This trend was observed in all stability zones but is arguably much weaker in the low and stable zones, which is likely due to other environmental factors such as poor soil quality, compaction at field edges, or water retention issues.

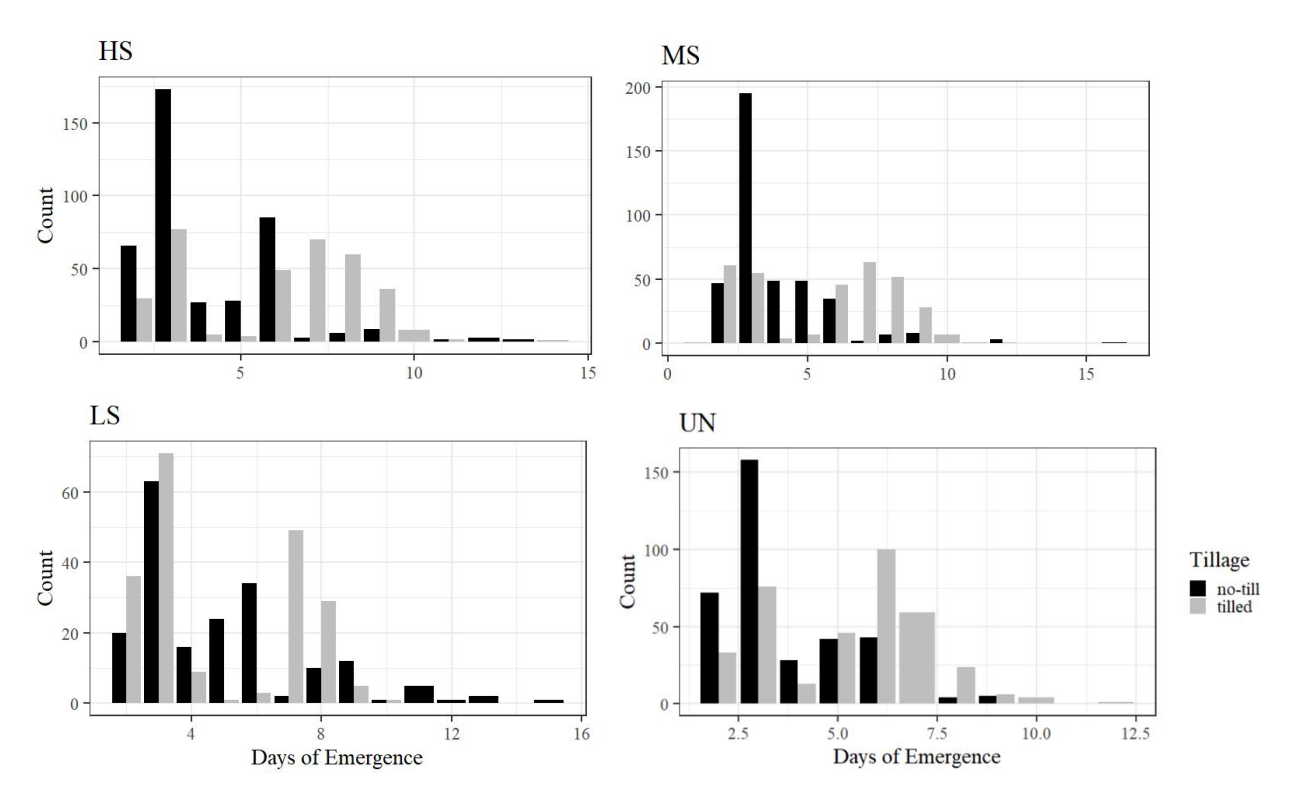


Figure 7. Showing emergence difference between no-till (darker shade) and tilled fields using data from 2016-2018, separated by yield stability zone.

Table 3. Output of field 105 in 2018 in which different emergence plots received differing nitrogen applications relating total kernel number per plant in comparison to the total amount of nitrogen applied and the yield stability zone.

Field	Yield Stability Zone	Total Nitrogen Applied (kg/ha)	Kernel Number per Plant
105	HS	145.73	455.7 a
		173.6	517.0 a
		192.8	486.6 a
	MS	145.73	468.7 a
		173.6	492.8 a

	181.6	468.4 a
UN	145.73	481.1 <i>a</i>
	173.6	479.0 a
	192.8	540.3 a

Uniformity of Stand Among Yield Stability Zones

All yield stability zones experienced variability in dates of emergence, but the unstable zone experienced the least variability among all groups, followed by the high and stable yielding zone (Figure 8 and 9). Plants in zones established as high yielding and unstable areas of the field emerged more quickly and had higher plant counts in four out of six study fields, while in the medium and low yielding zones, more variability was shown in DAP (Figure 10 and 11). Plants in the medium and low stable zones were more susceptible to skips in planting or plants that did not emerge. The medium categorical emergence contained the highest number of emerged plants (1123), followed by early (1086) and late (369). Over 800 of the total plants (2578) emerged in 7 days. Unstable zones saw the most plants emerge early categorically and had the least number of plants emerge late amongst all study years. This result shows the importance of delineating by stability zones and by year, and considering other environmental factors such as soil moisture, texture, and topography in explaining the differences within a single field.

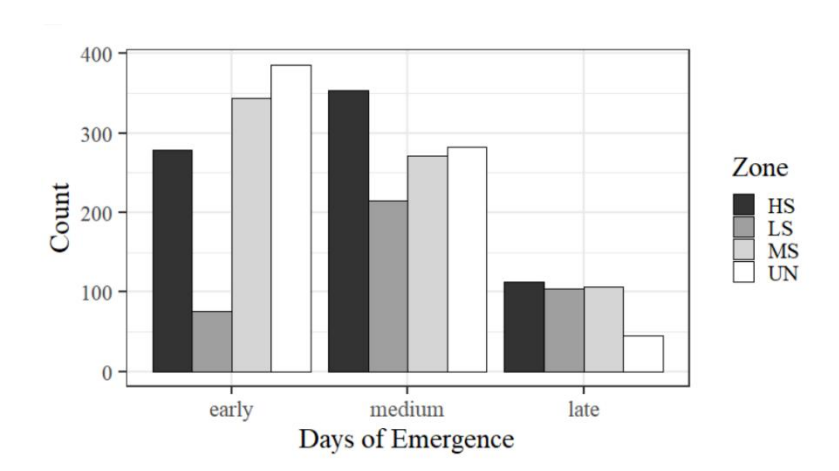
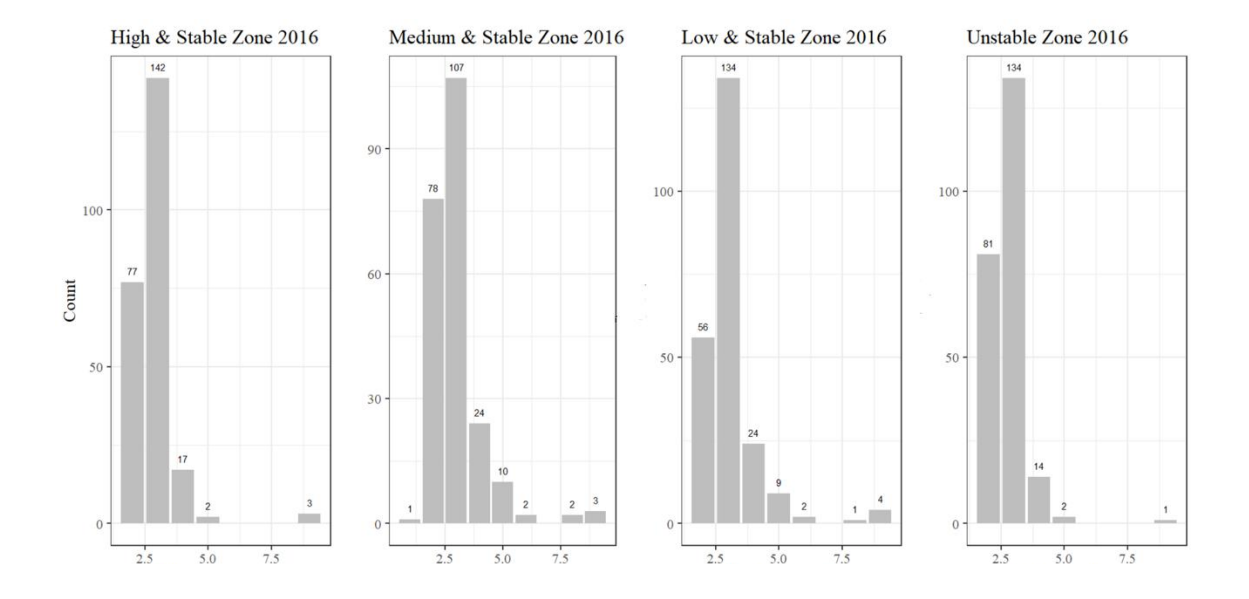


Figure 8. Frequency diagram of the amount of corn plants emerged by yield stability zone and categorical emergence of early, medium, and late. Categorical emergence was determined each year for each field using quartiles.



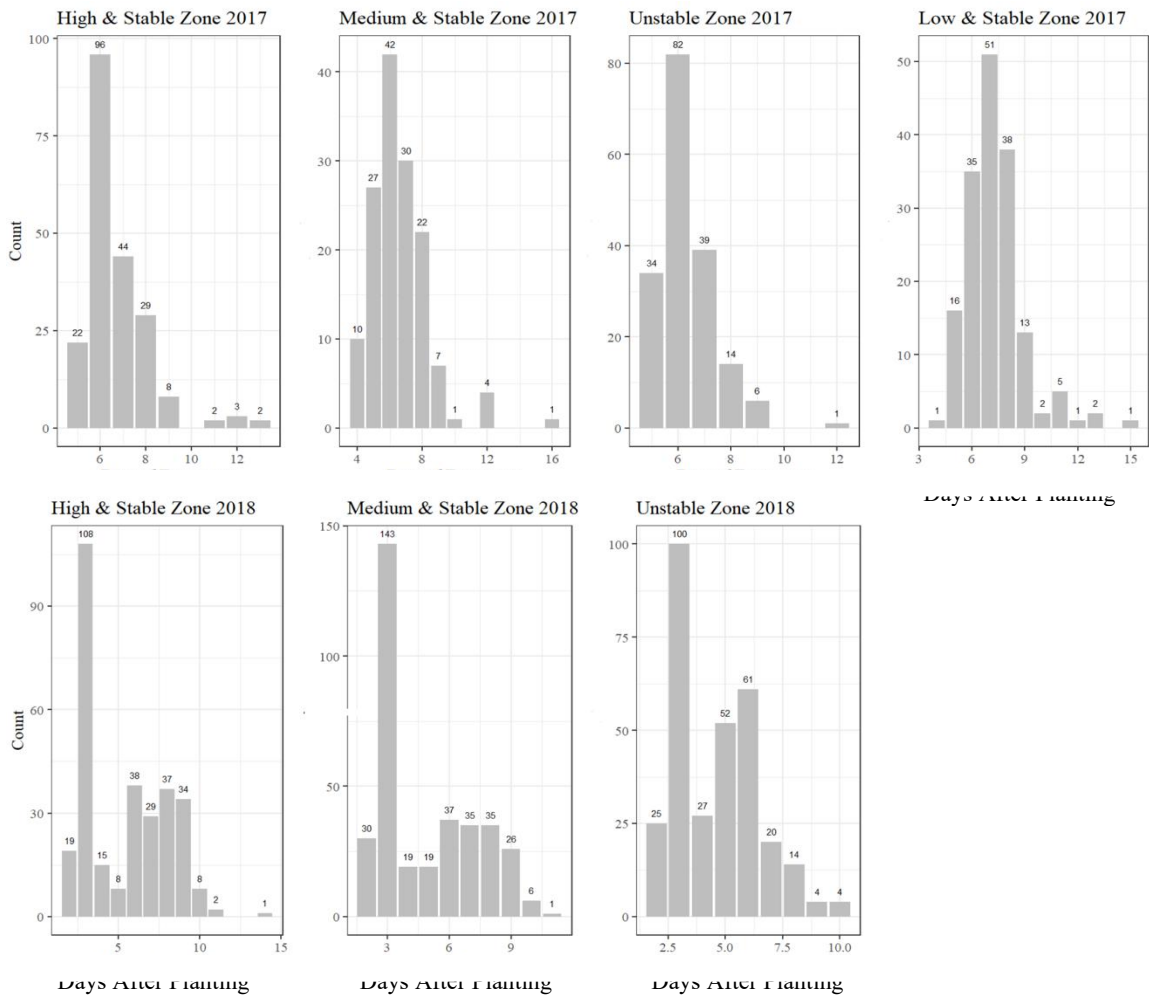


Figure 9. Frequency diagrams of emergence days by year and stability zone, where each plot shows the two study sites utilized for emergence studies in the given year.

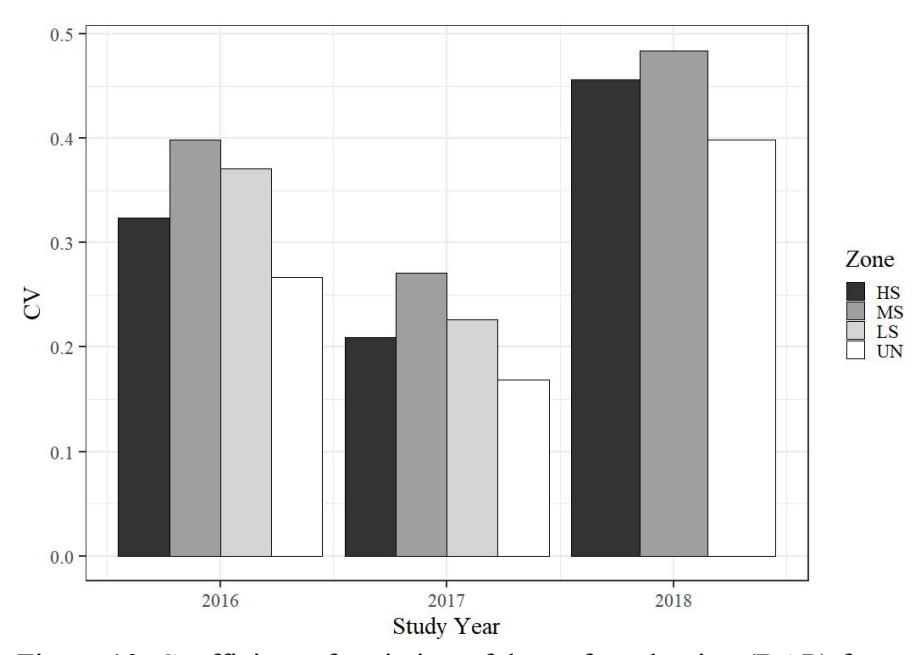


Figure 10. Coefficient of variation of days after planting (DAP) for each study year by stability zone

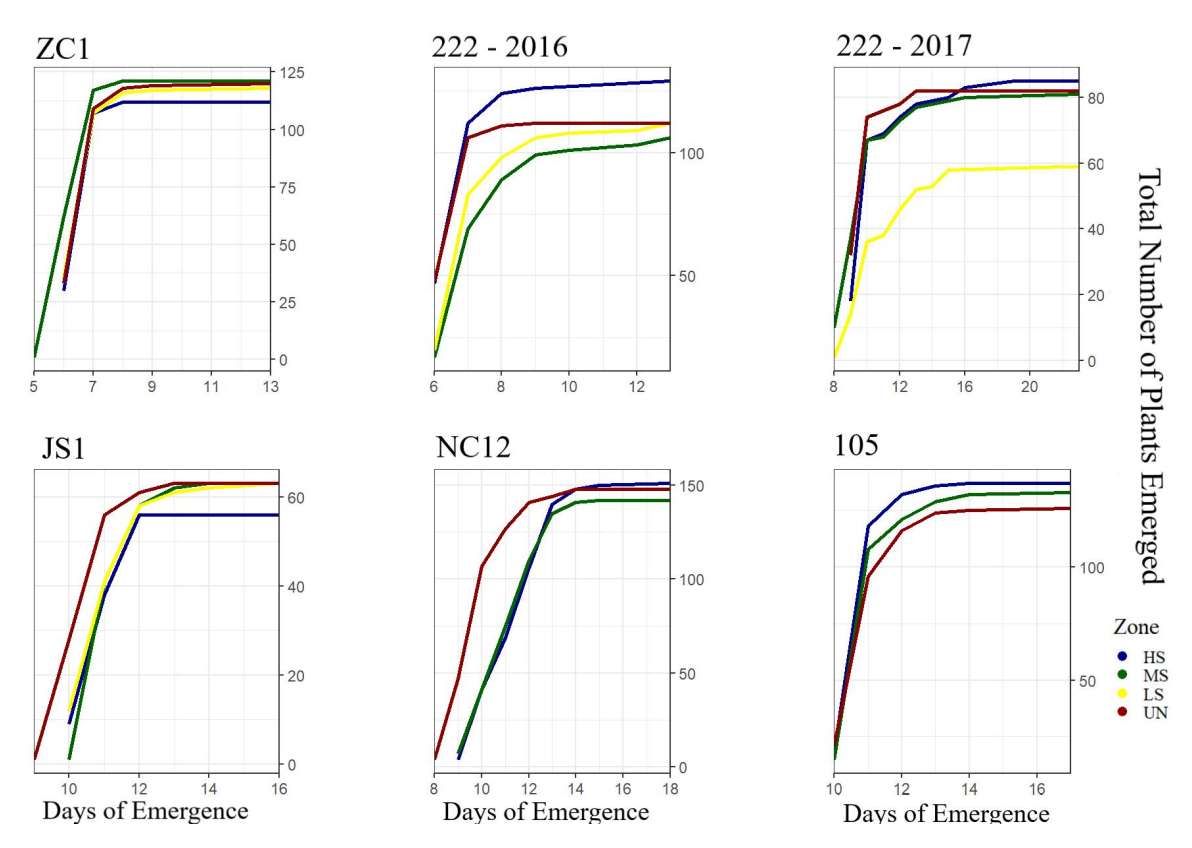


Figure 11. Illustrating the accumulation of emerged plants in all plots at each study site by stability zone. Some study plots were randomly excluded to have an equal number of plots in each stability zone, and hence comparison between the plots is not encouraged.

Kernel data confirmed the results of previous studies (Pommel et al., 2002; Hodgen, 2007) that with an increase in DAP, there is a significant negative response of number of kernels and total grain weight, and an insignificant difference in weight per kernel contributing to yield loss (Figure 12a-c). Mixed model analysis considering yield stability zone, growing space and categorical emergence (E, M, L) showed no significant difference in weight per kernel between emergence category, while showing slight significance in differences in weight per kernel between stability zones (Figure 12 and 13). In most field sites, high yielding zones experienced the highest number of kernels and total grain weight amongst all stability zones, following by unstable, medium and stable, and low and stable zones respectively. Unstable areas showed higher kernel numbers and total grain weight in several field sites, which is likely to have occurred due to differences in rainfall and topography. Each stability zone response was significantly less than high and stable yielding zones in kernel weight and total kernel weight except for total kernel weight in the unstable zone.

Considering all study fields and study years, mixed model analysis of stability zone with replicate as a random variable indicated significant differences between all stability zones besides high stable and unstable. There was a 12.7-gram decrease per plant in total kernel weight (1,053 kg/ha) from HS to MS and a 19.9-gram decrease in total kernel weight (1,651 kg/ha) from HS to LS with a mean total kernel weight in HS of 135 (11,203 kg/ha) (Figure 12, Table 4). This difference between stability zones was also reflected in kernel number, showing a decrease of 22 kernels from HS to MS, and 69 kernels from HS to LS, with a mean kernel number in HS of 471. Per field analysis showed similar differences between stability zone and between emergence category (Figure 13, Table 5).

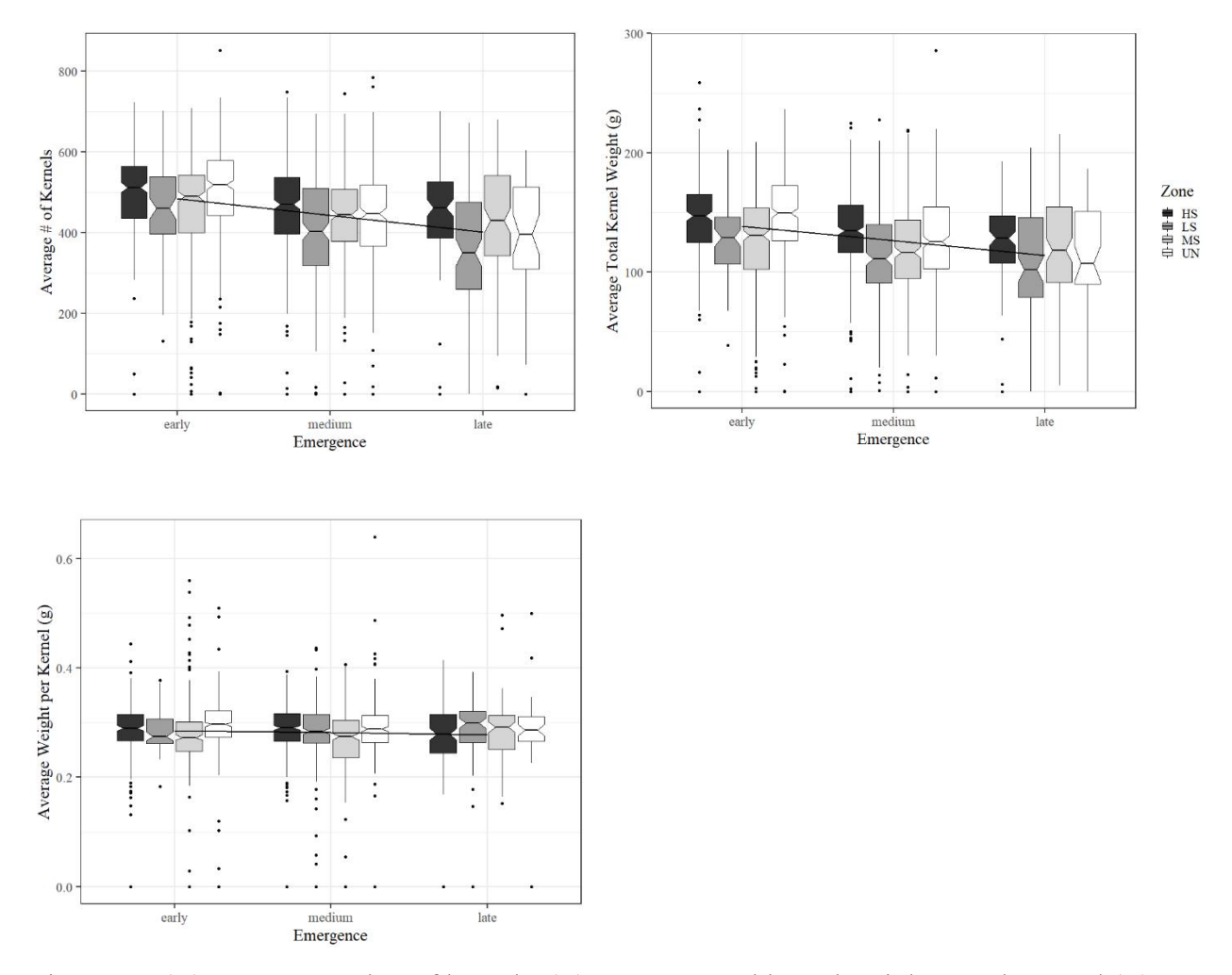


Figure 12. (A) average number of kernels, (B) Average total kernel weight per plant, and (C) Average weight per kernel by plant, for each emergence category grouped by yield zones.

a.

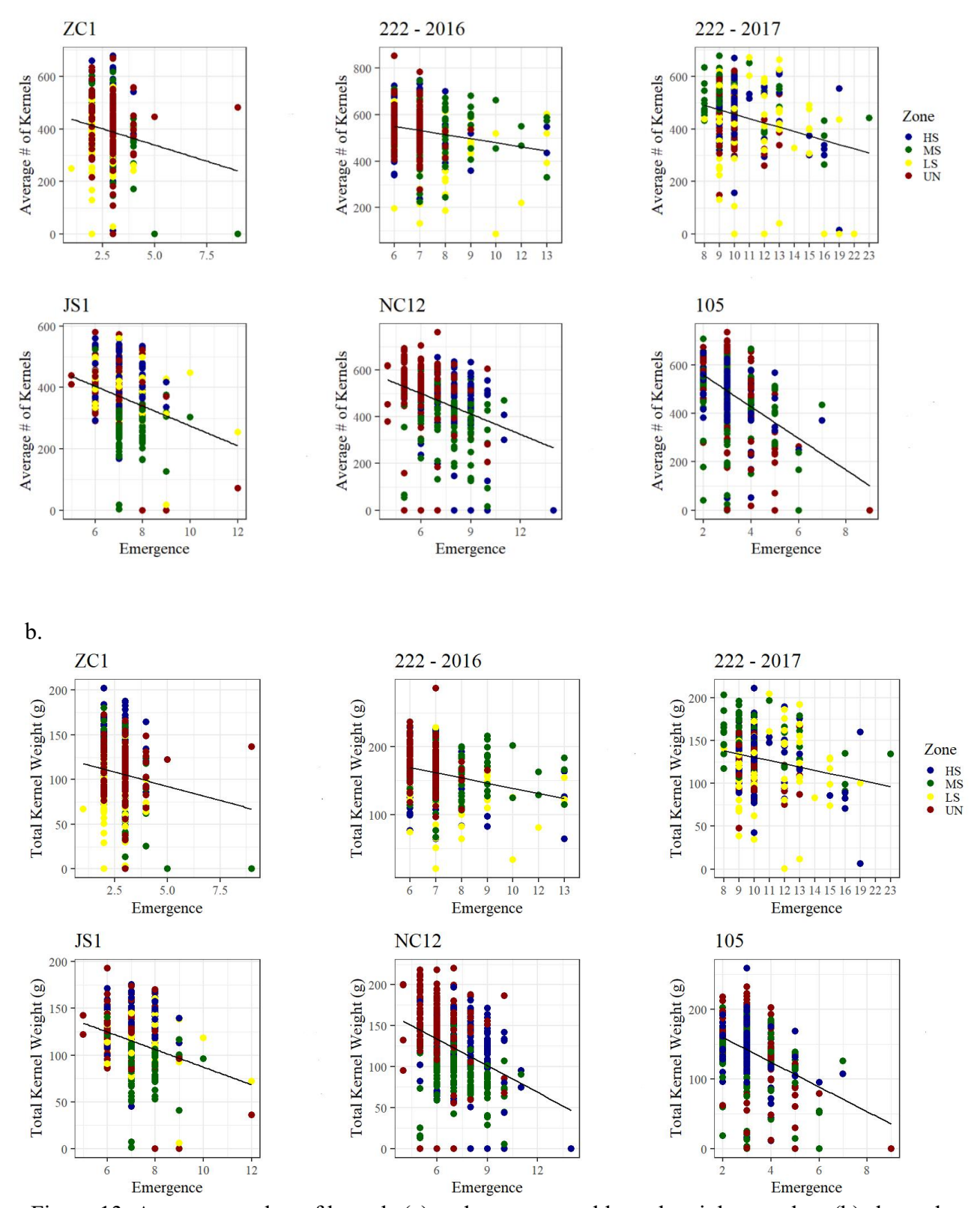


Figure 13. Average number of kernels (a) and average total kernel weight per plant (b) shown by

days after planting and separated by yield stability zone. Each plot represents a different study site and includes all of the emergence plots at the site.

Table 4. Analysis considering all fields in one mixed model $kernel\ weight = DOE + Zone + growing\ space + DOE:Zone:growingspace$ with replicate as the random variable. Letter separation was performed using Tukey's test of mean separation calculated by zone.

Emergence	YSZ	EMMEAN	Standard Error	LSD (TUKEY)
	UN	149.12	2.82	A
Early	HS	137.58	3.35	В
Larry	MS	132.00	2.98	В
	LS	104.89	8.72	С
	UN	125.18	3.46	AB
Medium	HS	130.34	3.11	A
Wicaram	MS	115.48	3.30	В
	LS	101.71	4.43	С
	UN	112.66	7.59	BC
Late	HS	123.12	4.66	В
Luic	MS	104.78	4.80	С
	LS	93.47	4.91	С

Table 5. Anova table by each field in each year of study. Letter separation was performed using Tukey's test of mean separation calculated by zone in the mixed model y = DOE + Zone + DOE:Zone:growingspace with replicate as the random variable.

Field	P value	R2	Emergence	UN	HS	MS	LS
105	DAP: 7.3 e -13	.12	Early	152.7 a	150.0 a	136.6 a	NA
(2018)	Zone: 0.002		Medium	115.8 <i>b</i>	104.0 <i>b</i>	113.1 <i>b</i>	NA
	DAP: Zone: 0.17		Late	NA	NA	NA	NA
NC12	DAP: .0007	.40	Early	160.0 a	113.7 a	98.5 a	NA
(2018)	Zone: $< 2.2 \text{ e} - 16$		Medium	145.5 ab	124.1 <i>a</i>	97.4 a	NA
	DAP: Zone: 0.05		Late	125.4 <i>b</i>	110.0 a	77.8 b	NA
JS1	DAP: 0.002	.40	Early	125.6 a	136.5 a	132.7 a	120.3 a
(2017)	Zone: <2.2 e -16		Medium	118.6 a	137.0 a	123.5 a	84.8 <i>b</i>
	DAP: Zone: 0.02		Late	96.8 <i>b</i>	139.4 a	113.8 a	86.1 <i>b</i>
222	DAP: 0.15	.17	Early	123.7 a	131.4 <i>a</i>	158.9 a	109.4 a
(2017)	Zone: 5.7 e -12		Medium	120.9 a	131.6 a	143.9 a	117.2 a
	DAP: Zone: 0.08		Late	106.2 a	117.3 a	139.6 a	122.0 a
222	DAP: 9.1 e -6	.10	Early	179.2 a	168.7 a	172.4 <i>a</i>	162.2 <i>a</i>
(2016)	Zone: 0.0002		Medium	164.2 <i>a</i>	163.0 ab	162.0 a	152.8 a
	DAP: Zone: 0.656		Late	153.4 <i>a</i>	142.5 b	158.5 a	132.1 <i>b</i>
ZC1	DAP: 5.4 e -5	.19	Early	115.7 a	140.8 a	89.9 a	123.0 a
(2016)	Zone: <2.2 e -16		Medium	102.4 <i>a</i>	121.3 <i>b</i>	92.9 a	100.4 <i>b</i>
	DAP: Zone: 0.003		Late	110.1 a	126.9 <i>ab</i>	78.4 <i>a</i>	68.5 c

Plant Spacing Variability

The highest value of plant space was observed in the low and stable zone, most likely due to skips or unmerged plants, and unfavorable soil conditions (Table 6). High and stable and unstable zones saw the smallest values of growing space. Similar mixed model analysis was performed, considering growing space and yield stability zone and their interaction, along with replicate as a random variable to predict total grain weight per plant (Table 7). Analysis of each field showed significant differences in kernel weights in all fields except field NC12, which was

only significant to p<0.1. Yield stability zone was significant in all cases, while the interaction between growing space and yield stability zone was not significant in any field.

When plant space was considered for all study sites with DAP and yield stability zone, 22.9% of the variation of total kernel weight and 18.6% of total kernel number was explained. A decrease of 56 kernels per ear from early to medium emergence and a decrease of 94 kernels from early to late emergence, and an 18- and 29-gram (1,493 kg/ha and 2,406 kg/ha) decrease in total grain weight per plant from early to medium and late emergence, respectively was observed.

There was a decreasing trend in grain yield among the low and stable yielding zone in 2017 and 2018 as the standard deviation increases. Variability was separately assessed with coefficient of variation (Figure 14 and 15) and point yield calculated over a two meter transect. Much of the variation is observed in the low and stable yielding zone, demonstrating that these areas are often affected by skips and plants that do not emerge, and are typically attributed to environmental factors such as soil type or water availability.

When viewing CV for all fields, point yield evaluated over a transect declines as CV increases, whereas total kernel weight per plant increases as growing space per plant increases (Figure 16). This supports the idea that compensatory growth can often makeup for skips, but that excessive variability over an area (large gaps or skips over a transect), in this case a 2 meter transect of a row, cannot be fully compensated for and can result in decrease of yield.

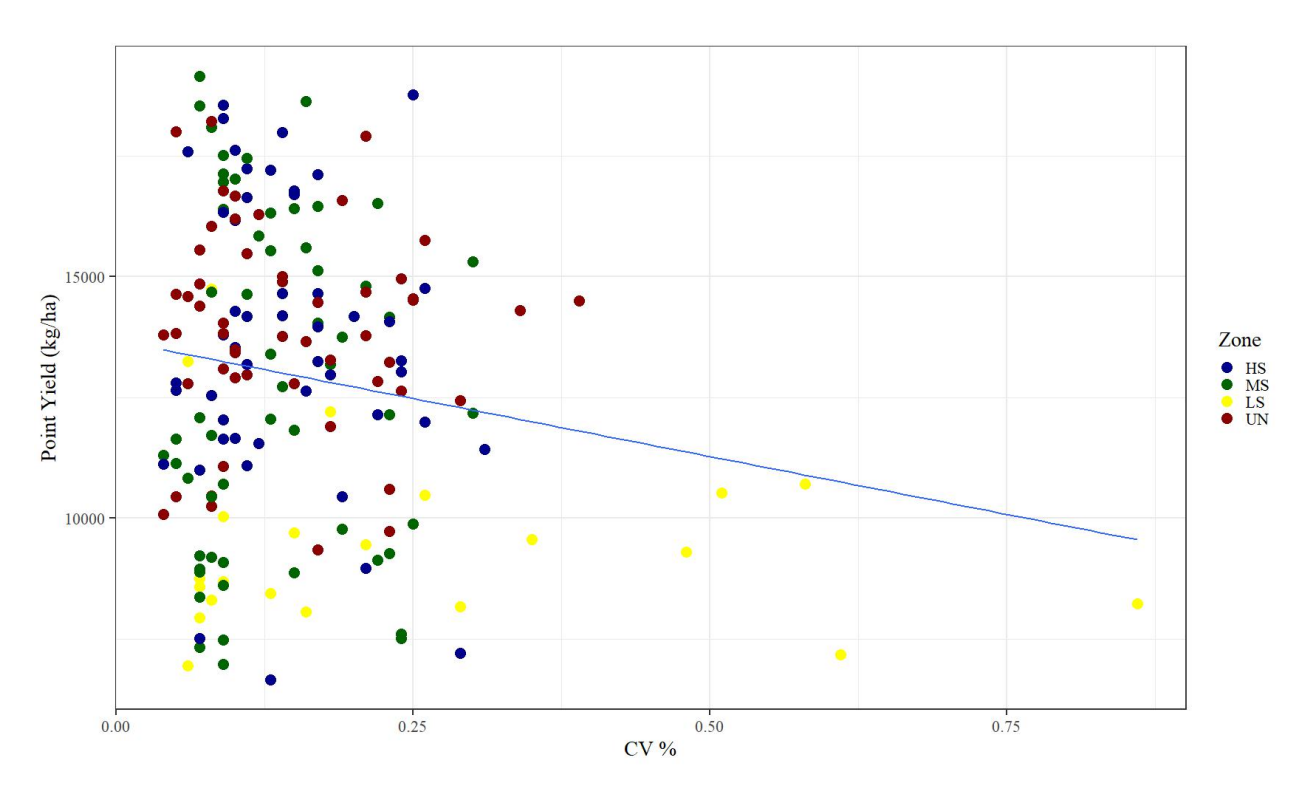


Figure 14. Coefficient of variation of growing space using equation 1 is shown versus the point yield (calculated using row spacing and plants per hectare calculations from number of plants within the sample plot) and grams of grain per plant, and converted to kilograms per hectare, and grouped by stability zone.

Table 6. The growing space is calculated by stability zone, and shown with standard error, and Tukey's mean separation performed to visualize any statistically significant differences of growing space between stability zones. This incorporated all study sites and all years of study

Zone	Growing Space (cm ²)	SE	Tukey Mean Separation
HS	1159.9	18.6	A
UN	1193.3	18.1	AB
MS	1231.58	17.9	В
LS	1343.1	31.0	С

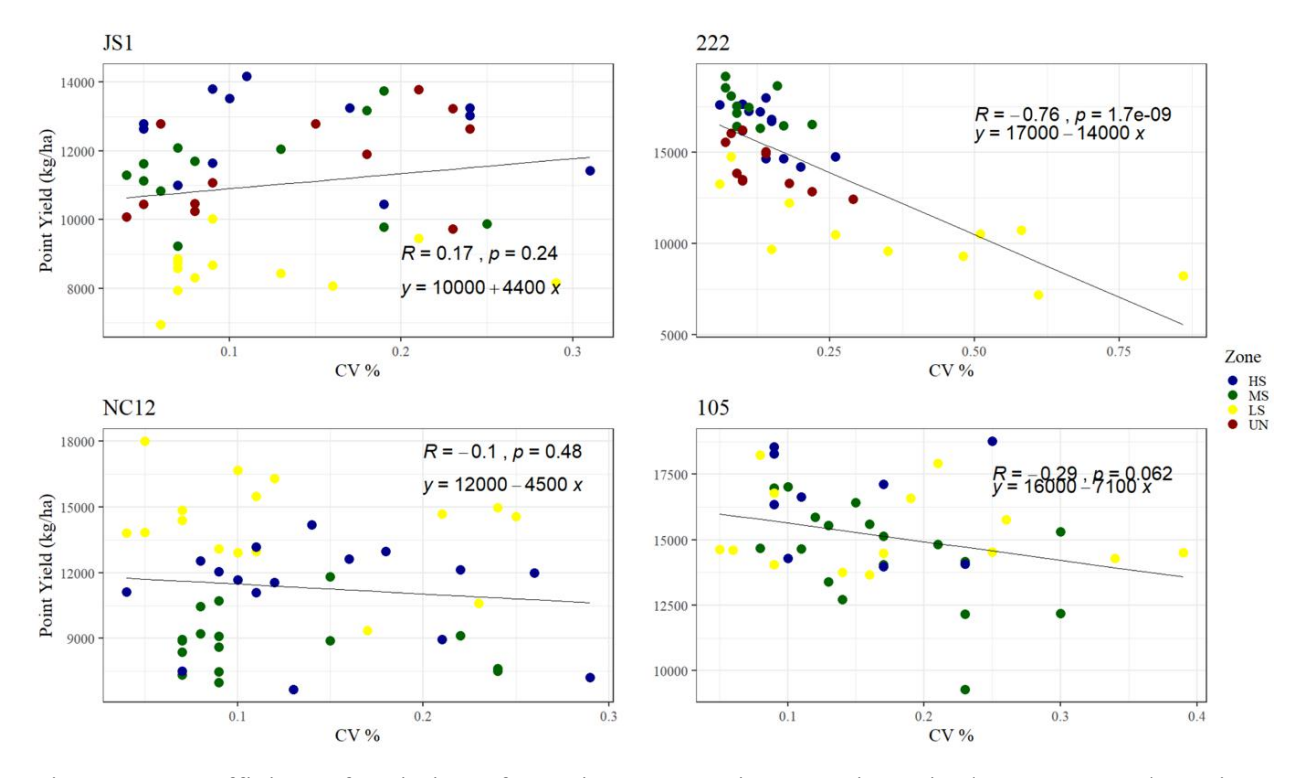


Figure 15. Coefficient of variation of growing space using equation 1 is shown versus the point yield (calculated using row spacing and plants per hectare calculations from number of plants within the sample plot) and grams of grain per plant, and converted to kilograms per hectare, and grouped by stability zone and separated by field with regression equation and coefficient of determination.

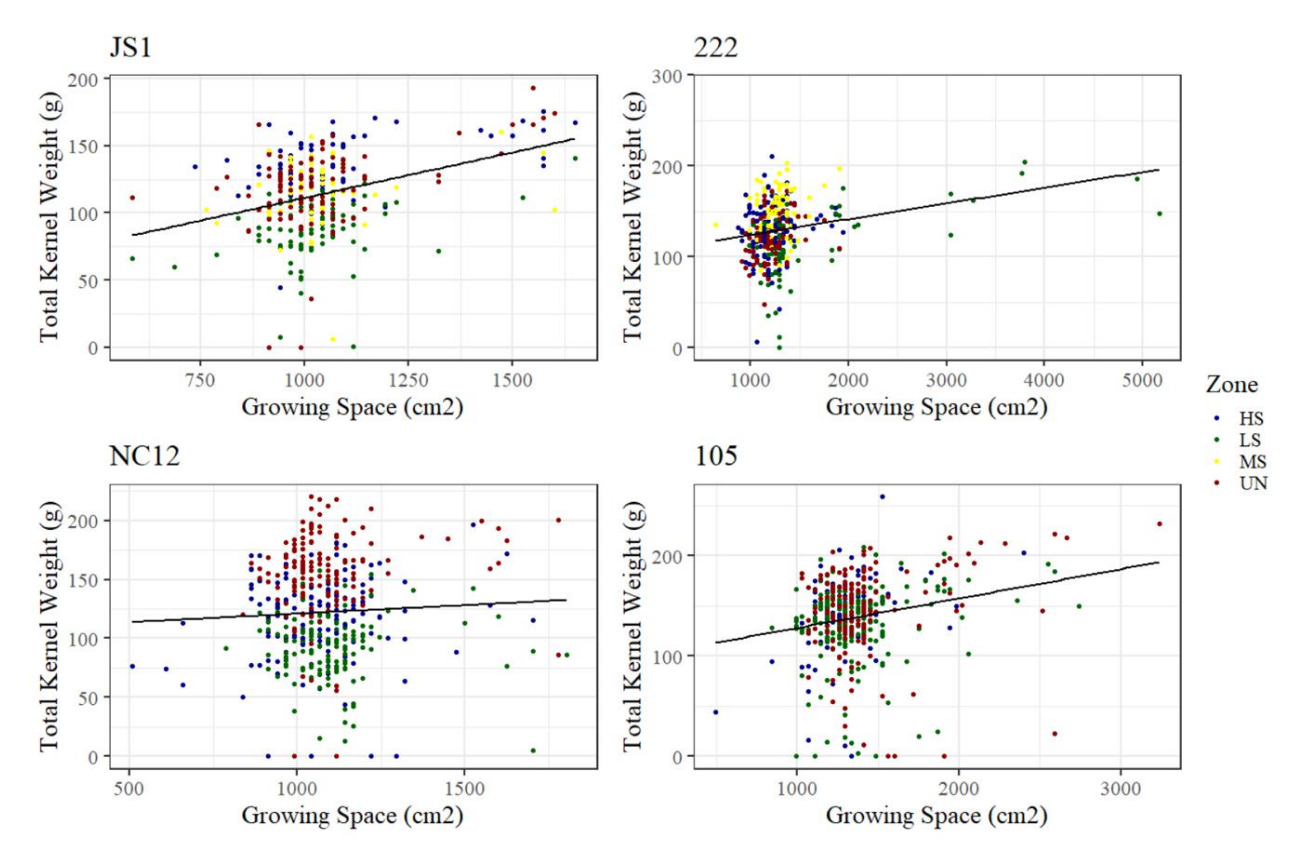


Figure 16. Utilizing by-plant grain weights to examine growing space (in square centimeters) vs the total kernel weight per plant in grams. Performed by field and separated by stability zone by color.

Table 7. ANOVA Table of predicting total grain weight using growing space, yield stability zone and their interaction.

Field	Factor	P value
105	Growing space (cm2)	3.871 e ⁻⁶
	Yield Stability Zone	0.007
	Growing space*Zone	0.085
NC12	Growing space (cm2)	0.081
	Yield Stability Zone	$< 2.00 e^{-16}$
	Growing space*Zone	0.236
JS1	Growing space (cm2)	2.458 e ⁻¹¹
	Yield Stability Zone	$< 2.2 e^{-16}$
	Growing space*Zone	0.2431
222	Growing space (cm2)	2.043 e ⁻¹¹
	Yield Stability Zone	< 2.2 e ⁻¹⁶
	Growing space*Zone	0.715

Discussion

Yield losses were observed from delayed emergence, and stability zone was an influential factor shown to behave similarly in each field. In all cases, high and stable yielding zones had higher yields than medium and low stable zones, while unstable varied by year and study site.

The low and stable zone saw the highest variability in days after planting and had the least amount of plants emerge of all stability groups.

Growing space was shown to be less influential on yield than yield stability zone. When analyzing by field, there was no clear trend between growing space and point yield, whereas considering all fields showed a decreasing trend of point yield as coefficient of variation increases. In each study site, an increase of growing space corresponded with an increase in total grain weight per plant.

More investigation behind the biological and physical mechanisms behind delayed plant emergence is required to fully quantify the importance of environmental factors to decreased yield shown from delayed emergence. The pattern between high and stable yield producing higher plant populations, higher, yields, and less DAP is likely sourced from a combination of topography, soil characteristics such as texture, microbiology, and porosity, and presence of organic matter. Evaluating the effects of natural delayed emergence versus emergence differences due to later planting dates can signify the environmental impacts on yield without using time as a control. The identification of the most important environmental factors affecting delayed emergence could be used to increase uniformity of plant stands and produce higher grain yields.

CHAPTER III: Spatial and Temporal Analysis of Nitrogen Use Efficiency Using Remotely Sensed Imagery and Crop Modeling

Introduction

The high mobility of Nitrogen (N) can lead to negative environmental effects, therefore, containing it within croplands is a major challenge in sustainable agriculture. Much of the nitrogen applied on farms is not utilized by the plants and is instead deposited to the environment through the air or water (Cassman et al., 2002; Basso et al., 2019, Basso and Antle, 2020) (Figure 17). Excessive application of nitrogen fertilizers causes release of N₂O to the atmosphere through oxidation of organic matter within the soil (denitrification), which contributes to greenhouses gas concentrations in the atmosphere. This process is one of the main concerns of large agricultural production, as N₂O is approximately 300 times more efficient at heating the Earth's atmosphere than CO₂ and a majority of N₂O emissions are generated by agriculture (Robertson and Vitousek, 2009; Robertson, 2014). An additional concern is nitrate leaching within the soil, which pollutes groundwater and surface water and depletes the nutrients in the soil, creating the need for further fertilization. This problem is of particular concern for humid areas such as Canada and the United States or areas that are not water limited, as leaching is a function of both NO₃⁻ in the soil and the rate of soil water drainage (Drury et al., 2014). Drainage is naturally related to soil texture, but tile drainage systems are often installed beneath the soil surface to remove surplus water in a controlled manner. Although considered a positive management tactic for water use efficiency, tile drainage can also allow for buildup of excess nutrients in nearby ditches (Drury et al., 1996). Leaching not only affects soil health but human health, as high levels of NO₃ in drinking water have been linked to cancer and blue baby syndrome (Basso and Ritchie, 2005; Knobeloch et al., 2000)). When groundwater or runoff

saturated with NO₃⁻ reaches surface water, it can cause ecologically damaging algae blooms in lakes or it can be transported through rivers to the ocean. As an abundance of inorganic nitrogen reaches lakes and rivers, algae blooms can create zones of oxygen depletion ("dead zones") that have been measured to be as large as 20,000 km² (Robertson and Vitousek, 2009).

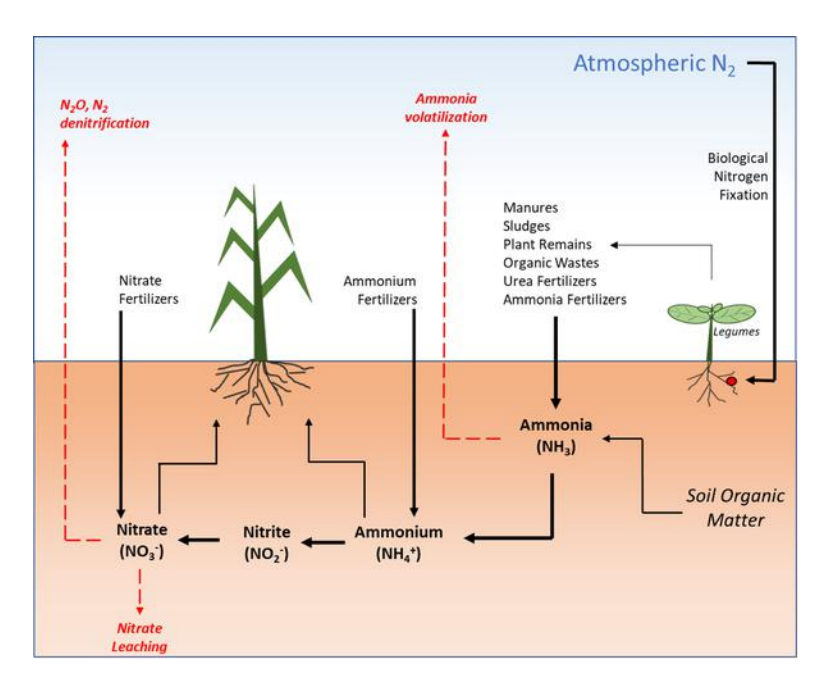


Figure 17. The nitrogen cycle pertaining to agricultural sources of fertilizer, and its effects on the atmosphere, surface water and ground water from North Carolina State Extension

Overview of Remotely Sensed Imagery and Nitrogen

While direct sampling techniques have been used to assess the nitrogen status of a field, the newest techniques involve remote sensing. Handheld and airborne sensors evaluate electromagnetic radiation, which reflects relative pigment levels (mainly chlorophyll) at certain wavelengths. The reflectance serves as an indicator of areas that suffer from nitrogen deficiency and can help develop "prescription" variable application plans to target these areas (Mulla, 2013). First developed in the 1990's, the Soil Plant Analysis Development (SPAD)-502 handheld meter is sensitive to chlorophyll content but requires labor intensive forms of measurement. SPAD

measurements were shown to correlate with level of nitrogen fertilization and used to detect nitrogen stress as early as 1992. While useful for relative plant health, SPAD reflectance values are not directly indicative of plant nutrient needs and cannot be used to decide the amount of nitrogen to apply.

The further development of accessible remote sensing technologies, from single band sensor data for sensing chlorophyll levels to multispectral and hyperspectral imagery capable of revealing many parameters of crop health, has allowed for an incredible increase in the degree to which researchers and farmers can monitor crops. The capacity of sensors today allows for high-resolution data collection and evaluation of nitrogen status; however, these crucial developments are still subject to limitations. Currently, the most severe limitation is that remote sensing data does not automatically produce a nitrogen prescription, thus a large amount of processing and estimation is required. The creation of vegetation indices such as Normalized Difference Vegetation Index (NDVI) from manipulation of the spectral bands can reveal relative plant health information but cannot be directly translated to nitrogen deficiency information without the examination of other possible deficiencies (Tucker, 1979). Combating these limitations by developing a better understanding of the crop-nitrogen relationship and obviating the need for reference strips will be key in the development of future sensor technologies and the management that follows.

Spectral Reflectance and Plant Health

Alongside remotely sensed imagery, handheld chlorophyll meters such as the SPAD have long since been used to attempt to quantify nitrogen application needs. Raun et al., (2001) found that variable nitrogen management should be managed at one-meter squared increments, attainable through a handheld optical sensor used to create a response index which increased

NUE (Nitrogen Use Efficiency) in their study by fifteen percent. J. A. Hawkins et al., (2007) attempted to quantify a relationship between chlorophyll meter values with the difference in nitrogen application from the optimum nitrogen rate with coefficient of determination values as high as 0.76 using relative chlorophyll measurements calculated by normalizing from the mean chlorophyll value in the area of the field with the highest nitrogen application rate. Argenta et al., (2007) confirmed the results of previous studies that the relationship between final yield and chlorophyll content is most variable at early stages of corn growth, and more predictive in later stages, around growth stage V10 or V11. This could be problematic in using chlorophyll content to infer nitrogen application due to the necessity of applying nitrogen before this relationship can be formed. Even so, this relationship paired with whole field remotely sensed imagery can be key to establishing a variable late side-dress. The downfall of handheld chlorophyll meters is the labor-intensive field sampling that accompanies it. To get a representative measurement across a field, many measurements must be taken not only across space but in the same area as well, as the variability in a single location can be extremely high. Similarly, handheld meters suffer from the limitation as remotely sensed imagery, as measurements cannot be translated into nitrogen application needed.

Since the adoption of the use of remotely sensed imagery to analyze crop health, many relationships have emerged between reflectance at many different wavelengths and crop nitrogen status, aided by destructive sampling. Chlorophyll content has also been examined remotely with the creation of Canopy Chlorophyll Content Index (CCCI), which is calculated from the red edge portion of the spectrum, from 680 to 750 nm where there is rapid change in reflectance values (Fritzgerald et al 2007). Basso et al., 2016 recorded change in reflectance before and after variable nitrogen application, with the highest correlation between nitrogen applied and index

value being the CCCI index combined with NDVI, as well as the second highest significance level (p=.007) in analysis of variance (ANOVA) results out of 19 vegetation indices. Rodriguez et al., 2006 takes another approach of CCCI calculation for assessment of wheat fertilization by normalizing to biomass accumulation to account for dilution of remotely sensed imagery. Using planar domain concepts to create CCCI from the upper and lower bounds of the NDRE to NDVI and Nitrogen Stress Index (NSI) from the relationship between nitrogen concentrations in biomass to dry weight of the biomass, CCCI explained 68 percent of the variation in nitrogen stress. This study highlighted an important limitation of direct correlation of nitrogen with reflectance, as water content and soil reflectance are not accounted for in the creation of indices and must be realized when comparing between early growing stages when much soil is visible between rows in remotely sensed imagery. One solution to this is the Excessive Greenness (ExG) index (Woebbecke et al., 1995), which emphasizes the green band from RGB (Red Green Blue) imagery to emphasize areas of higher biomass and can be used to separate green pixels from pixels with absence of green. Ponti (2013) used a combination of segmentation using mean-shift and the ExG index to eliminate errors within the imagery such as shadows from variable weather conditions. Mean-shift uses a kernel density function to classify similar pixels, locating local maxima. This combination showed the highest accuracy out of four indices tested with and without mean shift, increasing the visibility of possible nutrition deficiency within the imagery. Schlemmer et al., (2013) found a relationship with an R2 value as high as 0.74 between leaf nitrogen content and the red-edge chlorophyll index, as well as a 0.94 R² value between chlorophyll content and this index. This study utilized an index relating Near Infrared (NIR) and red-edge, with formula (NIR/Red Ege)-1 that was created by Gitelson et al., (2005). Measurements in this study were captured with a mounted sensor one meter above the canopy,

which were then destructively sampled at the same resolution. This labor-intensive practice, like many other studies that show high correlation between nitrogen status and reflectance values, shows promising results, yet is limited by time-intensive measurements.

The red band of RGB imagery (650 nm) has been highly utilized in crop health detection, and is negatively correlated with nitrogen concentration, or photosynthesis, as the higher red reflectance level shows the amount of light not absorbed by the canopy. NDVI, which utilizes near infrared and red reflectance values, is shown to be positively correlated with photosynthesis, and hence is one of the most popular indices to identify crop health. Maestrini and Basso (2018) confirmed this positive correlation in a big data study over much of the Midwest, analyzing the seasonal time when the NDVI values are most indicative of historical crop yield. Results showed that the last week of July to the first week of August showed the highest correlation to final yield. The study indicated that in stable yielding zones in maize fields and the combination of stable and unstable yielding zones, historical yield is the highest indicator of final yield in comparison to the significance of NDVI, whereas solely in unstable yielding zones of the field, NDVI of late July showed to be most indicative of final yield.

Like NDVI, Green Normalized Difference Vegetation Index (GNDVI) is indicative of biomass accumulation, utilizing the green band instead of the red band with the near infrared band. Shanahan, et al., 2001 showed GNDVI to be more significant than NDVI in predicting grain yield utilizing digital imagery converted to reflectance, most especially during grain fill, when NDVI becomes saturated at high values. This is said to be true due to the sensitivity of green band to changes in chlorophyll, which is said to be higher than the red band at high LAI values (Gitelson et al., 1996).

Each spectral band can indicate an aspect of crop health, and there is extensive research in the uses of each. Utilizing this research with simulation crop models allows for informed, inseason decision making for crop management backed by current remotely sensed imagery and years of weather, crop and soil data allowing for initialization of model simulation. The future of this research is to move towards larger scale detection of plant health, i.e. by-field detection using remotely sensed imagery without the need for destructive sampling, using relationships established in literature and knowledge gained from previous extensive destructive sampling to detect nitrogen.

Crop Modeling Integration

Many process-based crop models exist in agricultural research, and serve as an important tool to estimate yield effects in response to varying weather and crop conditions, even in areas where there has been no prior research. These models give the ability to simulate greenhouse gas emissions, water use, nitrogen uptake and leaching, soil carbon and nitrogen, and more (Jones et al., 2017). Using multiple management and weather scenarios, best management practices can be identified to maximize yield and limit overfertilization. This will become increasingly important as increased cases of extreme weather are expected with climatic changes in the near future (IPCC, 2014).

Basso et al., (2011) introduced the idea of utilizing crop simulation model to select optimal nitrogen application rates using decades of weather and yield data for a strategical approach and the current conditions of the experiment year for a tactical approach. Optimal rates were then chosen using criteria of yield response to fertilization, the marginal net return and the amount of N leached. Considering these criteria allows for analysis of the environmental and economic effects of differed nitrogen fertilization amounts. Results showed that the optimal

economic rate was a lessened rate than the traditional, uniform N rate. The interdisciplinary work of utilizing remotely sensed imagery with crop modelling to select nitrogen application rates is strongly adopted in industry, while less adopted in the research. Many companies provide prescription services using satellite imagery data, and how these rates are established remains proprietary. While businesses providing these services are important to the advancement of precision agriculture, more research is needed to connect the link between spectral reflectance and optimal nitrogen application for yield and profit. Creating an industry where these methods are well-researched and demonstrated through field-scale research is crucial for precision nitrogen application adoption.

Precision Nitrogen Management Adoption

Adoption of precision agriculture has been attributed to the farm size, income, education level, familiarity and access of technology, and location of the farmer (Pierpaoli et al., 2013). The most important component of consideration for adoption of precision N management for a farmer is the economic gain, whether it is gained from increased yield, hypothetical incentives for environmental consideration, or the costs saved from a decrease in amount of fertilizer purchased over time (Basso and Antle, 2020). This economic gain is also challenged by the initial costs of technology necessary to adopt precision N practices, and the lack of ease of use of existing technologies. To make sustainable nitrogen management informed by remotely sensed imagery a common norm, the ease of use needs to be improved and made less expensive.

Farmers' collaborating with research universities has been a valuable relationship in which the advantages of precision N management can be demonstrated in field studies and the barrier of intimidation of utilizing technology can be overcome. Even so, many data analysis methods

necessary for adoption of these practices require labor-intensive data manipulation and expensive software.

Research Questions and Objective

The overarching objective of this study was to evaluate the effects of in-season tactical N fertilizer management on NUE, nutrient uptake and yield. Tactical N management consists in adapting to the season and its dynamics due to weather to better match soil N supply with plant N demand, at field-scale. This study questioned if in-season fertilization management decisions increased NUE as well as yield, and if yield stability zones showed significant yield differences in response to variable nitrogen application. Another objective was to determine if remotely sensed imagery and crop modeling can identify optimal N fertilization rate to increase yield and NUE efficiency.

The hypothesis of this study was that spatial and temporal variability of soil, weather, topography, management and their interaction affect NUE, N uptake and yield and that tactical nitrogen fertilization management informed by remotely sensed imagery and modeling increases NUE, grain yields and profit while reducing environmental impact.

Methods

Field Experiment

In 2016, the focus of the field experiment was overloading amount of N applied at second side-dress in ZC1 and splitting the application amount of the second side-dress into two applications in 222 to test the impact of the timing of tactical N application (Table 8). In 2017, application at planting was decreased in field JS1, and in 222 pre-plant N was eliminated for the tactical zone strips, which also received variable N rates at the second side-dress while

conventional areas did not receive any fertilizer during the 2nd side-dress, in order to examine decreased N amounts and timing of application. In 2018, field NC12 received reduced N at planting in tactical strips and variable conventional rates at side-dress, one equaling the tactical side-dress amount and the other 20 lb/ac less. Field 105 received two different rates of reduced fertilization in 6 tactical strips, while at planting the whole field received a uniform amount, and at side-dress the tactical strips received increased fertilization while conventional management areas received four different rates, all lower than the tactical strips. These rates were selected based on a combination of remote sensing and SALUS modeling results addressed later in this chapter.

Table 8(a-b). The fertilizer application dates (a) and amounts (b) for six research fields from 2016 through 2018.

a.

Field	Target Population (seeds/m2)	Row Space (cm)	Plant Date	Harvest Date	Pre- Planting N Date	Side-dress 1 Date	Side-dress 2 Date
ZC1	9.39	50.8	5/24/16	11/12/16		6/11/2016	7/16/16 (CON) 6/21/16 (TAC)
222	7.78	76.2	5/25/16	11/3/16	4/27/16	6/30/16	7/25/16
JS1	9.39	50.8	5/18/17	10/13/17		6/19/17	7/15/17
222	7.78	76.2	5/20/17	10/31/17	4/26/17	7/5/17	7/19/17
NC12	9.39	50.8	5/1/18			6/7/2018	
105	7.78	76.2	6/4/18		6/3/18	7/31/18	
	ZC1 222 JS1 222 NC12	Population (seeds/m2) ZC1 9.39 222 7.78 JS1 9.39 222 7.78 NC12 9.39	Population (seeds/m2) Space (cm) ZC1 9.39 50.8 222 7.78 76.2 JS1 9.39 50.8 222 7.78 76.2 NC12 9.39 50.8	Population (seeds/m2) Space (cm) Date ZC1 9.39 50.8 5/24/16 222 7.78 76.2 5/25/16 JS1 9.39 50.8 5/18/17 222 7.78 76.2 5/20/17 NC12 9.39 50.8 5/1/18	Population (seeds/m2) Space (cm) Date Date ZC1 9.39 50.8 5/24/16 11/12/16 222 7.78 76.2 5/25/16 11/3/16 JS1 9.39 50.8 5/18/17 10/13/17 222 7.78 76.2 5/20/17 10/31/17 NC12 9.39 50.8 5/1/18	Population (seeds/m2) Space (cm) Date Date Planting N Date ZC1 9.39 50.8 5/24/16 11/12/16 222 7.78 76.2 5/25/16 11/3/16 4/27/16 JS1 9.39 50.8 5/18/17 10/13/17 222 7.78 76.2 5/20/17 10/31/17 4/26/17 NC12 9.39 50.8 5/1/18	Population (seeds/m2) Space (cm) Date Date N Date Planting N Date 1 Date ZC1 9.39 50.8 5/24/16 11/12/16 6/11/2016 222 7.78 76.2 5/25/16 11/3/16 4/27/16 6/30/16 JS1 9.39 50.8 5/18/17 10/13/17 6/19/17 222 7.78 76.2 5/20/17 10/31/17 4/26/17 7/5/17 NC12 9.39 50.8 5/1/18 6/7/2018

Table 8 (cont'd)

b.							
Year	Field	N Management	Pre-plant N applied (kg/ha)	N at planting (kg/ha)	N at Side- dress 1 (kg/ha)	N at Side- dress 2 (kg/ha)	Total N Applied (kg/ha)
2016	ZC1	conventional	(8)	68.9	93.2	31.1	193.1
	tactical		68.9	93.2	44.8	206.9	
	222	conventional	129.5		61.9		191.4
		tactical	129.5		36	25.9	191.4
2017 JS1	JS1	conventional		62.1	77.6	46.5	186.2
		tactical		30.9	77.6	46.5	155.0
	222	conventional	112.1	28.0	50.4		190.6
		tactical		28.0	50.4	89.7, 100.9, 112.1, 123.3	168.2, 179.4, 190.6, 201.8
2018	NC12	conventional		62.1	155.3	123.3	217.4
		tactical		62.1, 31.1	124.2, 155.3		186.3
	105	conventional	108.7	28.0	33.6, 44.8, 56.1, 67.3		170.3, 181.5, 192.8, 204
		tactical	28.0, 56.1	28.0	89.7		145.7, 173.8

Tactical Management and In-Season Destructive Sampling

Within the same fields as the emergence experiment, 8 sample points were established in each field in 2016 and 2017 based on the fertilization application type (conventional or tactical) (Basso et al., 2011) and on stability zone, totaling two of each yield stability zone per field. One meter squared destructive sampling of whole plants were collected throughout the season, weighed for dry biomass, and analyzed for N concentration. In 2018, because emergence zones were based on tactical application and not solely on yield stability, most recent UAV imagery from mid to late growing season was used to pick new sample points within and outside of our plots. In this way, picking new points based on where the UAV imagery showed the most

extreme reflectance values allowed for the further development of the relationship between reflectance and biomass and plant health status, as well as to assess the spatial variability. Similarly, these tactical/conventional points were sampled for biomass, N concentrations, and kernel counts at harvest. Drone flights were done seven to ten times throughout the growing season in each field, attempting to correlate flight dates with destructive sampling and PhotosynQ measurement dates for comparison. UAV remotely sensed imagery and SALUS modelling results were used to establish tactical N application rates.

UAV Imagery and Chlorophyll Meter Measurements

Drones used were the DJI Matrice 100 and 600 for multispectral imagery, including red edge, NIR, and the R, G, and B bands. The DJI Mavic Pro was also used for RGB visual imagery. imagery was also used, which is a company that utilizes imagery collected from an aircraft, collecting visual and thermal imagery. A reflectance panel (MicaSense, USA) was used to radiometrically calibrate the images, which were stitched with Pix4D (Pix4D S.A., Switzerland), creating an orthomosaic image. These stitched images are used to calculate multiple vegetation indices, including normalized difference vegetation index (NDVI), normalized difference red edge (NDRE), excessive greenness (ExG), and green normalized difference vegetation index (GNDVI) (Equations 2-5, Table 9). Vegetation indices are used for data analysis in comparison with nitrogen content of destructively sampled samples and PhotosynQ data, recording plant physiological properties. The proposed relationship between nitrogen content and remotely sensed imagery will be used to evaluate field scale variability and establish nitrogen prescription that is easy to use from the farmers' perspective, and informative of the spatio-temporal variation observed through various forms of sampling. In the future, this research could be utilized to

avoid labor-heavy destructive sampling, and instead use remotely sensed imagery to inform fertilization needs.

$$GNDVI = \frac{Near Infrared - Green}{Near Infrared + Green}$$
 (2)

$$NDVI = \frac{Near Infrared - Red}{Near Infrared + Red}$$
 (3)

$$NDRE = \frac{Near Infrared - Red Edge}{Near Infrared + Red Edge}$$
(4)

$$ExG = \frac{(2 x Green) - Red - Blue}{Red + Green + Blue}$$
 (5)

Table 9. Description of wavelengths pertaining to visible, multispectral, and thermal imagery and the pertaining vegetation indices produced.

Sensor	Wavelength (nm)	Primary Output
Visible	580 – 700	RGB, ExG
Multi-spectral	475, 560, 668, 717, 840	NDVI, GNDVI, NDRE
Thermal	7,500 – 13,500	Heat reflectance

PhotosynQ devices (Kramer, 2016) were used in 2017 and 2018 on six to nine occasions in each field, taking 6 measurements at each emergence plot, and 24 measurements per tactical/conventional point in 2017. These devices measure many physiological parameters, including relative chlorophyll, Phi2, PhiNPQ, and Light Intensity (PAR). Included within the PhotosynQ device is the microprocessor, and a multitude of sensors used for temperature, humidity, CO2, light, and light emitting diodes (LEDs) at wavelengths 530, 605, 650 and 940 nm, as well as an additional wide band sensor for examination of chlorophyll and absorbance in NIR (Near Infrared) (Kuhlgert, S. et. Al., 2016). Relative chlorophyll content measured with this device, similar to the SPAD chlorophyll meter, is often used to examine plant stressors such as nitrogen status by examining red (650 nm) and infrared (950 nm) relative reflectance. This data will be used to compare nitrogen content from destructive samples and remotely sensed imagery

to relative chlorophyll. The measurements are taken by hand by clipping the device onto the most recently collared leaf of the individual corn plant, and the data is automatically uploaded to a cellular device with Bluetooth capabilities.

SALUS Crop Modeling

Historical crop rotation and yield information, as well as management information, will be entered into the crop model, Systems Approach to Land Use Sustainability (SALUS) (Basso et al., 2006). Management decisions such as tillage, planting date, planting depth, planting density, fertilizer application and type are included. Weather data is collected from NLDAS-2 (North American Land Data Assimilation System Phase 2) and includes historical daily minimum and maximum temperatures, solar radiation, and precipitation values beginning in 1979 to the present. Information of historical yield response and growing degree-days required for the planted hybrid are used to determine cultivar parameters for each field scenario. The SALUS crop model will be used for a better understanding of the spatio-temporal variation at the field scale pertaining to soil type, soil water content and weather as pertaining to nitrogen response (Basso et al., 2006). This simulation model allows the user to assess all the variables contributing to yield response and their interactions. Similarly, the SALUS model will be used to assess the validity of variable nitrogen application regarding the yield response and decreased leaching of inorganic nitrogen to the surrounding environment and nitrous oxide emissions to the atmosphere.

The establishment of management zones created through historical yield and simulation modeling (Basso et al., 2001) creates a further delineation technique to assess field scale variation, and used with remotely sensed imagery and destructive sampling, it will aid in creating prescription nitrogen applications. Yield stability zones are created from average yield over

space for as many years as yield monitor data is available, combined with the variation of the yield values over the study years to create zones of high, medium and low yield zones, along with unstable zones. Currently, homogeneous yield zones identify optimal N rate to create a prescription using cumulative probability density functions of different application values and aided by vegetation indices segmentation.

Procedures To Develop Nitrogen Fertilization Prescription Map (Rx)

Industry Methodology

While prescription mapping of N is not a new custom in the age of precision agriculture, each company or research institute that provides N prescription mapping have differing beliefs on what the spectral response, environmental factors and management suggest the best application amount would be. For example, Climate FieldView uses satellite imagery and crop modelling to incorporate management decisions and climate. The imagery is categorized by the value of N deficiency present into several zones. The company aims to increase yield and maximize profit, and in 2017, the Climate Group performed a study showing that the recommended rates presented by Climate FieldView were above average conventional N applications. Similarly, Corteva of DowDuPont, Inc offers prescription mapping using satellite imagery, management and climate, but offers an additional option that allows visualization of the risk of N loss through leaching, variably across a field. AirScout, a company that uses a fixed wing manned aircraft to collect imagery, creates prescription mapping based solely on thermal imagery and Advanced Difference Vegetation Index (ADVI), their own created index similar to NDVI. A prescription map can be generated with up to five different rates across a field. While the prescription editor interface creates the zones based on the imagery, the product rates are determined by the user for each zone. Therefore, the applications are not established based on

needs of the plant but on segmentation of the imagery collected, leaving the user to interpret what each zone requires and what methodology to use regarding plant health.

Much of these companies provide a prescription based on the idea that if there is poor plant health indicated from reflectance values and environmental factors, more nitrogen should be applied to make up for nutrient deficiencies. Methods implored in this study will use the contrasting belief that increased rates of nitrogen should be applied to the areas showing healthy reflectance, as not to waste nitrogen applications on areas of the field with low uptake. In this way nitrogen is applied in areas that have shown high utilization of nitrogen and maintain areas of the field predicted to perform well in final yield, as to maximize the sink strength in areas of high source capacity.

UAV Imagery Prescription Aided by Systems Crop Modeling

The segmentation of the NDRE, NDVI and the ExG indices identified regions of higher or lower biomass (ExG) and chlorophyll content (NDVI and NDRE) based on strength of reflectance. The most recent imagery on the date of prescription creation was used for segmentation analysis unless earlier imagery showed a higher degree of variability. For example, if there was prolonged span of time without rain and rainfall the day before the imagery was captured, the plants response to the rainfall could fail to show variability needed to establish segmentation. Segmentation was performed in ENVI or ArcMap, using an iterative, unsupervised tool (Iso Cluster Unsupervised Classification Tool in ArcMap), with the option to change the number of clusters created and the minimum class size (number of pixels within a classification group). Using the Fishnet tool in ArcMap, segmentation is modified to the width of the farmer's applicator using majority classing techniques in a grid fashion.

Once segmentation was performed (Figure 18 and 20), SALUS crop model simulated 30 years of historical weather scenarios considering soil conditions including SSURGO (Soil Survey Geographic Database) information and nitrate data known from soil samples taken at the beginning of the growing season, crop hybrid data and various fertilization amounts based on the farmers conventional application amounts along with reduced rates accepted by the farmer (Table 10 and 11). This data was used to establish an empirical cumulative density function (ECDF) to visualize yield probabilities by fertilization amount (Figure 19) considering field conditions. Comparatively ECDF visualizes the trade-off of various fertilization amounts and illustrates the point of plateau in nitrogen application amount, where more fertilization will not increase use efficiency or yield. The combination of crop modeling and remotely sensed imagery is used directly by the farmer on a USB containing the shapefile.

Table 10. The chosen application rates based on the segmentation of NDRE imagery of field 105 in 2018. After performing segmentation, each class of pixels is assigned a rate based on agreed upon rates with the farmer, as well as crop modeling results (Figure 17) showing the tradeoff of yield probability with application amount.

N Management	Pre-Planting on July 3 (lb N/ac)	Planting on June 4 (lb N/ac)	Side-dress on July 31 (lb N/ac)	Total N Applied (lb N/ac)
Conventional, low NDRE class	97	25	30	152
Conventional, mid NDRE class	97	25	40	162
Conventional, high NDRE class	97	25	50	172
Conventional, highest NDRE class	97	25	60	182
Tactical, low rate	25	25	80	130
Tactical, high rate	50	25	80	155

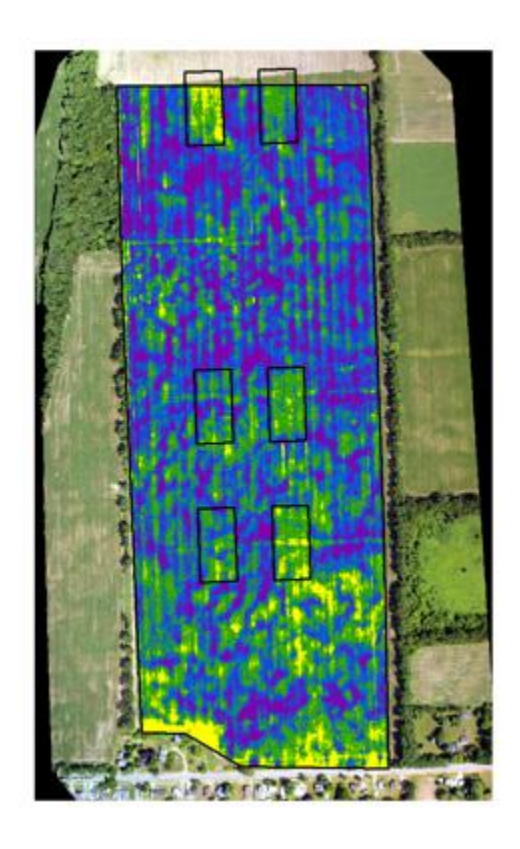


Figure 18. This image is a segmentation of NDRE imagery taken on July 24, 2018 and used to create the nitrogen prescription used. The yellow represents low reflectance, increasing to green, blue and at the highest reflectance, purple.

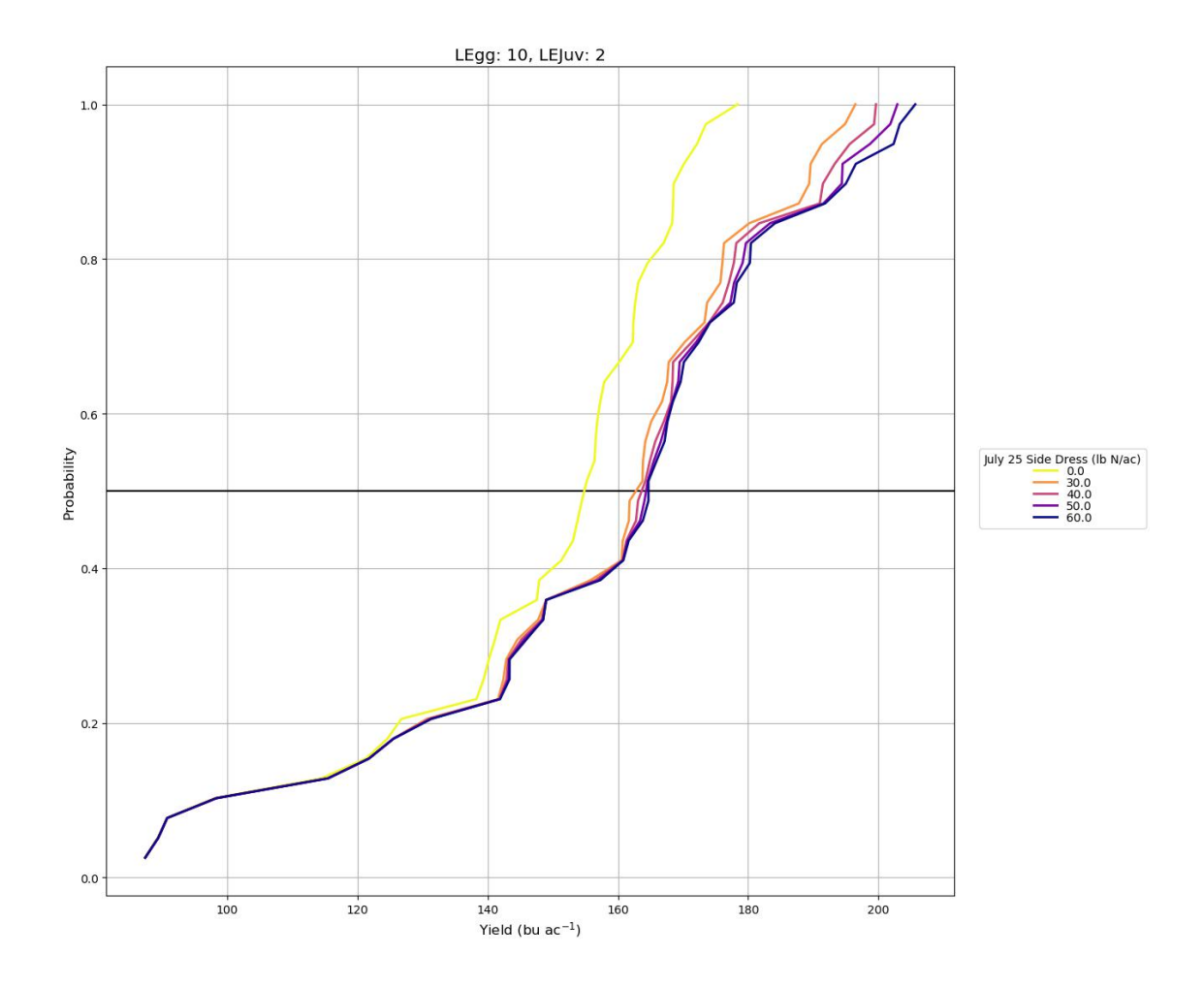


Figure 19. ECDF of field 105 in 2018 several days before the planned fertilization date. This ECDF was made from SALUS output data utiling the current conditions from soil sampling, and 30 potential weather scenarios. This plot shows the probability of achieving a certain level of yield dependent upon the level of fertilization. It is visible here that in many circumstances, yields will be incredibly similar regardless of application type, and visualizes the trade-off of no nitrogen application.

Table 11. The chosen application rates based on the segmentation of ExG imagery of field NC12 in 2018. After performing segmentation, each class of pixels is assigned a rate based on agreed upon rates with the farmer, as well as crop modeling results showing the tradeoff of yield probability with application amount.

N Management	Planting on May 1	Side-dress on June 5	Total N Applied
	(lb N/ac)	(lb N/ac)	(lb N/ac)
Conventional, low ExG class	55.4	110.8	166.2
Conventional, high ExG class	55.4	138.5	193.9
Tactical	27.7	138.5	166.2

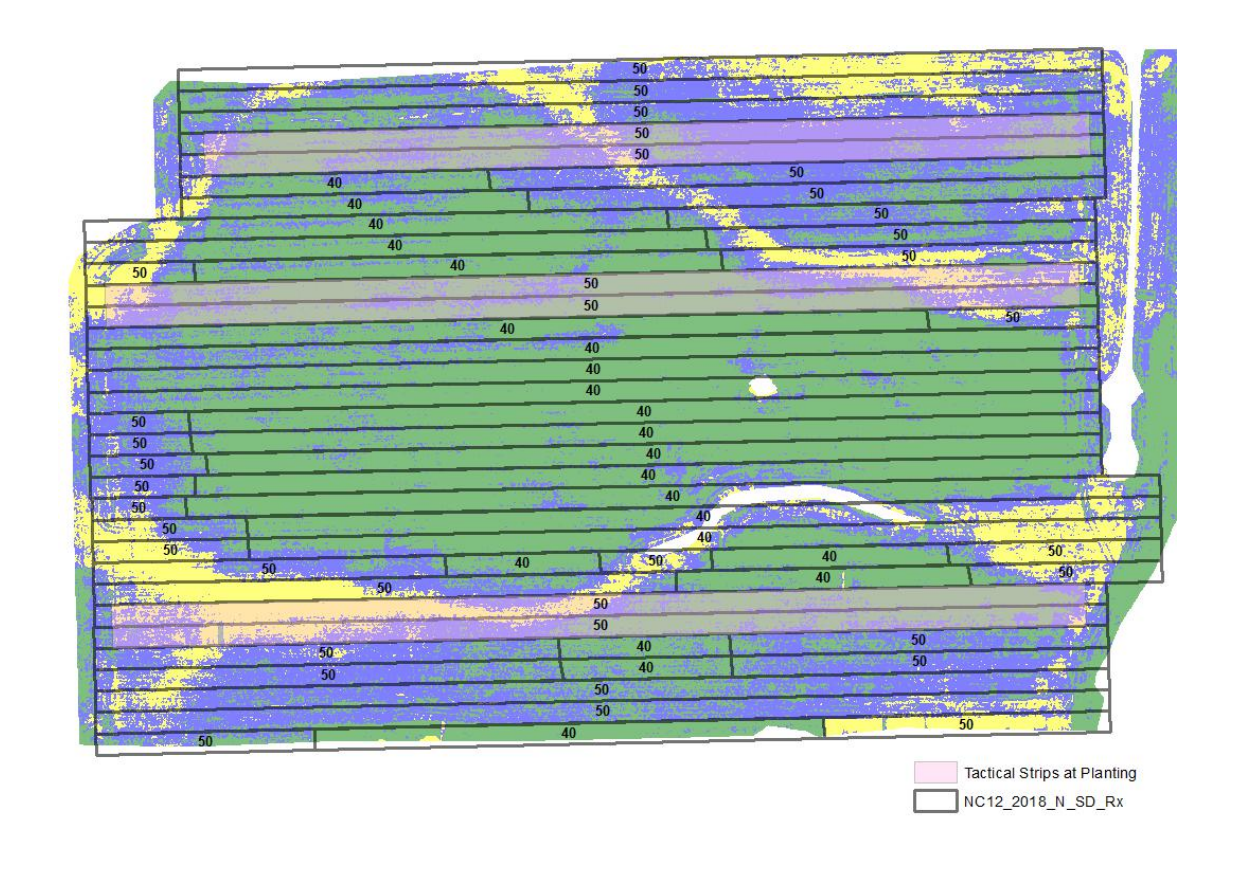


Figure 20. Segmentation of the ExG index, with suggested N rates of 40 gpa (gallons per acre, as the farmer applies liquid fertilizer) for green areas, or lower values of excessive greenness, and increased rates of 50 gpa for blue or yellow areas. On top of the segmentation image is the fishnet tool the width of the planter, which can be directly loaded into the farmer's applicator as a shapefile.

Statistical Analysis

Nitrogen Use Efficiency

Multiple methods have been established for calculating nitrogen use efficiency. In this study the NUE analyzed originated from Xie et al., (2007), which found basis in Crasswell et al., (1984) (Equation 6), and used by Basso et al., (2016).

ANUE or NFE =
$$Y(\frac{kg}{ha})/N app(\frac{kg}{ha})$$
 (6)

Where ANUE is agronomic nitrogen use efficiency or nitrogen fertilizer efficiency (NFE), Y is yield in kilograms per hectare (kg/ha), and NApp is nitrogen applied in kg/ha. A yield monitor mounted on the combine records the yield data in bu/ac at high-resolution. These data are interpolated using ordinary kriging into raster form at two-meter squared resolution using ESRI's ArcMap software and is used to calculate yield at the field scale, and further used in the calculation of ANUE. Randomized rectangular polygons created in ArcMap within each fertilization zone in each field overlaid a yield monitor raster and a raster created to delineate different fertilization zones. For analysis of all fields of study, zonal statistics calculated the mean of each polygon, and were exported and sorted to each fertilization scheme and ANUE, profit and yield were analyzed. Additionally, randomized points were created in each polygon, data from yield monitor was exported and used to calculate the ANUE and profit analysis in order to create more data points for a by-field analysis with higher statistical significance. The data was analyzed using mixed model analysis with replicate (or polygon the point is associated with) as a random variable. Analysis was performed in RStudio to run statistical tests, including ANOVA results and mixed model in the lme4 package, as well as in ArcMap to process UAV imagery.

Grain price was calculated based on a fixed \$ 3.99/bushel rate equaling \$0.157/kg, and nitrogen price was determined based on USDA fertilizer prices of \$571 per short ton of urea, equaling \$0.2895 /kg N. In situations where N data was not available for the field or stability zone, literature values were used and notated in table 12. Profit was calculated (Basso et al., 2011) using equation 7:

$$MNR = \left(Yield \left(\frac{kg}{ha}\right) x \ Grain \ Price \left(\frac{\$}{kg}\right)\right) - \left(Napp \left(\frac{kg}{ha}\right) x \ N \ Price \left(\frac{\$}{kg}\right)\right)$$
(7)

Where MNR is Marginal Net Return and Napp is the nitrogen application amount in kilograms per hectare.

Spatial Analysis

Whole field analysis of nitrogen use efficiency was also calculated in ArcMap using yield monitor data and nitrogen concentration in grain and stover (leaves and stalks of the corn plant) to create a raster file of each study field. Raster calculations were made from the yield monitor data and nitrogen values from field sampling using the following equations (Equations 8-12), and averaged over stability zone, as well as the MNR profit equation mentioned previously, but varied in N price and grain price by year.

$$N Grain = Yield \left(\frac{kg}{hg}\right) x N_{perc}$$
 (8)

$$N \, Stov = StW \, \left(\frac{kg}{ha}\right) x \, N_{st} \tag{9}$$

$$StW = \frac{Yield \left(\frac{kg}{ha}\right) - (Yield \left(\frac{kg}{ha}\right) x HI)}{HI}$$
 (10)

$$Nup = Ngrain + Nstov (11)$$

$$NUE = \frac{Nup}{Napp} \tag{12}$$

where Ngrain is the amount of grain in kg/ha, and Nperc is the percentage of nitrogen in grain, Nstov is the nitrogen in stover in kg/ha, StW is stover weight in kg/ha, Nst is percentage of nitrogen in stover, HI is the harvest index, Nup is nitrogen uptake, NUE is nitrogen use efficiency, and NFE is the nitrogen fertilizer efficiency. If nothing else is given due to sample processing errors, 2 % of total grain weight is considered nitrogen in grain and 0.5 % of total stover weight is nitrogen in stover (Table 12).

Table 12. Values used for spaital NUE calculation in ArcGIS using the raster caculator tool. The HI is the same for both treatments because only camera zones had HI values but they were placed in conventional only. The asterisk next to the N values indicates this was an arbitrary value chosen from literature.

Field		Treatment	HS	MS	LS	UN
222	N% Grain	Tactical	1.22	1.2	1	0.92
		Conventional	1.18	1.2	0.97	1.26
	N% Stover	Tactical	0.59	0.6	0.38	0.44
		Conventional	0.71	0.6	0.4	0.59
	HI	Tactical	0.6	0.6	0.56	0.6
		Conventional	0.6	0.6	0.56	0.6
JS1	N% Grain	Tactical	1.24	1.23	1.24	1.17
		Conventional	1.33	1.35	1.57	1.26
	N% Stover	Tactical	0.48	0.51	0.59	0.4
		Conventional	0.56	0.57	0.68	0.53
	HI	Tactical	0.53	0.56	0.47	0.51
		Conventional	0.53	0.56	0.47	0.51
105	N % grain	Tactical (25)	1.73	1.59	1.59	1.63
	-	Tactical (50)	2.06	1.65	1.65	1.11
		Conventional	1.98	1.44	1.44	1.79
	N% Stover	Tactical (25)	0.5*	0.5*	0.5*	0.5*
		Tactical (50)	0.5*	0.5*	0.5*	0.5*
		Conventional	0.5*	0.5*	0.5*	0.5*
	HI	Tactical (25)	0.61	0.62	0.62	0.64
		Tactical (50)	0.65	0.6	0.6	0.62
		Conventional	0.67	0.61	0.61	0.56
NC12	N % grain	Tactical	1.12	1.27	1.27	1.09
		Conventional	1.15	1.26	1.26	1.21
	N% Stover	Tactical	0.49	0.46	0.46	0.57
		Conventional	0.54	0.52	0.52	0.71
	HI	Tactical	0.65	0.64	0.64	0.65
		Conventional	0.64	0.65	0.65	0.64

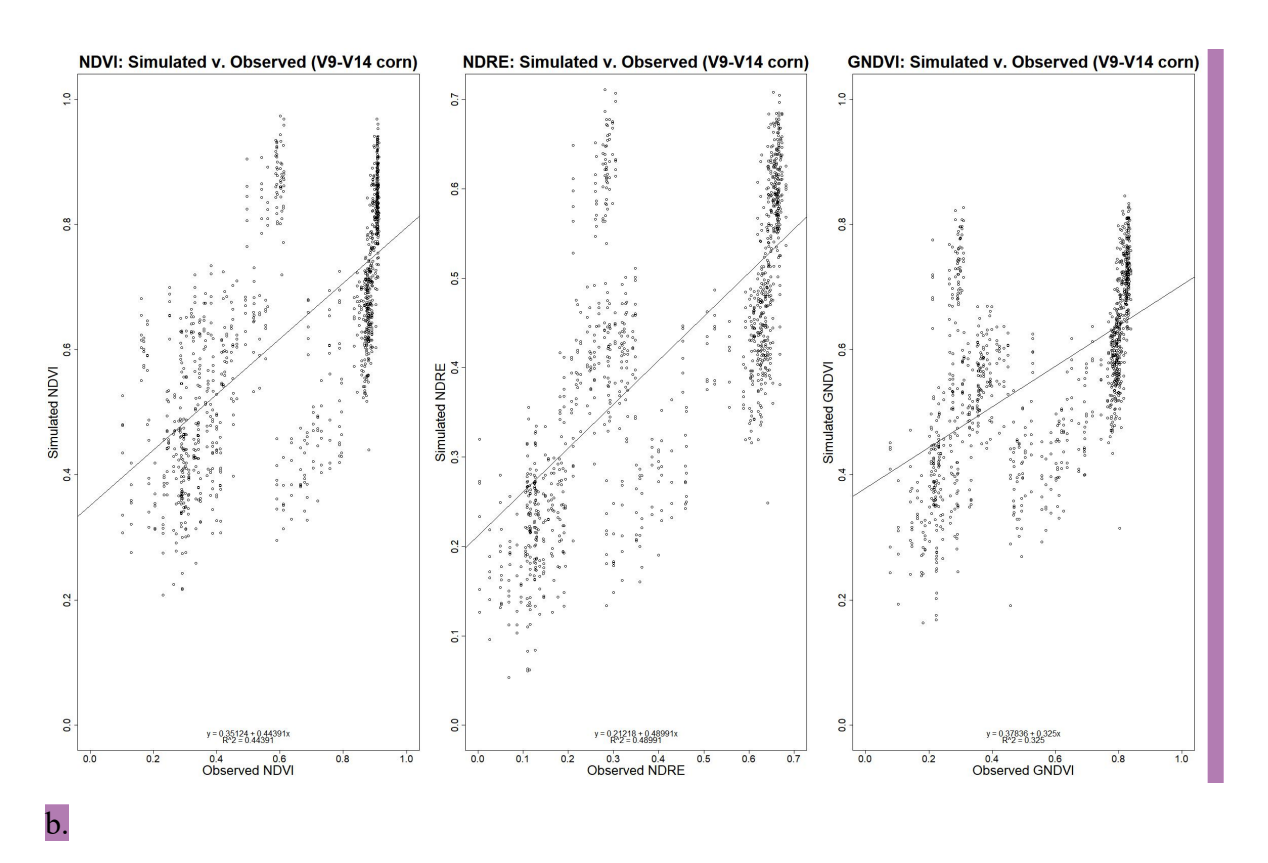
Results

Chlorophyll Meter Analysis

PhotosynQ measurements were tested to assess correlation with NDVI, GNDVI and NDRE, as well as the predictability of nitrogen content using NDVI from the remotely sensed imagery and PhotosynQ measurements. Parameters used included relative chlorophyll, ambient humidity, and temperature, Phi2 and PhiNO (photosynthesis parameters), and SPAD reflectance wavelengths of 420, 530, 605, 650, 730, 850 and 880. Results showed limited predictability of GNDVI, NDVI and NDRE from PhotosynQ parameters, with coefficient of determination not reaching 0.50 (Figure 21a). This is due to extreme variability between measurements, and the need for extensive number of sampling points both across the field and at the same sampling location to fully capture variability at each sampling point and predict vegetation indices with accuracy. The results showed that scale of which these experiments have been performed have not shown beneficial results to relate to reflectance to create a nitrogen prescription in regard to utilizing vegetation indices. Without extending the number of sampling points and replicates at each point, drone imagery is more easily attainable after startup costs, and gives more information about spatial variability over a field. Visualizing nitrogen content with relative chlorophyll measurements showed positive correlation (Figure 21b) validating the relationship between chlorophyll content and nitrogen. Each dot on Figure 6 indicates an averaged value of all the measurements taken at that location, and still shows wide variability in the relationship overall and by study site. Further, examining by each field (Table 15, Appendix), 105 showed no statistically significant differences in relative chlorophyll between stability zones when considering sampling date or treatment type. Field NC12 and 222 showed significant differences between sample date and stability zone and treatment. Field JS1 showed differences between

date and zone but was not included in the table because there was only one date that photosynQ measurements were taken in which both treatments were represented.

a.



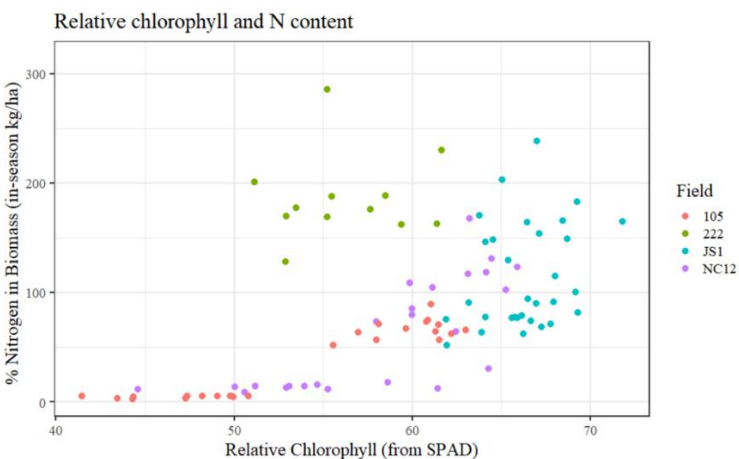


Figure 21. The plots show simulated vegetation index (NDVI, NDRE and GNDVI) using Photosynq measurement parameters versus the true vegetation index value from UAV imagery (a). The correlation of nitrogen in biomass to the relative chlorophyll estimated from SPAD reflectance values from the PhotosynQ devices. Each color indicated a different field from 2017 to 2018 (b).

Reflectance from Remotely Sensed Imagery and Nitrogen Status

Reflectance from remotely sensed imagery was analyzed for all fields from 2017 to 2018 with all hand-sampled dates (Figure 22) to confirm the relationship between nitrogen content and reflectance in red band, green band, red edge, NDVI, NDRE, and GNDVI from UAV imagery, and ADVI provided by Airscout. Nitrogen was analyzed in kg/ha, calculated from the percentage of total N from a subsample analyzed using combustion methods, related to the biomass weight of the hand sample. There is a negative correlation between nitrogen and reflectance in the red band, green band, and the red edge band and a positive correlation between NDRE, NDVI, and GNDVI and nitrogen content. This confirms results in previous studies relating nitrogen content and spectral reflectance and helps to validate the methodology to create a variable rate prescription. By field analysis showed mixed results due to small sample size at each field and date, attributed to the difficulty of whole plant field sampling, especially late in the season.

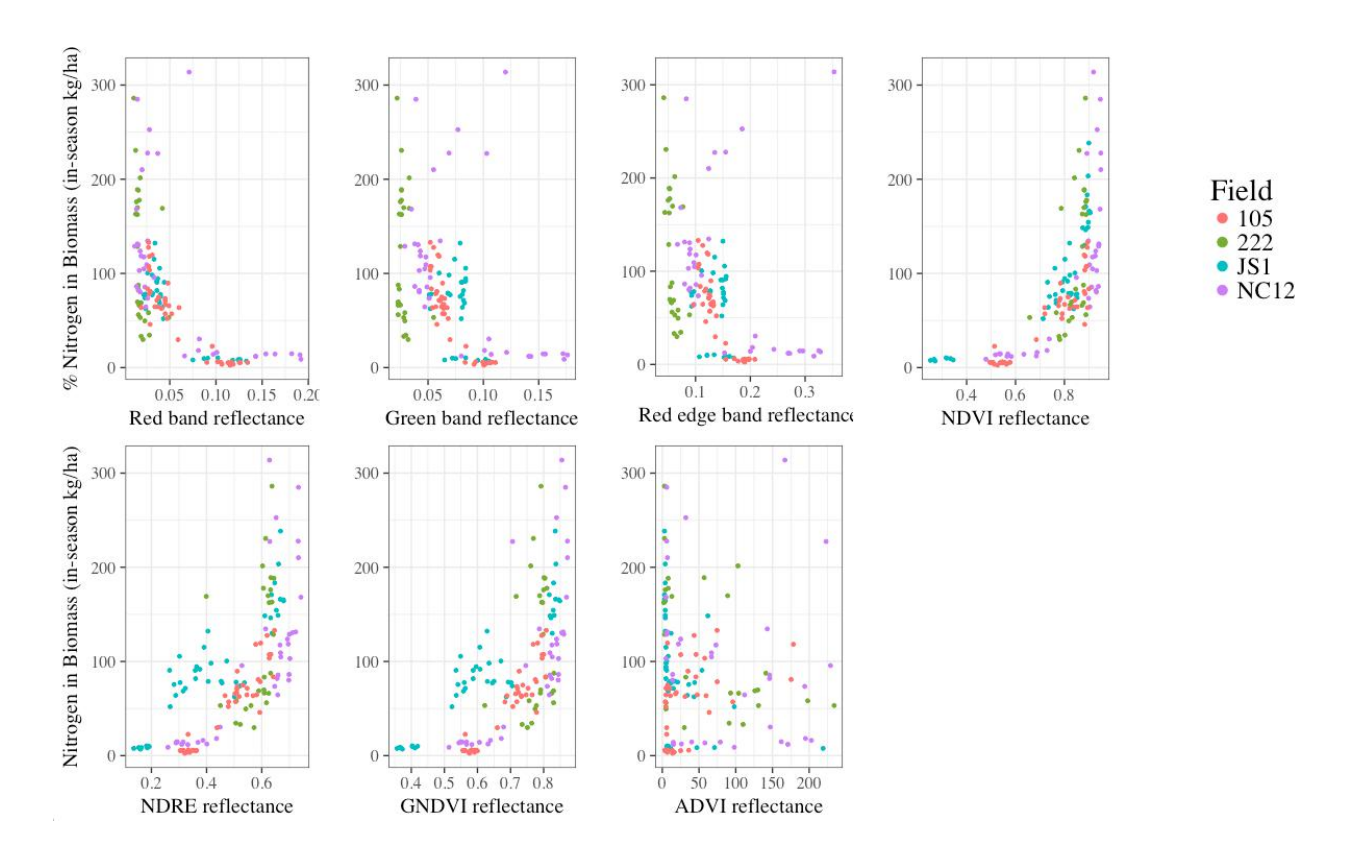


Figure 22. Plots of the red band, green band, blue band, red edge band, NDVI, NDRE, GNDVI and ADVI reflectance values, plotted against the nitrogen content in the biomass. This content was calculated using biomass weight values, referenced to percent nitrogen analyzed from a subsample of the ground biomass.

Yield and Use Efficiency Response to Variable Rate Application

Utilizing zonal statistics on randomly created polygons within treatment types, nitrogen data and yield monitor raster data was used to analyze the ANUE, profit, and yield to identify significant differences in treatment. Four different regressions were tested for significance, showing differences in yield between treatments only in field 105 in 2018 (Table 13).

Table 13. Single variate regression analysis with profit, yield, or ANUE as the dependent variable and treatment as the covariate by field. The letters represent the Tukey's mean separation test showing if profit, yield, and ANUE are statistically significantly different from one another.

Field	Treatment Type	Application Amount (kg/ha)	Profit (\$/ha)	Yield (kg/ha)	ANUE (kg/kg)
.22	Tactical Split application	191	1659 a	10921 a	57 a
'	Conventional One application	191	1714 a	11271 a	59 a
ZC1	Tactical	193	1810 a	11883 a	62 a
2016)	Conventional	207	1813 a	11932 a	57 b
	Tactical	168	1617 a	10611 a	63 ab
	reduced	179	1751 a	11485 a	64 a
222 (2017)	Tactical Overload Pre-plant N Overload 2 nd Side-dress N	191	1672 a	11571 a	61 <i>ab</i>
		191	1761 a	10999 a	58 b
	Conventional	202	1762 a	11595 a	57 b
S1	Tactical reduced side-dress	155	1868 a	12183 a	79 a
(2017) -	Conventional	186	1857 a	12172 a	65 b
NC12 ½ (2018) ½	Tactical ½ at planting	186	1818 a	11923 a	64 a
	½ at side-dress	186	1667 a	10963 a	59 a
	Conventional	217	1864 a	12273 a	56 a
105 _ (2018)	Tactical decreased at	146	1516 b	9924 c	68 a
	planting	174	1600 ab	10512 abc	60 b
	Conventional	182	1581 <i>ab</i>	10405 ab	57 bc
	varied at	193	1630 a	10735 ab	56 c
	Side-dress	204	1664 a	10972 a	54 d

Field Summaries (Figure 23 a-c, Table 13)

No statistically significant differences were observed in the field 222 in 2016 for what concerns profit, yield, or ANUE across the two treatments. This is expected because the only difference in management was the timing, in which one was split, and one was applied all at once.

There were no significant differences in the tactical versus conventional treatment in profit or in yield, but there was a significant increase in ANUE in the reduced, tactical treatment for the ZC1 field in 2016.

For the field 222 in 2017, there were no significant differences in profit or yield in any of the treatments, but the tactically reduced rates showed significantly higher ANUE than the conventional rates.

No significant differences in profit or yield among the tactical and conventional treatments were found in JS1 in 2017. The ANUE in the reduced treatment was much higher than the conventional treatment.

Analyzing NC12 in 2018 using a linear model showed no differences in yield or profit between management zones but showed significant differences in ANUE by Tukey's test. The reduced treatment in which fertilization was halved at planting had the highest ANUE, followed by the treatment halved at side-dress, and the conventional treatment. Alternatively, using a mixed model with replicate as a random variable showed no significant difference in yield, profit, or ANUE.

The field 105 in 2018 presented the most varied results and is the only field study that saw contrasting results in yield from the five other field sites. Significant differences in profit, ANUE and yield were observed among management zones. From the smallest application amount (146 kg/ha) to the highest (204 kg/ha) there is a 148 \$/ha loss in profit, a 1048 kg/ha loss in yield, and a 14 kg/kg N increase in ANUE. Tukey's mean separation test is a conservative test, and all other applications besides the lowest (second lowest 174 kg/ha N) were considered within the same grouping as the highest application amount and saw a 64 \$/ha loss in profit and 460 kg/ha loss in yield. ANUE did not show this pattern, as almost each increment of fertilization amount showed mean separation. Examining the second lowest application (174 kg/ha), there was no true mean separation of yield or profit between this rate and the highest rate.

Insignificant results show that decreasing the amount of nitrogen applied neither affects profit or yield in any study site besides field 105 in 2018 and in some cases, increases profitability. In all study sides, increased ANUE rates were observed in reduced application management zones.

a.

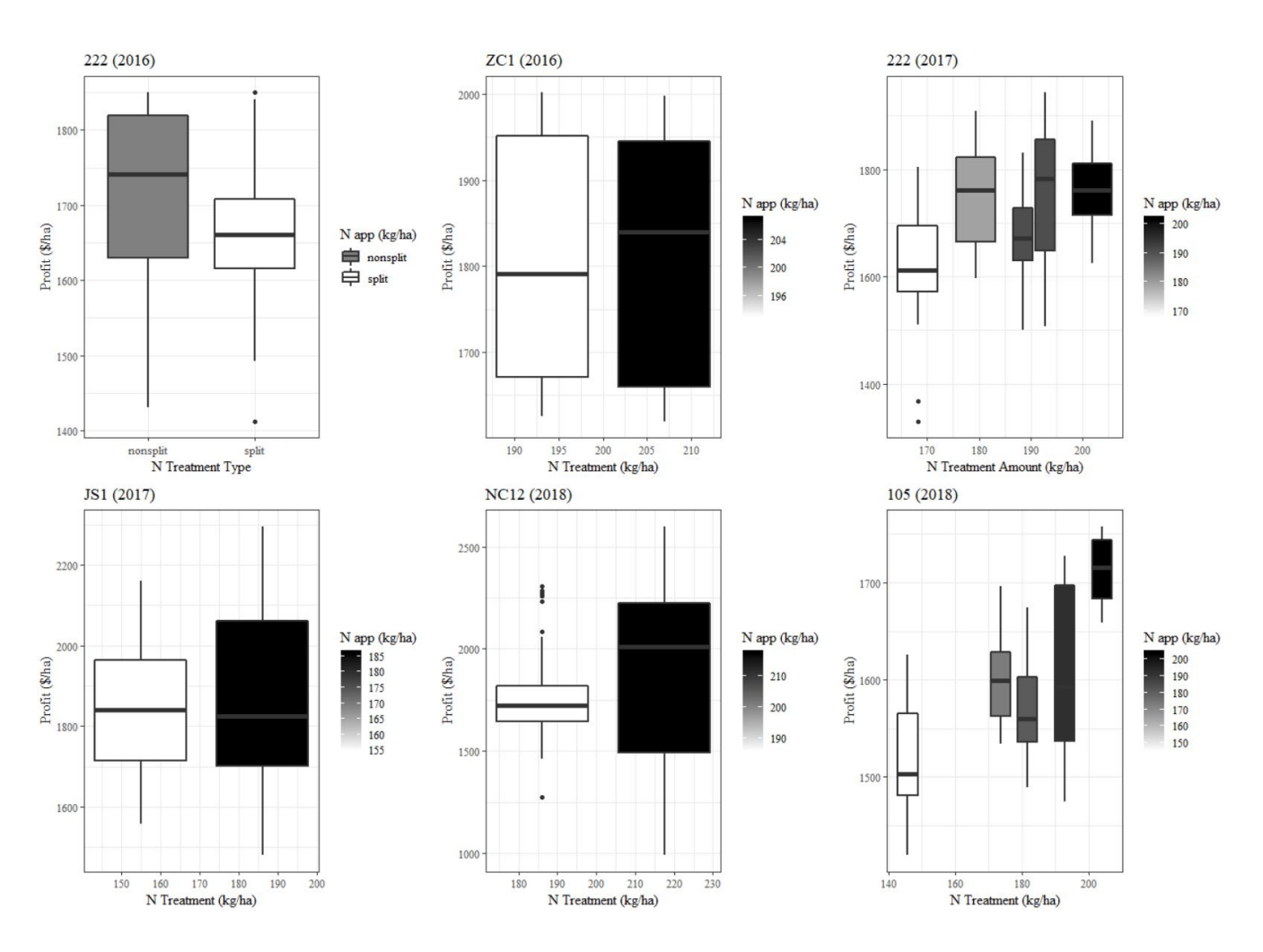


Figure 23. Yield, Nitrogen Use Efficiency and Profit by each application in six field studies from 2016-2018.

Figure 23 (cont'd)

b.

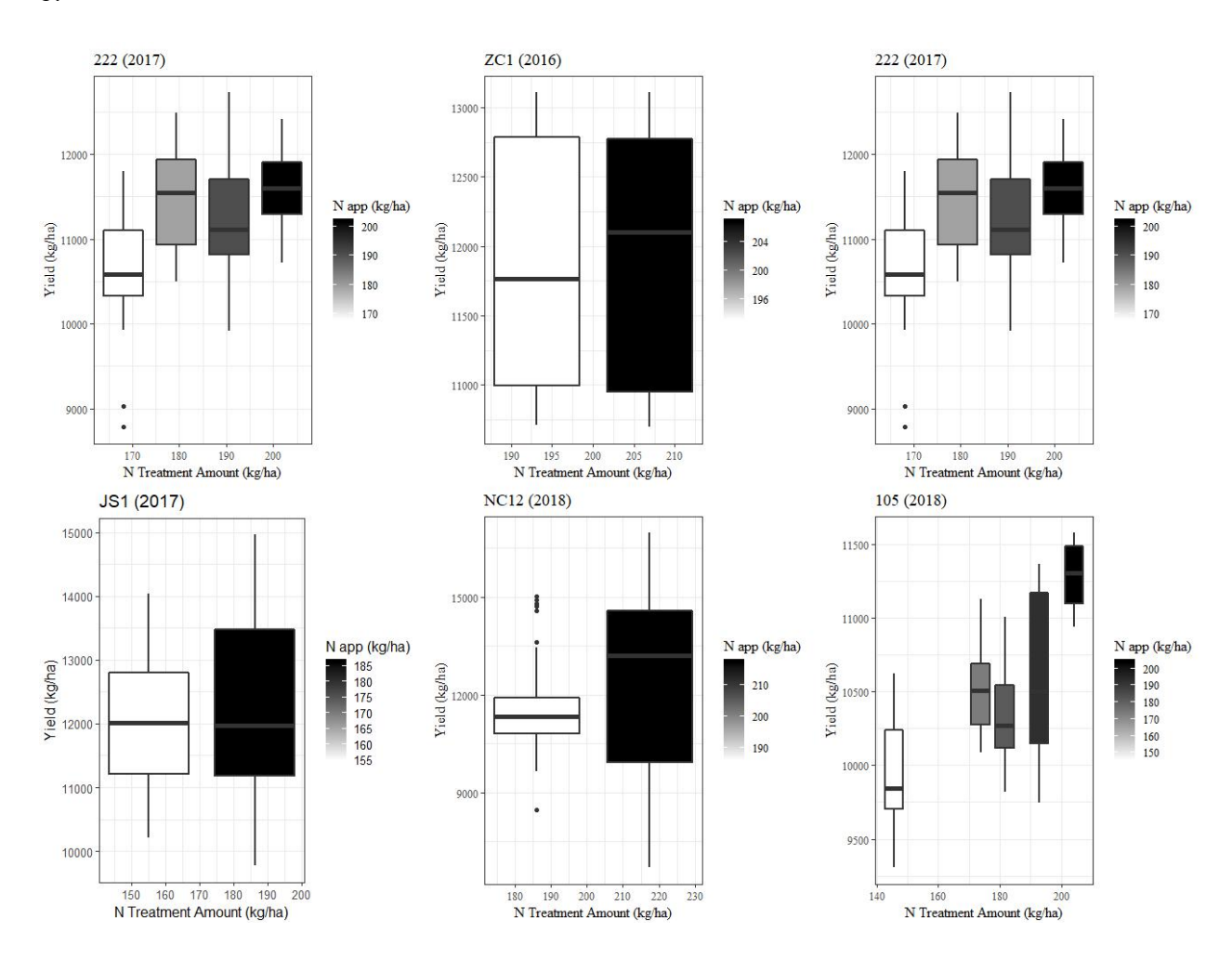
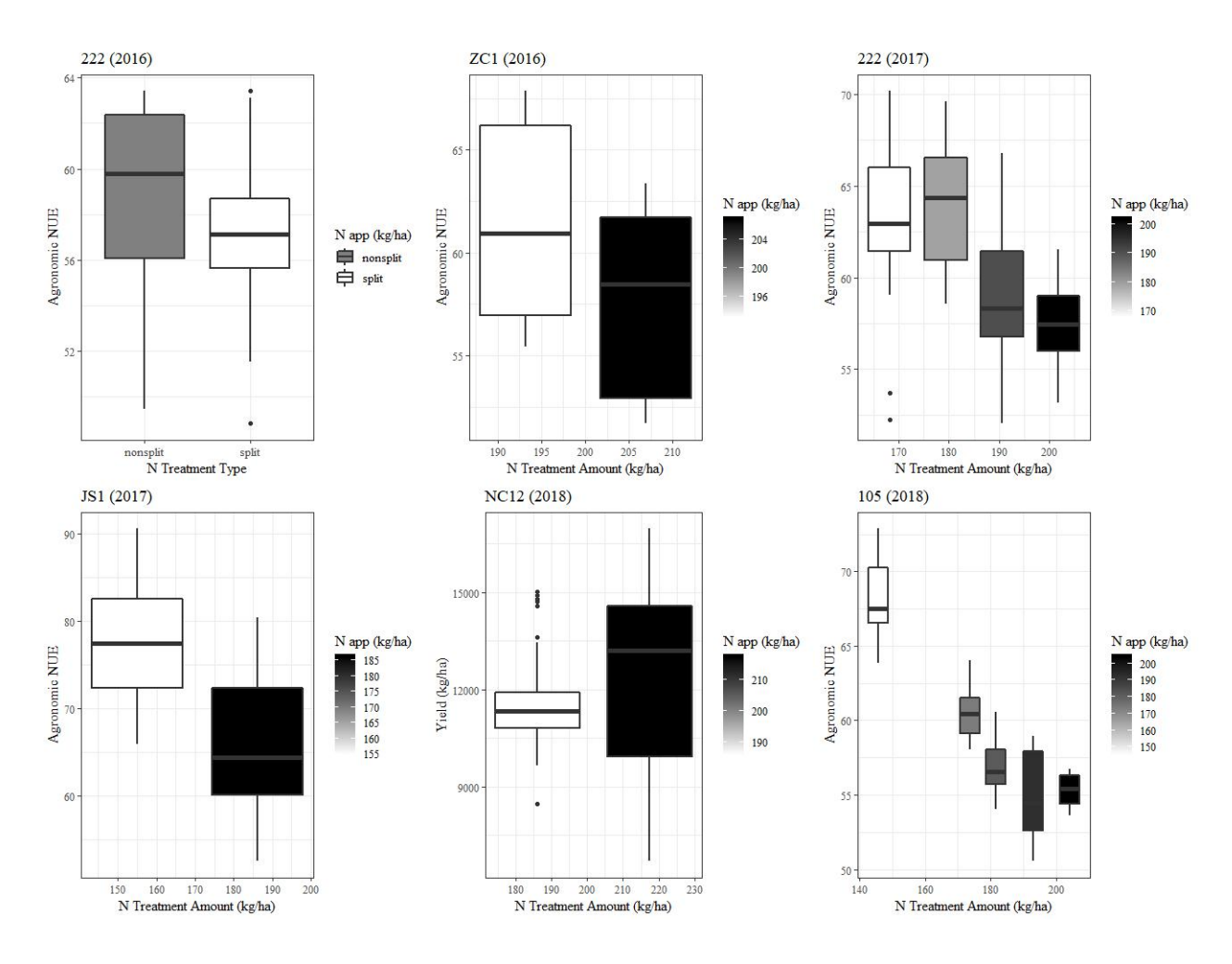


Figure 23 (cont'd)

c.



Mixed model analysis on randomly sampled point data of yield monitor data with stability and fertilization amount showed significant differences in yield between stability zones in each field besides field ZC1 in 2016 (Table 14a and Figure 24). Low and stable zones displayed the smallest yield values, followed by medium and stable and high and stable, while unstable zones varied by field and year. Additionally, there were statistically significant differences in yield between conventional and tactical management (Table 14b) in all fields excel ZC1 in 2016. There were only two field studies in which the highest application amounts saw the highest yield results. Considering all field sites, Nitrogen Supplied by Soil, Nitrogen Use

Efficiency, and ANUE experience increases as fertilization application amount increases, while Nitrogen Uptake (Figure 25) saw a slight decrease as application amount increases.

Table 14(a-b). Regression using equation $y = \mu + stability + N$ applied + replicate + error with mean separation using tukey adjustment. The letters represent the Tukey's mean separation test showing if yields were significantly different between stability zones and by amount of fertilization.

a.

Field	Stability Zone	Yield (kg/ha)			
ZC1 (2016)	Medium and Stable	11882 a			
	High and Stable	12084 a	12084 a		
	Unstable	11803 a			
222 (2017)	Low and Stable	9881 a			
	Medium and Stable	11080 b			
	High and Stable	11637 c			
	Unstable	10031 a			
JS1 (2017)	Low and Stable	10837 a			
	Medium and Stable	12233 <i>b</i>			
	High and Stable	13195 d			
	Unstable	12771 <i>c</i>			
105 (2018)	Medium and Stable	10428 a			
	High and Stable	10730 <i>b</i>			
	Unstable	10383 a			
NC12 (2018)	Medium and Stable	11175 a			
	High and Stable	12210 <i>b</i>			
	Unstable	13072 c			

b.

Field	Total N applied (kg/ha)	Yield (kg/ha)		
ZC1 (2016)	193	11904 a		
	207	11943 a		
222 2017)	168	10063 a		
	179	10925 bc		
	191	10920 <i>c</i>		
	202	10723 <i>b</i>		
JS1 (2017)	155	12222 a		
	186	12295 a		
105 (2018)	146	10011 a		
	174	10593 <i>c</i>		
	182	10230 <i>b</i>		
	193	10651 c		
	204	11084 d		
NC12 (2018)	186	11947 a		
	217	12357 <i>b</i>		

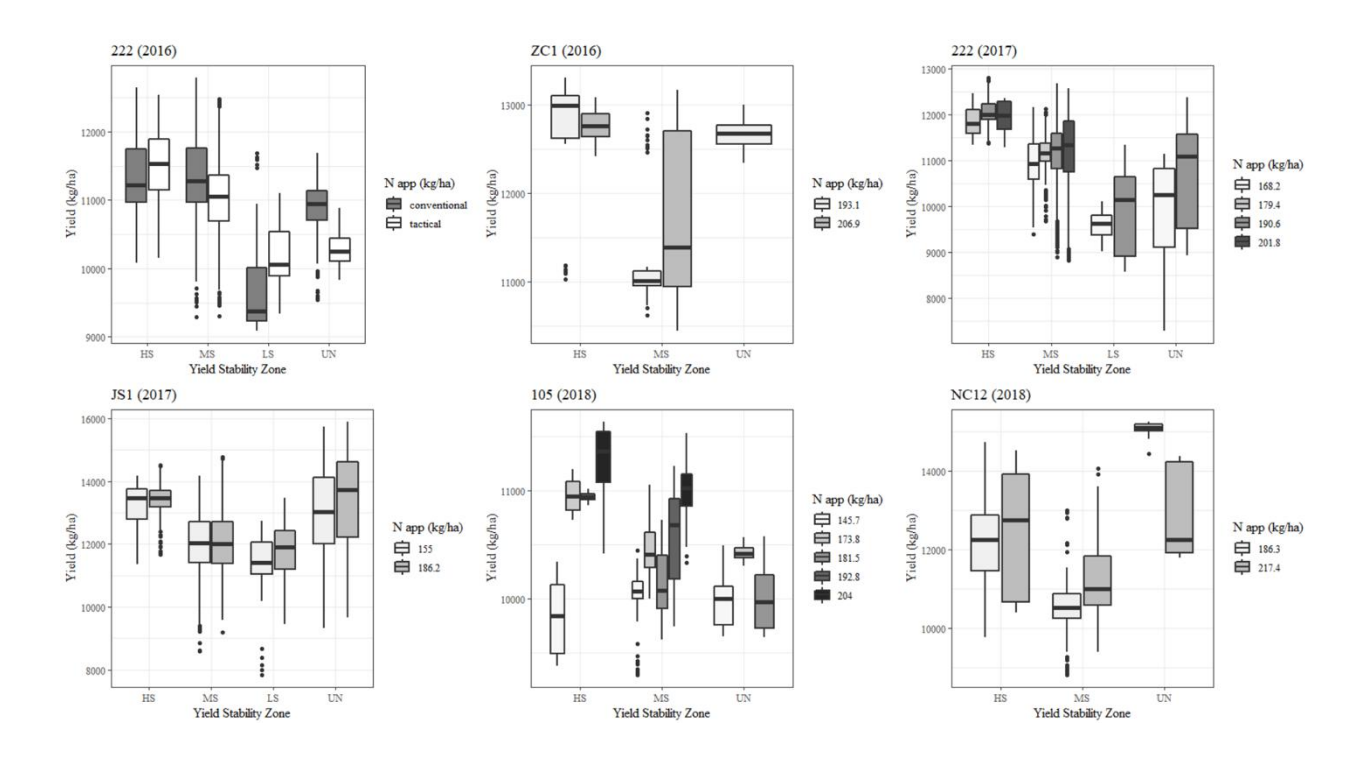


Figure 24. Differences in yield between stability zones by application types for each study field between 2016-2018. In 2016 field 222 received different color scheme because the difference in application was timing of fertilization, and not application amount.

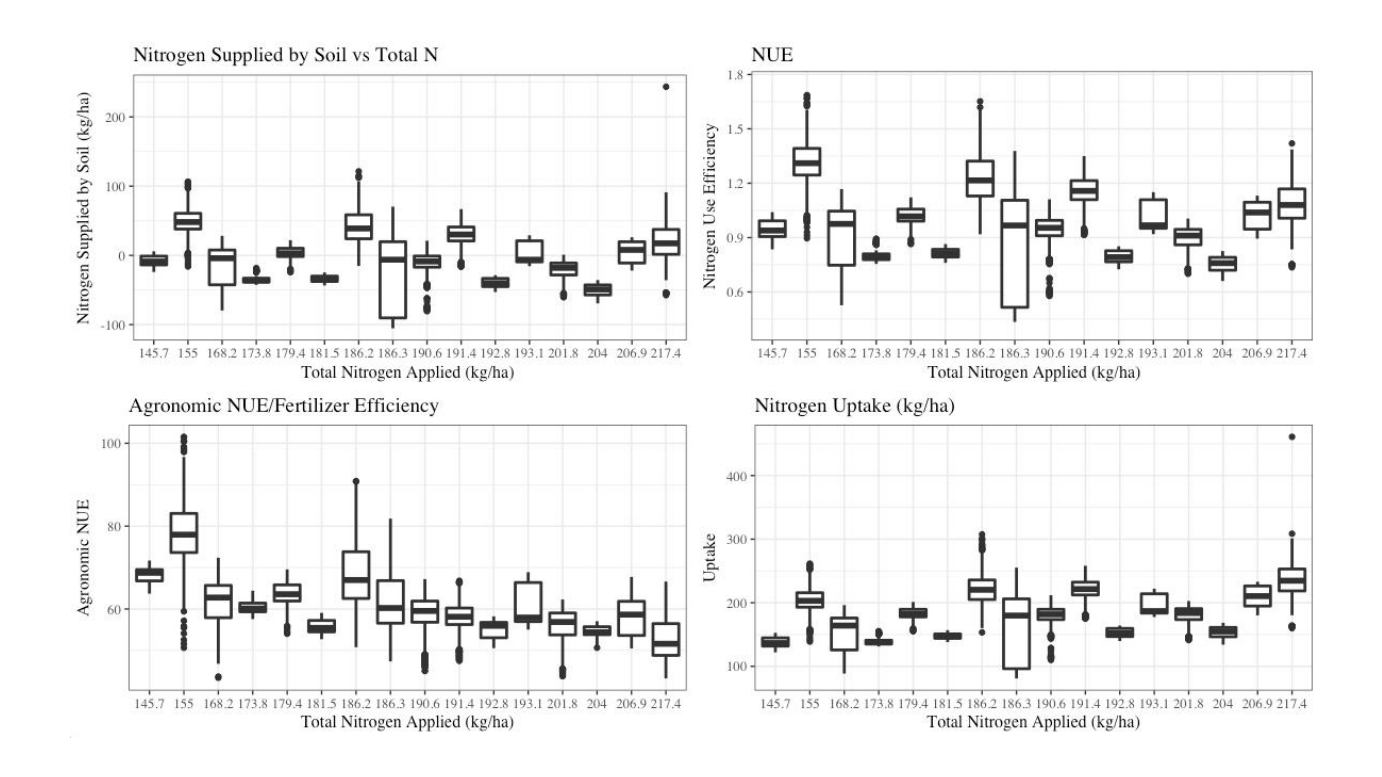


Figure 25. Nitrogen Supplied by Soil, Nitrogen Use Efficiency, ANUE, and Nitrogen Uptake were calculated using N data from plant samples (Table 11) and yield monitor data from all six study sites from 2016-2018, using raster calculation in ArcMap and extracting point data.

Discussion

Each study site experienced differing yield affects from varied fertilizer management schemes from 2016-2018, although most study sites showed unaffected significant yield differences between study sites when using a tactically chosen, decreased fertilization amount. In fields 222 (2016), ZC1 (2016), 222 (2017) and JS1 (2017) and NC12 (2018) there was no statistically significant differences in yield or profit. In years 2016 and 2017, test strips created in the field were expected to show these results, as overapplication of nitrogen fertilization is prevalent, and the goal of this study was to illustrate increased rates do not equal increased yields. ANUE was increased in the tactical zones in all fields where increased rates were applied in 2016 and 2017. In 2018 where fertilization prescriptions were created for each field using modelling and remote sensing, NC12 saw similar yield results in each application zone due to similar application rates across the field that were not variable enough to capture differences. Field 105 saw significant differences in yield, ANUE and profit between management zones. The smallest application amount (146 kg/ha) to the highest (204 kg/ha) showed a 148 \$/ha loss in profit, a 1048 kg/ha loss in yield, and a 14 kg/kg N increase in ANUE. While these results seem to dissuade the hypothesis made, these results illustrate the desired effect of a variable nitrogen rate. We expect lower profits with underperforming areas but applying less nitrogen in those areas and more nitrogen in productive areas, as shown by remotely sensed imagery, increases the utilization of nitrogen fertilizer in well performing and underperforming areas of the field. In this regard, we are increasing yield in areas where more nitrogen is applied and saving money on fertilizer by applying lower rates to underperforming areas. The concept behind the method used for fertilization application prescriptions in this study aimed to apply more fertilizer in areas of the field shown to have increased use efficiency, and less applied in underperforming regions. It

has been suggested that skipping fertilization in these areas altogether or planting native grasses for biodiversity and soil health (Basso, et al., 2019). Therefore, areas that received higher rates of fertilizer application achieving higher yields in some cases is expected, and often when this is the case, the profit achieved by both study regions are not statistically significantly different due to funds saved from cost of fertilizer.

When stability zones were also considered in analysis of differences in yield between management zones, there were significant decreases in yield in areas of decreased fertilization, although never amounting to more than ~860 kg/ha. In cases where low and stable yielding zones were represented (field 222 in 2017 and field JS1 in 2017), these areas showed the lowest relative yield in the year of study with a decrease of 1,756 kg/ha and 2,385 kg/ha from high and stable yielding zones, respectively. Interestingly, field 105 that saw the biggest yield differences among management zones, experienced a difference of 347 kg/ha, suggesting this field is more highly affected by management and weather patterns than historical yield.

Future work will include developing a stricter algorithm for utilizing the SALUS crop modeling technology and creating a fertilizer application prescription considering the remotely sensed imagery and the yield stability zones. The yield stability zones proved to be extremely indicative of the yields that will be produced, and unstable zones can be better managed based on the expected weather conditions, and further account for the variability observed in those zones.

CONCLUSIONS

Delay in individual corn plant emergence was shown to be correlated with lower yield levels, showing an over 1,800 kg/ha decrease in grain yield, scaled from individual plant grain weights using plant populations and averaged over all study sites. Yield stability zones were also significant in predicting individual plant grain weights, showing a 20-gram decrease, or over 1,600 kg/ha from the high and stable zone to the low and stable zone, over all study sites. In most cases, the high and stable yielding zones emerged more quickly as well, with a lower number of skips or plants that did not emerge. Knowing the effects of delayed plant emergence can provide insight on management decisions such as replanting, for example if an area of the field experiences abundance or extreme lack of water. Additionally, areas that have low yield and often experience delayed emergence, may be more suitable as native grasses, a cover crop, or unplanted, as costs of production may not account for low yield levels. In most cases, fields that received no-till management also saw a decrease in days after planting, suggesting that no-till management may be more beneficial to uniform plant emergence and could contribute to higher yields.

Remotely sensed imagery paired with the SALUS crop model method of producing a fertilization prescription demonstrates the capabilities for informed management decisions based on a multitude of data and improves upon industry methods of prescription creation. Variable rate fertilization has been proved in previous literature to increase nitrogen use efficiency without sacrificing yield or profit. This study reiterated this concept, and in some cases even increased profit where less fertilization was applied. While the SALUS model remains a technology usable by technologists with modelling training, future work could be done to create

a user-friendly, adaptable technology, and create a service usable by farmers to create informed fertilization prescriptions that consider both environmental impact and profit for the farmer.

The evaluation of spatial and temporal variation of yield across a single field has shown to be affected by a multitude of environmental factors and management practices. While this variation continues to be difficult to predict, utilizing remotely sensed imagery, crop modelling and field sampling validation methods continues to identify trends in which management decisions can be informed. Yield stability zones created from historical yield data considering variability from year to year as well as overall yield performance across a single field proved to be an important factor in simulating future yields.

APPENDIX

APPENDIX: Nitrogen Fertilization Scheme Spatial Data



Figure 26. Nitrogen fertilizer sidedress prescription developed from remotely sensed imagery for field NC12 in 2018, created in ESRI ArcGIS.



Figure 27. Nitrogen fertilizer sidedress prescription developed from remotely sensed imagery for field 105 in 2018, created in ESRI ArcGIS.

a.

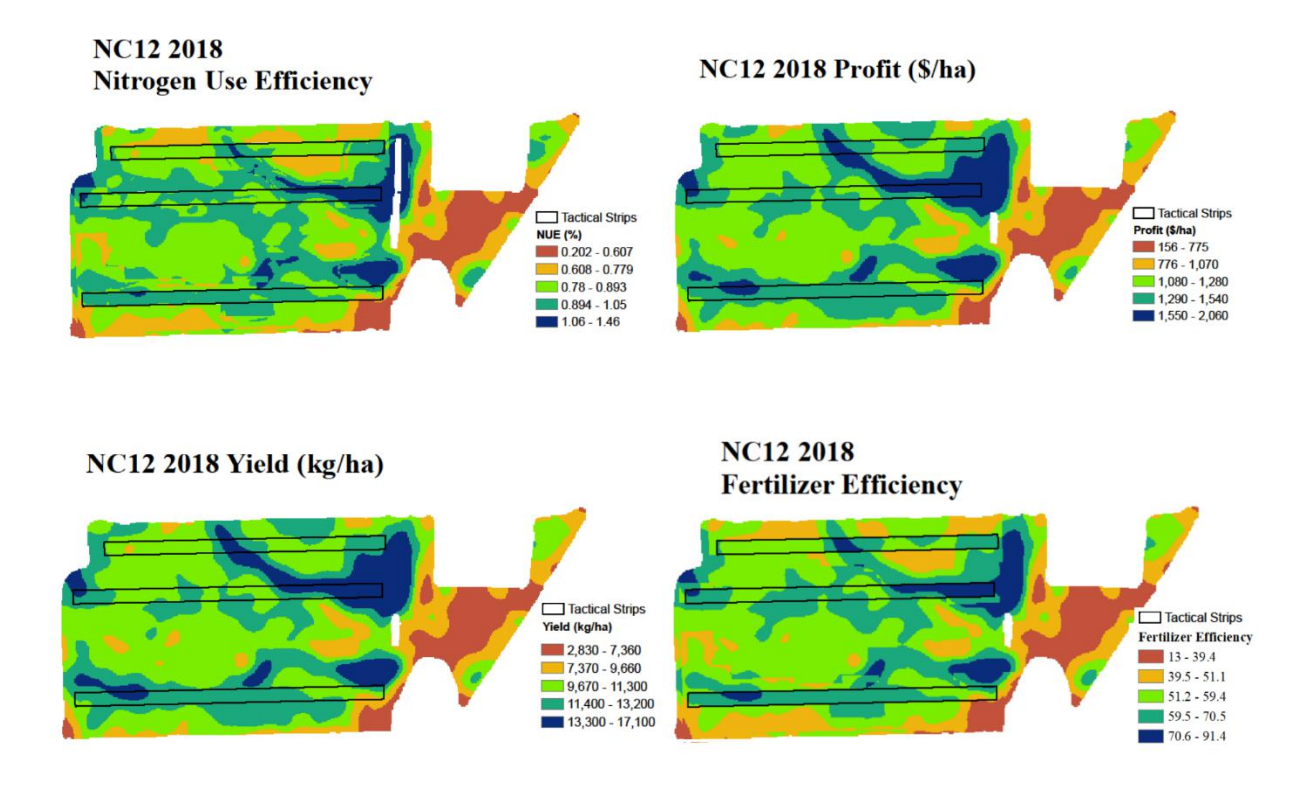


Figure 28. NUE, Profit, Yield, and Fertilizer Efficiency/ANUE maps created in ESRI ArcMap from yield monitor data and N data from hand samples.

Figure 28 (cont'd)

b.

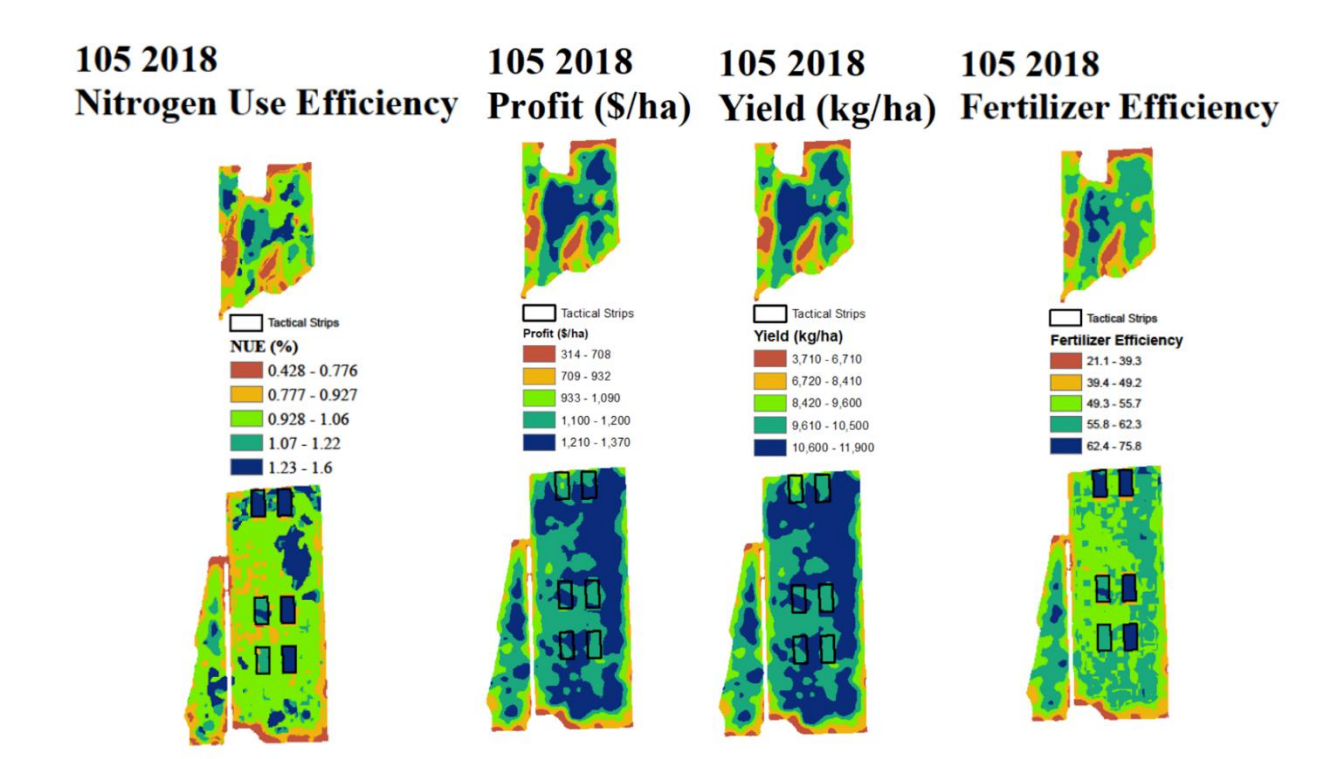


Figure 28 (cont'd)

c.

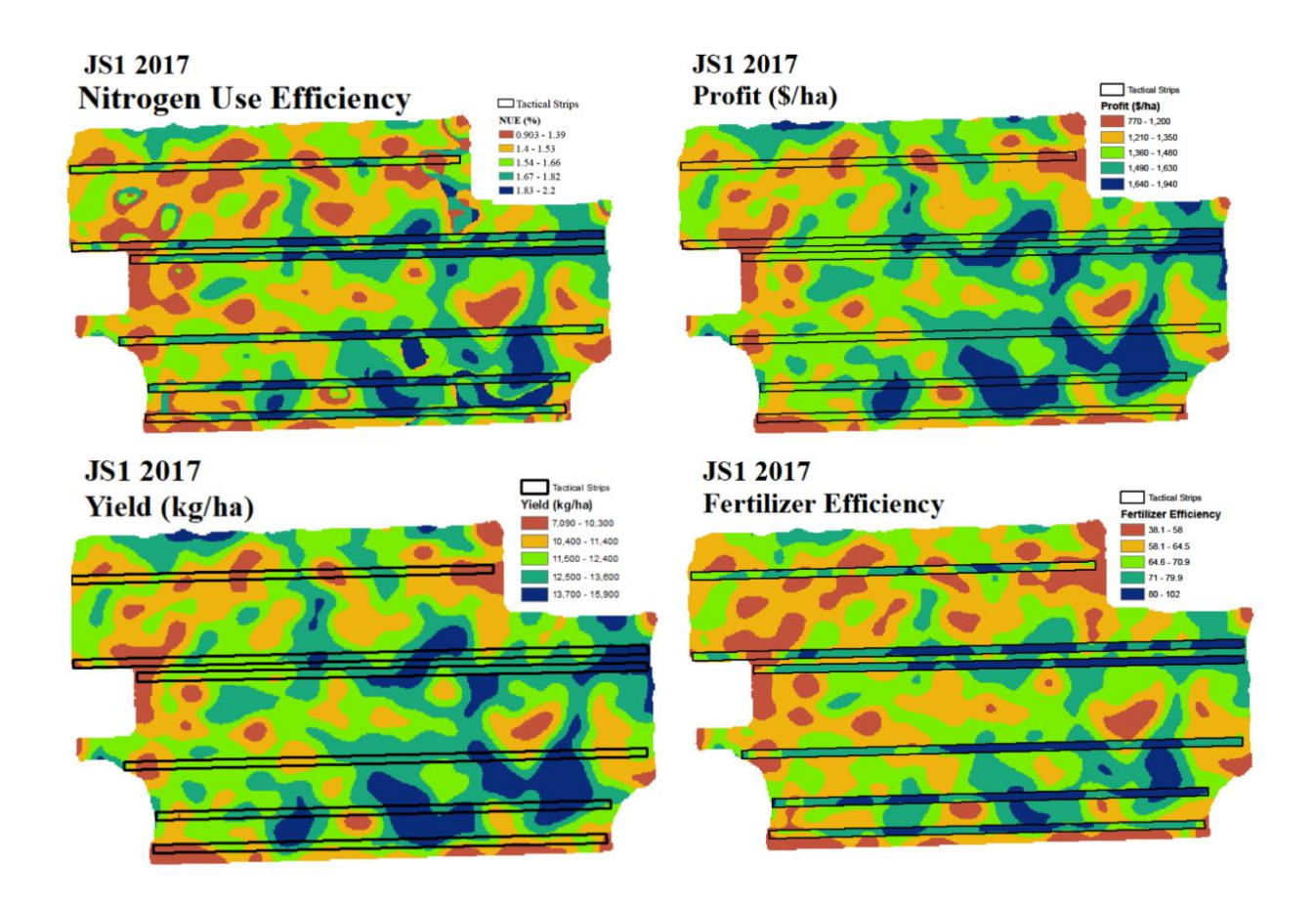


Figure 28 (cont'd)

d.

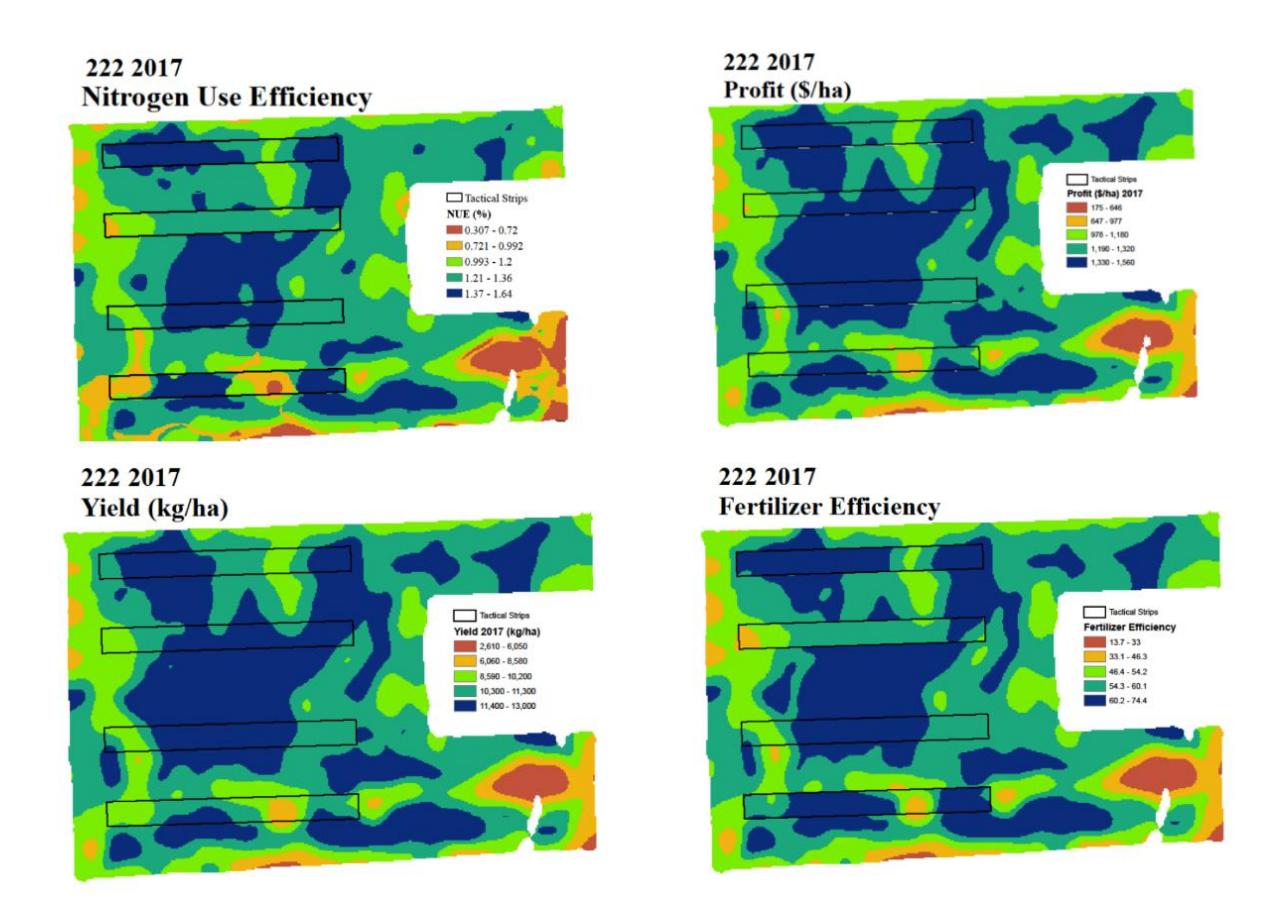
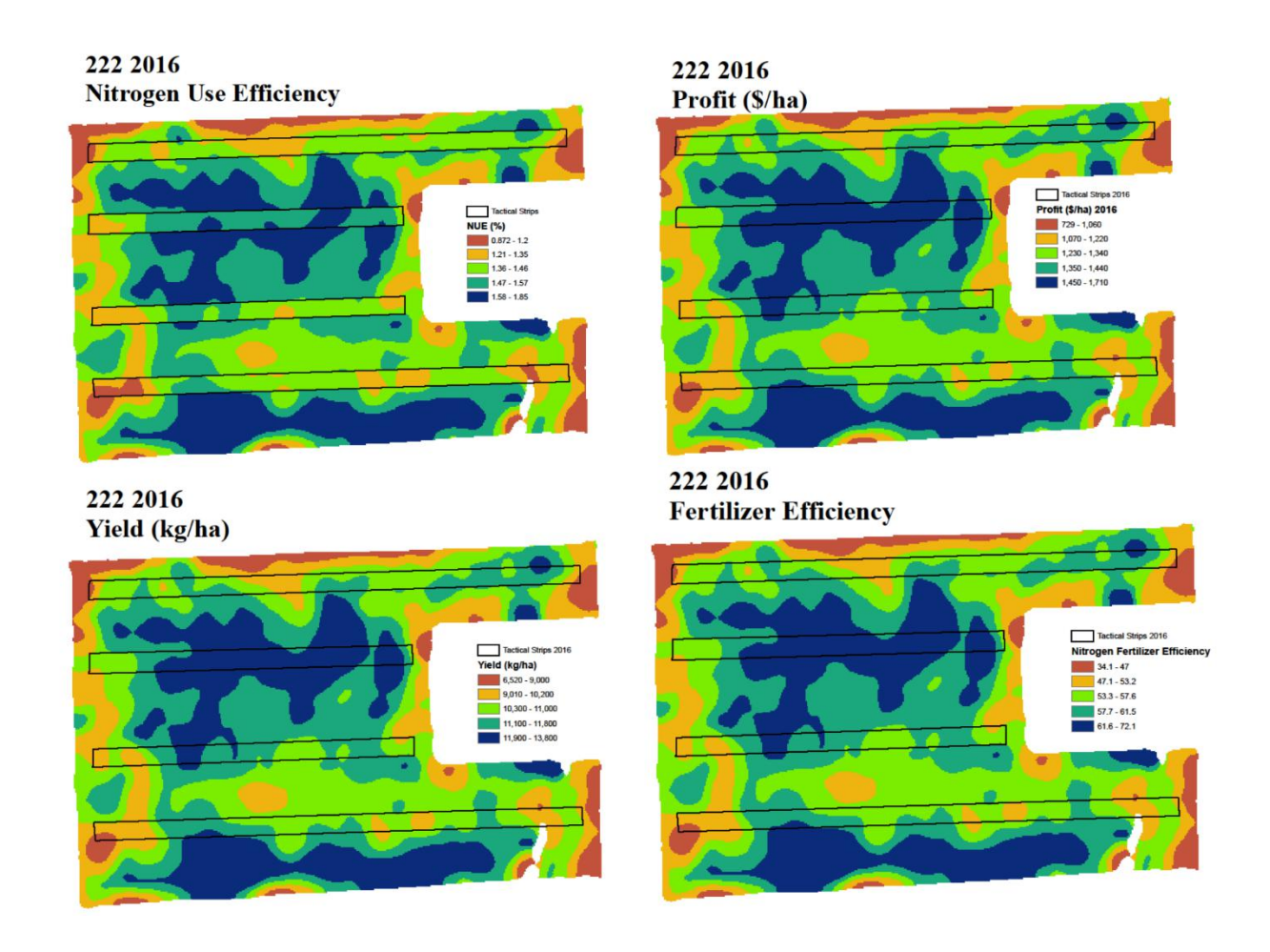


Figure 28 (cont'd)

e.



ZC1 2016 Yield and Sampling Technique

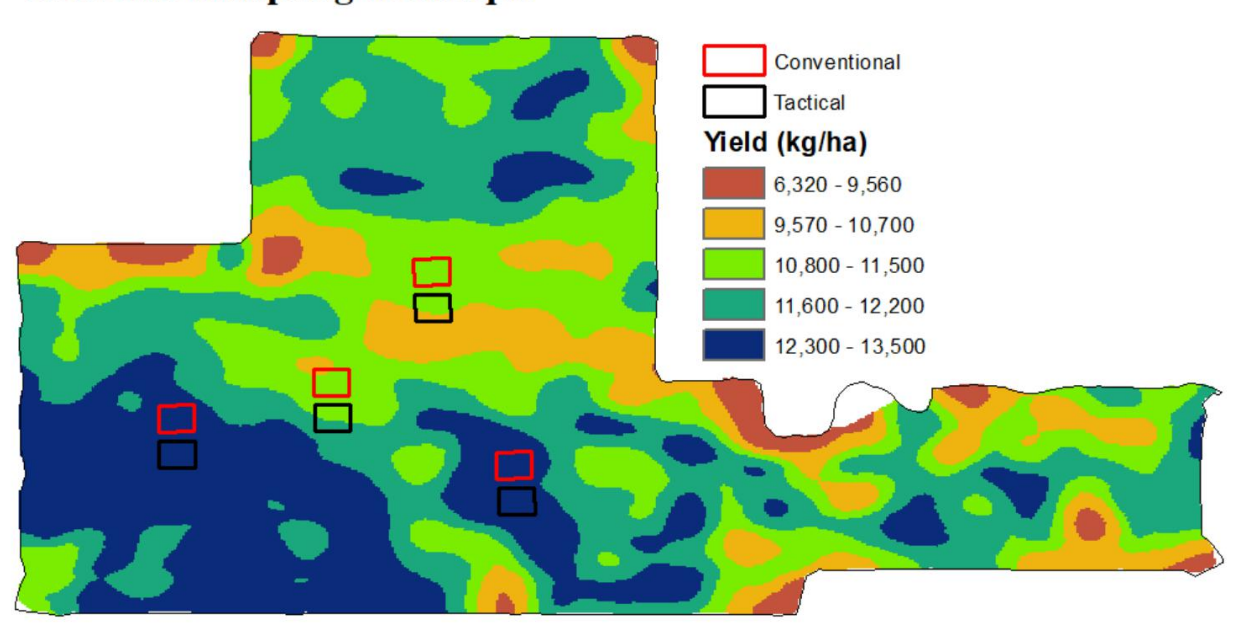


Figure 29. Yield monitor data of field ZC1 in 2016 showing sampling locations where N was overloaded by hand.

Table 15. ANOVA significance results (p values) relating relative chlorophyll from photosynq measurements to date of measurements, yield stability zone, and nitrogen treatment type (tactical or conventional, trt=treatment) and their interactions, indicated by a colon.

Field	Date	Zone	Trt Type	Date:Zone	Trt: Zone	Trt:Date	Trt:Date: Zone
222	< 2.2e-16	5.69 e-08	8.33 e- 16	0.0002	0.005	0.0001	0.0006
105	< 2.2e-16	0.28	0.37	0.14	0.74	0.75	0.62
NC12	< 2.2e-16	6.19 e-11	0.001	0.0003	0.06	0.26	0.73

REFERENCES

REFERENCES

- Basso, B., Ritchie, J.T., Pierce, F.J., Braga, R.P., Jones, J.W. 2001. "Spatial validation of crop models for precision agriculture". *Agricultural Systems*. 68, 97–112.
- Basso, B., Cammarano, D., & De Vita, P. 2004. "Remotely Sensed Vegetation Indices: Theory and applications for crop management". *Rivista Italiana Di Agrometeorologia* (1), 36–53. Retrieved from http://wwww.agrometeorologia.it/documenti/rivista9 1/Basso2004 1.pdf
- Basso, B., & Ritchie, J. T. 2005. "Impact of compost, manure and inorganic fertilizer on nitrate leaching and yield for a 6-year maize—alfalfa rotation in Michigan". Agriculture, Ecosystems & Environment 108(4), 329–341.
- Basso, B., Ritchie, J. T., Grace, P. R., & Sartori, L. 2006. "Simulation of Tillage Systems Impact on Soil Biophysical Properties Using the SALUS Model". Italian Journal of Agronomy 1(4), 677-688. https://doi.org/10.4081/ija.2006.677
- Basso, B., Ritchie, J. T., Cammarano, D., & Sartori, L. 2011. "A strategic and tactical management approach to select optimal N fertilizer rates for wheat in a spatially variable field". European Journal of Agronomy 35(4), 215–222. https://doi.org/10.1016/J.EJA.2011.06.004
- Basso, B., Liu, L., & Ritchie, J. T. 2016. "A Comprehensive Review of the CERES-Wheat, Maize and -Rice Models' Performances". Advances in Agronomy 136, 27-132. https://doi.org/10.1016/bs.agron.2015.11.004
- Basso, B., Dumont, B., Cammarano, D., Pezzuolo, A., Marinello, F., & Sartori, L. 2016. "Environmental and economic benefits of variable rate nitrogen fertilization in a nitrate vulnerable zone". Science of The Total Environment 545, 227–235. https://doi.org/10.1016/j.scitotenv.2015.12.104
- Basso, B., & Schulthess, U. 2016. "Variable rate nitrogen fertilizer response in wheat using remote sensing". Precision Agriculture, 17, 168–182. https://doi.org/10.1007/s11119-015-9414-9
- Basso B. and Antle J. 2020. Digital agriculture to design sustainable agricultural systems. Nature Sustainability, 4, 254-256
- Blacklow, W. M. 1974. "Simulation model to predict germination and emergence of corn (zea mays 1.) in an environment of changing temperature". Crop Science 13, 604–608
- Bongiovanni, R. 2004. "Precision Agriculture and Sustainability". Precision Agriculture, 5, 359–387. Retrieved from https://link.springer.com/content/pdf/10.1023%2FB%3APRAG.0000040806.39604.aa.pdf
- Cassman, K.G., Dobermann, A., Walters, D.T. 2002. "Agroecosystems, nitrogen-use efficiency, and nitrogen management". AMBIO: A Journal of the Human Environment 31, 132-140.
- Drury, C.F., Tan, C.S., Gaynor, J.D., Oloya, T.O., Welacky, T.W. 1996. "Influence of controlled drainage-subirrigation on surface and tile drainage nitrate loss". Journal of Environmental Quality 25, 317-324.

- Drury, C.F., Tan, C.S., Welacky, T.W., Reynolds, W.D., Zhang, T.Q., Oloya, T.O., McLaughlin, N.B., Gaynor, J.D. 2014. "Reducing nitrate loss in tile drainage water with cover crops and water-table management systems". Journal of Environmental Quality 43, 587-598.
- Erickson, B., D. Widmar, and J. Holland. 2013. "Precision Agriculture in 2013," Crop Life 16th Purdue U. Retailer Precision Adoption Survey, W. Lafayette, IN. June. http://agribusiness.purdue.edu/precision-ag-survey.
- Ford, J. H., & Hicks, D. R. 2013. "Corn Growth and Yield in Uneven Emerging Stands." Journal of Production Agriculture 5(19006), 185–188.
- Gitelson, A. A., Kaufman, Y. J., & Merzlyak, M. N. 1996. "Use of a green channel in remote sensing of global vegetation from EOS- MODIS". Remote Sensing of Environment 58(3), 289–298. https://doi.org/10.1016/S0034-4257(96)00072-7
- Havlin, J.L., Heiniger, R.W. 2009. "A variable-rate decision support tool". Precision Agriculture 10, 356-369.
- Hawkins, J. A., Sawyer, J. E., Barker, D. W., & Lundvall, J. P. 2007. "Using Relative Chlorophyll Meter Values to Determine Nitrogen Application Rates for Corn". Agronomy Journal 99(4), 1034. https://doi.org/10.2134/agronj2006.0309
- Hodgen, Paul J, "Individual corn plant nitrogen management." 2007. ETD collection for University of Nebraska Lincoln.

 https://digitalcommons.unl.edu/dissertations/AAI3271926
- IPCC. 2014. "Climate Change 2014: Synthesis Report. Contribution of Working Groups I, II and III to the Fifth Assessment Report of the Intergovernmental Panel on Climate Change [Core Writing Team, R.K. Pachauri and L.A. Meyer (eds.)]". IPCC, Geneva, Switzerland, 151 pp.
- Jones, J. W., Antle, J. M., Basso, B., Boote, K. J., Conant, R. T., Foster, I., ... Wheeler, T. R. 2017. "Toward a new generation of agricultural system data, models, and knowledge products: State of agricultural systems science". Agricultural Systems 155, 269–288. https://doi.org/10.1016/J.AGSY.2016.09.021
- Knobeloch, L et al. "Blue babies and nitrate-contaminated well water." Environmental health perspectives vol. 108,7 (2000): 675-8. doi:10.1289/ehp.00108675
- Kotak, B. G., Kenefick, S. L., Fritz, D. L., Rousseaux, C. G., Prepas, E. E., & Hrudey, S. E. 1993. "Occurrence and toxicological evaluation of cyanobacterial toxins in Alberta lakes and farm dugouts". Water Research 27(3), 495–506. https://doi.org/10.1016/0043-1354(93)90050-R
- Kuhlgert, S., Austic, G., Zegarac, R., Osei-Bonsu, I., Hoh, D., Chilvers, M. I., ... Kramer, D. M. 2016. "MultispeQ Beta: a tool for large-scale plant phenotyping connected to the open PhotosynQ network". Royal Society Open Science 3(10), 160592. https://doi.org/10.1098/rsos.160592
- Liu, W., M. Tollenaar, G. Stewart, and W. D. 2004. "Within- row plant spacing variability does not affect corn yield". Agronomy Journal 96(1), 275–280.

- Liu, W., Tollenaar, M., Stewart, G., & Deen, W. 2004. "Response of Corn Grain Yield to Spatial and Temporal Variability in Emergence." Crop Ecology, Management & Quality 854(March 2003), 847–854
- Liu, L., & Basso, B. 2020. "Impacts of climate variability and adaptation strategies on crop yields and soil organic carbon in the US Midwest". PLOS ONE 15(1). https://doi.org/10.1371/journal.pone.0225433
- Maestrini, B., & Basso, B. 2018. "Drivers of within-field spatial and temporal variability of crop yield across the US Midwest". Scientific Reports 8(1), 1–9. https://doi.org/10.1038/s41598-018-32779-3
- Martin, K. L., Hodgen, P. J., Freeman, K. W., Melchiori, R., Arnall, D. B., Teal, R. K., ... Raun, W. R. 2005. "Plant-to-plant variability in corn production". Agronomy Journal 97(6), 1603–1611. https://doi.org/10.2134/agronj2005.0129
- Meyer-Aurich, A., Weersink, A., Gandorfer, M., Wagner, P. 2010. "Optimal site-specific fertilization and harvesting strategies with respect to crop yield and quality response to nitrogen". Agricultural Systems 103, 478-485.
- Mulla, D.J. 2013. "Twenty-five years of remote sensing in precision agriculture: Key advances and remaining knowledge gaps". Biosystems Eng 114, 358-371.
- Mulla, D., and R. Khosla. 2016. "Historical Evolution and Recent Advances in Precision Farming." Soil-Specific Farming Precision Agriculture, 1–35. Boca Raton, FL: CRC Press. doi:10.1201/b18759-2.
- Nafziger, E. D., Carter, P. R., & Graham, E. E. 1991. "Response of Corn to Uneven Emergence". Crop Science 31(3), 811–815. https://doi.org/10.2135/cropsci1991.0011183x003100030053x
- Nielsen, R. L. 2018. "Stand Establishment Variability in Corn". Iowa State University. https://doi.org/10.31274/icm-180809-430
- Nielsen, D. R., Biggar, W, & Erh, K. T. 1973. "Spatial Variability of Field-Measured Soil-Water Properties." Hilgardia 42, 215-259.
- Pierce, F. J., & Nowak, P. 1999. "Aspects of Precision Agriculture". Advances in Agronomy 67(C), 1–85. https://doi.org/10.1016/S0065-2113(08)60513-1
- Pfost, D., Casady, W., Shannon, K. 1998. "Precision Agriculture: Global Positioning System (GPS)". Water Quality University Extension, University of Missouri-System Precision Agriculture Center.
- Pommel, B., Mouraux, D., Cappellen, O., & Ledent, J. F. 2002. "Influence of delayed emergence and canopy skips on the growth and development of maize plants: a plant scale approach with CERES-Maize". European Journal of Agronomy 16. Retrieved from www.elsevier.com/locate/eja
- Ponti, M. P. 2013. "Segmentation of Low-Cost Remote Sensing Images Combining Vegetation Indices and Mean Shift". IEEE Geoscience and Remote Sensing Letters 10(1), 67–70. https://doi.org/10.1109/LGRS.2012.2193113

- Rademaher, J.J., Young, T.B., Kanarek, M.S. 1992. "Gastric cancer mortality and nitrate levels in Wisconsin drinking water". Arch. Environ. Health 47 (4), 292–294
- Raun, W. R., Solie, J. B., Johnson, G. V, Stone, M. L., Mullen, R. W., Freeman, K. W., ... Lukina, E. V. 2002. "Improving Nitrogen Use Efficiency in Cereal Grain Production with Optical Sensing and Variable Rate Application." Agronomy Journal 820, 815–820.
- Robertson, G.P., Vitousek, P.M. 2009. "Nitrogen in agriculture: Balancing the cost of an essential resource". Annual Review of Environment & Resources 34, 97-125.
- Robertson, G.P. 2014. "Soil greenhouse gas emissions and their mitigation". Encycl. Agric. Food Syst., San Diego 185-96. Doi:10.1016/B978-0-444-52512-3.00097-8
- Rosegrant, Mark W.; Koo, Jawoo; Cenacchi, Nicola; Ringler, Claudia; Robertson, Richard D.; Fisher, Myles; Cox, Cindy M.; Garrett, Karen; Perez, Nicostrato D.; and Sabbagh, Pascale. 2014. "Food security in a world of natural resource scarcity: The role of agricultural technologies". Washington, D.C.: International Food Policy Research Institute (IFPRI). http://dx.doi.org/10.2499/9780896298477
- Rutto, E., Daft, C., Kelly, J., Chim, B. K., Mullock, J., Torres, G., & Raun, W. 2014. "Effect of Delayed Emergence on Corn (Zea Mays L.) Grain Yield". Journal of Plant Nutrition 37(2), 198–208. https://doi.org/10.1080/01904167.2013.859691
- Schimmelpfennig, David. "Farm Profits and Adoption of Precision Agriculture. (2016). "ERR-217, U.S. Department of Agriculture, Economic Research Service, October 2016
- Schimmelpfennig, David, and Robert Ebel. 2011. "On the Doorstep of the Information Age: Recent Adoption of Precision Agriculture." EIB-80, U.S. Dept. of Agriculture, Economic Research Service, August 2011.
- Shanahan, J. F., Schepers, J. S., Francis, D. D., Varvel, G. E., Wilhelm, W. W., Tringe, J. M., ... Major, D. J. 2001. "Use of Remote-Sensing Imagery to Estimate Corn Grain Yield." Agronomy Journal 93(3), 583. https://doi.org/10.2134/agronj2001.933583x
- Shockley, J. M., Dillon, C. R., & Stombaugh, T. S. 2011. "A Whole Farm Analysis of the Influence of Auto-Steer Navigation on Net Returns, Risk, and Production Practices." Journal of Agricultural and Applied Economics 43(1), 57–75. https://doi.org/10.1017/s1074070800004053
- Solie, J. B., Monroe, A. D., Raun, W. R., & Stone, M. L. 2012. "Generalized Algorithm for Variable-Rate Nitrogen Application in Cereal Grains". Agronomy Journal 104(2), 378. https://doi.org/10.2134/agronj2011.0249
- Teal, R. K., Tubana, B., Girma, K., Freeman, K. W., Arnall, D. B., Walsh, O., & Raun, W. R. 2006. "In-Season Prediction of Corn Grain Yield Potential Using Normalized Difference Vegetation Index". Agronomy Journal 98:1488–1494 https://doi.org/10.2134/agronj2006.0103
- Vieira, S. R., Nielsen, D. R., & Biggar, J. W. 1981. "Spatial Variability of Field-Measured Infiltration Rate". Soil Science Society of America Journal 45(6), 1040–1048. https://doi.org/10.2136/sssaj1981.03615995004500060007x